University of New Mexico
UNM Digital Repository

Biology ETDs | Electronic Theses and Dissertations

Spring 5-11-2018

Linking Climate Change and Mortality in Piñon-Juniper Woodlands, from Leaf to Ecosystem

Amanda I. Liebrecht
University of New Mexico

Follow this and additional works at: https://digitalrepository.unm.edu/biol_etds

 Part of the Biology Commons

Recommended Citation
Liebrecht, Amanda I.. "Linking Climate Change and Mortality in Piñon-Juniper Woodlands, from Leaf to Ecosystem." (2018).
https://digitalrepository.unm.edu/biol_etds/276

This Dissertation is brought to you for free and open access by the Electronic Theses and Dissertations at UNM Digital Repository. It has been accepted for inclusion in Biology ETDs by an authorized administrator of UNM Digital Repository. For more information, please contact disc@unm.edu.

Amanda I. Liebrecht
Candidate

Biology
Department

This dissertation is approved, and it is acceptable in quality and form for publication:

Approved by the Dissertation Committee:

Marcy E. Litvak , Chairperson

William T. Pockman

William R.L. Anderegg

Robert L. Sinsabaugh

LINKING CLIMATE CHANGE AND MORTALITY IN PIÑON-JUNIPER WOODLANDS, FROM LEAF TO ECOSYSTEM

by

AMANDA I. LIEBRECHT

B.A. Biology, Biochemistry, St. Mary's College of Maryland, 2011

DISSERTATION

Submitted in Partial Fulfillment of the
Requirements for the Degree of

Doctor of Philosophy
Biology

The University of New Mexico
Albuquerque, New Mexico

July, 2018

ACKNOWLEDGEMENTS

The research in this dissertation was supported by DOE Office of Science TES, SC DE-SC0008088 and NSF Ecosystems NSF-DEB-1557176 awards to MEL and WTP. Additional support from the Sevilleta LTER REU program and a scholarship from the Department of Biology at the University of New Mexico were provided to AIL.

I would like to acknowledge Deer Canyon Preserve for allowing access to the open space where all study sites were located. I would like to thank my committee, and all members (current and former) of the Litvak and Pockman labs for their help with experimental design, data collection, instrument installation, instrument and site maintenance and endless feedback. Finally, I would like to thank my family, friends, and partner for supporting me throughout this journey and making this dissertation possible.

LINKING CLIMATE CHANGE AND MORTALITY IN PIÑON-JUNIPER WOODLANDS, FROM LEAF TO ECOSYSTEM

by

Amanda I. Liebrecht

B.A. Biology, Biochemistry, St. Mary's College of Maryland, 2011
Ph.D. Biology, University of New Mexico, 2018

ABSTRACT

As global climate changes, the Southwestern US is predicted to experience more frequent and intense drought events. Extreme droughts can drive decreases in both physiological and ecosystem function, and can result in widespread tree mortality. Piñon-juniper (PJ) woodlands are a prevalent ecosystem in the region, co-dominated by two tree species, piñon (*Pinus edulis*) and juniper (*Juniperus monosperma*). Drought-induced piñon mortality has occurred over the past few decades, coinciding with outbreaks of a piñon-specific bark beetle. Piñon and juniper have different hydraulic strategies (isohydry and anisohydry, respectively) that should affect the way each species responds to drought. In this dissertation, I used PJ woodlands to quantify both physiological and ecosystem effects of drought and mortality, and the ways in which they interact. First, I focused on a PJ woodland where all of the large piñon had been girdled to simulate drought-related mortality. I looked for evidence of competitive release in both species by measuring photosynthetic and hydraulic parameters in the girdled plot vs. an intact control plot. I did not find evidence of competitive release in response to piñon mortality, likely due to the multi-year drought that followed the girdling event. I next examined whether hydraulic strategy affected piñon and juniper responses to two components of

drought, atmospheric and soil moisture drought. I used sap flow measurements at an intact control site to quantify tree responses to soil water potential and vapor pressure deficit (VPD). Over seven years, both species were more sensitive to drying soil than high VPD, and both species were similarly affected by concurrent dry soil and high VPD. Finally, I quantified tree and ecosystem responses to a three year drought and the natural piñon mortality event that followed, combining sap flow and eddy covariance data. Tree and ecosystem function both decreased during drought, and ecosystem net carbon uptake decreased after mortality, although wet conditions following mortality offset this decrease. Taken together, these findings suggest that increasing drought and associated mortality in the region will decrease productivity, but climate conditions following drought will ultimately determine whether the ecosystem recovers or shifts to an alternate state.

Table of Contents

List of Figures

List of Tables

Chapter 1

Introduction

Semi-arid piñon-juniper woodlands, the focus of this dissertation, are an ideal study system for tree mortality and climate change. In addition to being prevalent throughout the Southwestern US, they are also the third-largest ecosystem in the Western US (West 1999). Climate predictions for the future suggest that the areas encompassing piñon-juniper woodlands will become hotter and drier, with more intense and frequent droughts (Overpeck and Udall 2010, Dai 2013). Piñon-juniper woodlands are dominated by two species, *Pinus edulis* (piñon) and *Juniperus monosperma* (juniper) that have very different hydraulic strategies (McDowell et al. 2008), which could have important ramifications for how each species responds to the predicted climate changes. This provides us a unique opportunity to explore how plant hydraulic strategy interacts with different types of drought to produce ecosystem-level responses, and could help inform predictions about future ecosystem behavior.

Piñon-juniper woodlands are also an example of an ecosystem that has been severely impacted by widespread tree mortality. Following a drought from 1999-2002, the western US experienced about 6% mortality of piñon (Shaw et al. 2005), although in some locations, piñon-juniper woodlands experienced up to 95% mortality of piñon, with a much smaller percentage (up to 25%) of juniper dying as well (McDowell et al. 2008). As a result of this differential mortality, these landscapes changed drastically and saw a shift toward domination by old, large juniper and young, small piñon (Clifford et al.

2008). This dissertation investigates the response of piñon-juniper woodlands to both changes in climate (increasing drought) and to piñon mortality, examining responses at scales from leaf to tree to ecosystem.

In chapter 2, I examined leaf and root physiological responses of the remaining piñon and juniper in a PJ woodland following the mortality of large, mature piñon. My study site was a piñon-juniper woodland where more than 1600 large piñon had been girdled in 2009 to simulate piñon mortality from drought. As a result of this mortality, I expected to see evidence of competitive release in the remaining trees, a phenomenon where removing competitors from an ecosystem leads to an abundance of resources such as water and nutrients that benefit the remaining plants (Anderegg et al. 2016b). This response is frequently observed in more mesic ecosystems, but has not been examined very often in semi-arid biomes. I measured leaf-level photosynthesis and root vulnerability to cavitation in the remaining juniper and piñon at the experimental site as well as an adjacent control site in 2011 and 2012. In response to competitive release, I expected the remaining trees of both species to acclimate to the wetter conditions in the ecosystem by up-regulating their photosynthetic activity and capacity, and changing their vulnerability to cavitation.

In chapter 3, I used the difference in hydraulic strategies between piñon and juniper to explore how each species responded at the tree level to two different drought types: soil moisture drought as a result of low soil water availability, and atmospheric drought as a result of rising temperatures and the associated high vapor pressure deficit (VPD). I used a seven-year time series (2010-2016) of sap flow measured in both piñon and juniper in a piñon-juniper site that experienced natural drought/bark beetle driven

piñon mortality beginning in 2013. The hydraulic strategy used by piñon is isohydry, where the plant closes its stomata under periods of soil moisture drought stress to conserve water, decreasing transpiration and maintaining stable leaf water potential (McDowell et al. 2008). On the other hand, the hydraulic strategy used by juniper is anisohydry, where the plant keeps its stomata open even during soil moisture drought stress, maintaining higher transpiration rates and allowing leaf water potential to decrease (McDowell et al. 2008). Here, I looked for evidence that the difference in hydraulic strategy between the two species would translate to a difference in sensitivity to the two types of drought. I used an existing framework (Sperry and Love 2015, Sperry et al. 2016) to help explain any species-specific differences I observed.

In chapter 4, I broadened the scale of my work to the ecosystem level, using what I had learned about species-specific responses to climate in chapter 3 to take a closer look at the natural mortality at my study site. I defined climate thresholds of soil water potential and VPD beyond which I saw impaired physiological function in both species, and quantified the number of days spent above those climate thresholds prior to mortality. I also explored the effects of drought conditions on both tree and ecosystem levels across the seven years of the study (again, 2010-2016). In addition, I compared ecosystem and tree function before and after mortality occurred, during drought and non-drought conditions and examined how the contributions from different components of the ecosystems changed after mortality.

As climate conditions in the Southwestern US continue to change, becoming hotter and drier, piñon-juniper woodlands (and semi-arid biomes as a whole) will become more stressed. My work in chapters 2 and 4 investigated whether there will be any

benefits for the surviving trees or the ecosystem as a result of piñon mortality to address possible recovery trajectories for piñon-juniper woodlands. In chapters 3 and 4, I investigated whether atmospheric and soil moisture drought will be detrimental to tree-level function in both species or to the function of the ecosystem as a whole to inform predictions of future productivity in piñon-juniper woodlands. The findings of this work will have implications for ecosystem recovery trajectories and productivity following disturbances such as drought and mortality. This work can help inform research on other semi-arid biomes as well as on other ecosystems with a mixture of isohydric and anisohydric species.

All three chapters are currently being prepared as manuscripts for publication. The chapters are included as elements of my dissertation, but the manuscripts will be the culmination of collaboration with multiple co-authors and advisors.

Chapter 2

Large-scale piñon mortality did not result in tree-level competitive release in a piñon-juniper woodland ecosystem.

2.1 Introduction

Anthropogenic climate forcing is expected to trigger climate changes globally and throughout the southwestern United States. Besides elevated atmospheric CO_2 levels, the projected regional changes include increased temperatures, decreased precipitation, and an increase in both the frequency and intensity of drought events (Overpeck and Udall 2010, Dai 2013). Extreme droughts have historically resulted in widespread tree mortality, which affects both ecosystem structure and carbon and water dynamics (Breshears et al. 2005, Allen et al. 2010, Carnicer et al. 2011, Peng et al. 2011, Rodrigues et al. 2011, Adams et al. 2012, Anderegg et al. 2013, Krofcheck et al. 2015, Anderegg et al. 2016b, Morillas et al. 2017). Given the frequency and severity of drought events that have led to climate-driven mortality over the past few decades, it is vital to understand how ecosystems will respond to these events moving forward (Allen et al. 2010).

Ecosystem-scale responses to mortality should depend on a variety of factors, including the magnitude of the mortality event, characteristics of the affected ecosystem, and how readily recovery processes occur (Anderegg et al. 2016b). Anderegg et al. (2016b) suggested that responses to climate-driven mortality may not be as extreme as responses to larger-scale disturbances such as stand-replacing fires or clear-cutting because recovery may be faster. One aspect that regulates the rate of ecosystem recovery

post-mortality is competitive release. Competitive release occurs when a competitor for resources such as water, light, or nutrients is removed from the ecosystem, thereby increasing the availability of resources for the remaining competitors (Rich et al. 2008, Lloret et al. 2012, Anderegg et al. 2016b). This effect has been well demonstrated in tree-thinning studies, particularly in mesic areas (e.g. Simard et al. 2004, Pretzsch 2005, Schuler 2006, Martínez-Vilalta et al. 2007, Ward 2008), where tree growth rates of remaining trees have increased in response to selective harvest. In addition to increased growth of remaining trees, the release effect may allow for higher recruitment and growth of understory vegetation, particularly if canopy loss enhances ground-penetrating radiation (Rich et al. 2008, Royer et al. 2011, Lloret et al. 2012, Anderegg et al. 2016b).

Competitive release should be observable at the leaf and tree level not only by measuring growth, as described above, but also through increased rates of leaf-level carbon uptake in the surviving plants. If the result of mortality is indeed increased water availability, plants should exhibit higher stomatal conductance (Sperry 2000), and thus, higher photosynthetic rates post-mortality. Another measurable effect of increased water availability may be an increase in hydraulic conductivity of remaining trees in the ecosystem, which could lead to increased cavitation vulnerability of those trees (Hudson et al. 2018). Cavitation, or damage to the hydraulic machinery as xylem cells fill with air, often occurs when plants are drought-stressed and the xylem is under excessive tension. The result is decreased hydraulic conductivity (Cochard et al. 1992). Plants in arid environments often have a higher resistance to cavitation (Maherali et al. 2004) as a physiological adaptation to more frequent and prolonged drought stress. It has been suggested (Maherali et al. 2004, Gleason et al. 2016) that there is a tradeoff between

efficiency of xylem (high conductivity) and safety (high resistance to cavitation), although the evidence for this tradeoff is weak (Gleason et al. 2016). If widespread mortality increases the availability of water in the ecosystem, hydraulic conductivity in surviving plants may also increase, leading to the production of more vulnerable but more efficient xylem.

During a recent severe, prolonged drought in the southwestern U.S. (1999 to 2002), differential tree mortality dramatically altered piñon-juniper (PJ) woodlands throughout the region. Although both piñon and juniper were physiologically stressed during the drought, piñon mortality (greater than 90% in some areas) was higher than juniper mortality (up to 25% in some areas) (Breshears et al. 2005), due to concurrent outbreaks in the piñon ips (*Ips confusus*) beetle (McDowell et al. 2008, Gaylord et al. 2013). In addition, larger and older piñon had higher mortality rates (Mueller et al. 2005, Floyd et al. 2009). This differential mortality transformed the traditional piñon-juniper woodland landscape from co-dominated juniper and piñon terrain into a landscape dominated by juniper and small, young piñon (Mueller et al. 2005, Clifford et al. 2008, Floyd et al. 2009). The death of a large fraction of the overstory and subsequent litter fall altered both abiotic and biotic processes in these ecosystems, including increased ground-penetrating radiation (Rich et al. 2008, Royer et al. 2011), increased water availability (Rich et al. 2008), and changes in albedo, erosion, nutrient cycling, and soil respiration (McDowell et al. 2008, Adams et al. 2010). In addition, understory species such as grasses and forbs increased in many areas (McDowell et al. 2008, Rich et al. 2008). It is unknown how piñon-juniper woodlands across the Southwestern US are going to respond in terms of both structure and function to this widespread mortality. Evidence of

competitive release of the remaining trees could be very important in predicting the trajectories of recovery in this biome.

We tested for competitive release in a piñon-juniper woodland following the death of large piñon (by girdling) to examine the ecosystem scale consequences of simulated drought-induced mortality on ecosystem function. We predicted that we would observe evidence of competitive release in the remaining trees, juniper (*Juniperus monosperma*), and small piñon (*Pinus edulis*), primarily due to increased water availability following the mortality of a canopy co-dominant. We predicted we would observe competitive release as 1) increased photosynthetic activity and capacity in both tree types, and 2) increased hydraulic conductance and an associated increased cavitation vulnerability in roots from both tree types.

2.2 Methods

2.2.1 Study site

The study site (referred to as the girdled site or girdled plot) is located south of Mountainair, NM, at 34.44649° N, 106.21446° W. The ecosystem is semi-arid piñon-juniper (PJ) woodland, dominated by *Pinus edulis* (piñon) and *Juniperus monosperma* (juniper) trees, along with several perennial species such as *Bouteloua gracilis* (a C4 grass), *Gutierezzia sarothrae*, *Yucca baccata*, and various cactus species in the *Opuntia* genus. In September 2009, we simulated drought-induced mortality (see Krofcheck et al. 2014, Morillas et al. 2017) across the 4 ha site by girdling all piñon that had a diameter at breast height (1.4 m) of greater than 7 cm, a total of >1600 trees. The girdle wounds were inflicted at breast height using chainsaws and were subsequently injected with 5%

glyphosate to ensure complete mortality. The girdled trees were chlorotic by November 2009 and lost their needles by July 2010. For the purposes of our gas exchange and cavitation vulnerability measurements, we used as our control a smaller (~1 ha) intact section of piñon-juniper woodland adjacent to the girdled plot, about 50 m away (referred to as the control plot).

2.2.2 Soil parameters

We measured volumetric soil water content and soil temperature beneath three piñon canopies, three juniper canopies, and three open areas throughout the girdled site and a nearby control site (located less than 3 km away at an intact piñon-juniper woodland). We installed CS610 soil moisture probes and T107 soil temperature probes (Campbell Scientific, Logan, Utah, USA) at 5, 10, and 30 cm depth in each location. Due to the presence of a petrocalcic "caliche" layer (Morillas et al. 2017), we could not measure deeper soil. The caliche layer was shallower at the girdled site, impairing our ability to install the same number of soil probes at 30 cm. Thus, there were only sensors at 30 cm under one piñon canopy, one juniper canopy, and one open area at the girdled site. For the purposes of this analysis, we averaged the data from the replicate probes by depth and cover type. We calculated a depth-averaged volumetric soil water content of the first 30 cm of the soil column ($VWC_{0\text{-}30}$) by assuming that the readings from the probe at 5 cm were representative of the first 7.5 cm of the soil column, the readings from the probe at 10 cm were representative of the next 7.5 cm of the soil column, and the readings from the probe at 30 cm were representative of the remainder of the soil column.

2.2.3 Photosynthetic parameters

To evaluate the effect of piñon mortality on the photosynthetic activity and capacity of the juniper and small piñon that remained, we measured the maximum carboxylation velocity of Rubisco (Vc_{max}) and the light-saturated photosynthetic rate under ambient levels of CO_2 (A_{max}) on five juniper and five small piñon (< 7 cm dbh) at the girdled plot from Fall 2011 – Spring 2012. These photosynthetic parameters were obtained from leaf-level gas exchange measurements in the field using a Li-Cor 6400XT portable photosynthesis system (Li-Cor, Lincoln, NE, USA) with the standard 2x3 cm chamber (6400-02B LED, Li-Cor, Lincoln, NE, USA). For all leaf-level gas exchange measurements, we used the youngest sun-exposed, south-facing mature foliage.

To evaluate whether or not competitive release was evident in photosynthetic capacity or activity, we compared these measurements of gas exchange in the girdled plot with simultaneous measurements made on five juniper and five small piñon (< 7 cm dbh) in the adjacent control plot. We also measured five large (> 7 cm dbh) piñon in the control plot.

We estimated Vc_{max} by measuring photosynthetic CO_2 (A/C_i) response curves on trees in the girdled and control plots under well-watered conditions. For each measurement piñon or juniper needles were sealed inside the chamber with G35 Qubitac Sealant (Qubit Systems, Kingston, ON, Canada) to prevent leaks and exposed to constant light (2000 µmol m^{-2} s^{-1}) and temperature (25 ºC) while a CO_2 mixer was used to expose the needles to a range of 15 CO_2 concentrations between 0 and 2400 µmol/mol, allowing at least 5 minutes at each CO_2 concentration for the assimilation rates to stabilize. The resulting assimilation values were corrected for projected leaf area and diffusion

(according to the manufacturer's recommendations). We measured projected leaf area by collecting the foliage that had been enclosed in the chamber and scanning the collected foliage on a flat-bed scanner within 24 hours of collection. We used ImageJ software (US National Institutes of Health, Bethesda, MD, USA) to calculate leaf area from the scanned images. We estimated Vc_{max} from the response curves following the method of Ethier and Livingston (2004), using an Excel macro developed by Kevin Tu (http://landflux.org/Tools.php). The resulting Vc_{max} values were adjusted to a temperature of 25 °C according to the methods of Bernacchi et al. (2001) and Harley et al. (1992), as the leaf temperature control on the Li-Cor did not always result in an exact leaf temperature of 25 °C.

We measured light-saturated photosynthetic rates (A_{max}) monthly from Fall 2011-Fall 2012 and more frequently during the March-October growing period of that year, for a total of 17 days of measurements. All measurements were performed in the morning (8 am – noon), as photosynthetic rates in these species reach a minimum by mid-afternoon (Limousin et al. 2013). Each time measurements were taken, all piñon were measured first, followed by all juniper, because we observed that piñon started decreasing their photosynthetic rates earlier in the day than juniper. We rotated between measuring the control plot trees and the girdled plot trees first, to avoid biases between treatments due to time of day. For each measurement, we sealed piñon or juniper needles inside the chamber as described above and exposed them to constant light (2000 μmol m^{-2} s^{-1}), CO_2 (390 μmol/mol), and temperature (25 ºC if ambient was above that, starting leaf temperature otherwise). We allowed the assimilation measurements to stabilize for 3-5

minutes before recording. We again corrected the resulting assimilation values for projected leaf area and diffusion, as described above.

2.2.4 Vulnerability curves

We estimated vulnerability to cavitation of roots using the air-injection method (Sperry and Saliendra 1994). During summer 2013 (5/23/13 – 7/16/13), we collected 3 root samples from juniper and 3 from small piñon in both the girdled and control plots. In the lab, each sample was rehydrated by submerging it in 20 mM KCl and leaving it in a vacuum chamber overnight. The day after collection, we used nitrogen gas to apply pressure to each root sample for two minutes in a double-ended metal pressure sleeve, followed by measurement of hydraulic conductivity. This procedure was repeated from 0 to 6 MPa for piñon, and from 0 to 10 MPa for juniper. We measured hydraulic conductivity (K_s) of the sample using a steady-state flow meter, consisting of a capillary tube with a known hydraulic conductivity, a pressure transducer, and a tubing manifold with plastic Luer fittings, as described by Feild et al. (2011) and Hudson et al. (2018).

We used the measured hydraulic conductivities to calculate the percent loss of conductivity at each pressure and then constructed a vulnerability curve by graphing the percent loss of conductivity versus the pressure (Neufeld et al. 1992, Hudson et al. 2018). We fit the data from each vulnerability curve to a Weibull function following the methods of Neufeld et al. (1992), which allowed us to estimate the pressure at which 50% of hydraulic conductivity had been lost (P_{50}) and the pressure at which the loss of hydraulic conductivity began to increase, also termed the air entry threshold (P_e) (Domec and Gartner 2001, Meinzer et al. 2009, Hudson et al. 2018).

2.2.5 Tree biomass

Each year, during the summer or fall (between June and October), we non-destructively surveyed biomass at the girdled site. We surveyed intensively within 6 circular plots (each with a 10 m radius) across the site and used these measurements to approximate the site as a whole. Within each plot, we measured the height, root crown diameter (juniper) or diameter at breast height (piñon), and canopy diameters of all the trees. We later converted the diameter at breast height measurements in piñon to root crown diameter (Chojnacky et al. 2013). We used allometric relationships from Grier et al. (1992) (Table 2.1) to calculate the total live foliar biomass (g C m^{-2}) and total live biomass (g C m^{-2}) for each species in each plot, then averaged the 6 plots together for each year.

Table 2.1: Allometric equations from Grier et al. (1992) used to calculate foliar and total biomass from root crown diameter (RCD) measurements in piñon and juniper. These allometries were based on measurements of 15 *Pinus edulis* and 21 *Juniperus monosperma* from piñon-juniper woodlands on the Colorado Plateau in northern Arizona. All equations are of the form: log Biomass = a + b*log RCD.

Species	Type	a	b	R^2
Piñon	Foliar	-0.946	1.565	0.94
	Total	-1.468	2.582	0.95
Juniper	Foliar	-1.737	1.382	0.79
	Total	-1.157	2.086	0.94

2.2.6 Statistical analysis

We used R (version 2.15.1) for all statistical analysis. We used t-tests to compare V_{cmax} values for small piñon between the control and girdled plots and to compare V_{cmax} values for juniper between the control and girdled plots. We placed A_{max} values into subsets by the day of year and within that day of year, we used t-tests to compare small

piñon between the control and girdled plots, and to compare juniper between the control and girdled plots. We looked at A_{max} by day of year to control for seasonal adjustments and seasonal changes in soil moisture. By comparing the control and girdled plots only on a daily scale, there should not be differences in soil water status between the two. To look for any evidence of changes in vulnerability to cavitation, we used t-tests to compare P_{50} and P_e values between trees in the control and girdled plots. We also used t-tests to compare P_{50} and P_e between species.

We compared soil characteristics (volumetric water content and temperature) between the girdled and control sites from 2009-2012. We used linear regressions to describe the relationship of VWC_{0-30} and soil temperature between the sites for each year, and compared the slope of these relationships over time to see if mortality at the girdled site changed the soil characteristics relative to the control site.

2.3 Results

2.3.1 Changes in soil moisture and temperature at the girdled site and a nearby control site

Soil water availability post-mortality did not increase. Before girdling occurred, the girdled site was slightly wetter, yet similar in soil temperature to the control site (Fig. 2.1). After girdling, we observed an immediate relative decrease in VWC_{0-30} in the girdled site compared to the control site in all three cover types (under piñon canopy, under juniper canopy, and open), which persisted through 2012 (Fig. 2.1, Table 2.2). In addition, post-girdling, soil temperatures in the girdled site were noticeably hotter below

piñon canopies, and to a lesser extent below juniper canopies and in open areas (Fig. 2.1, Table 2.3).

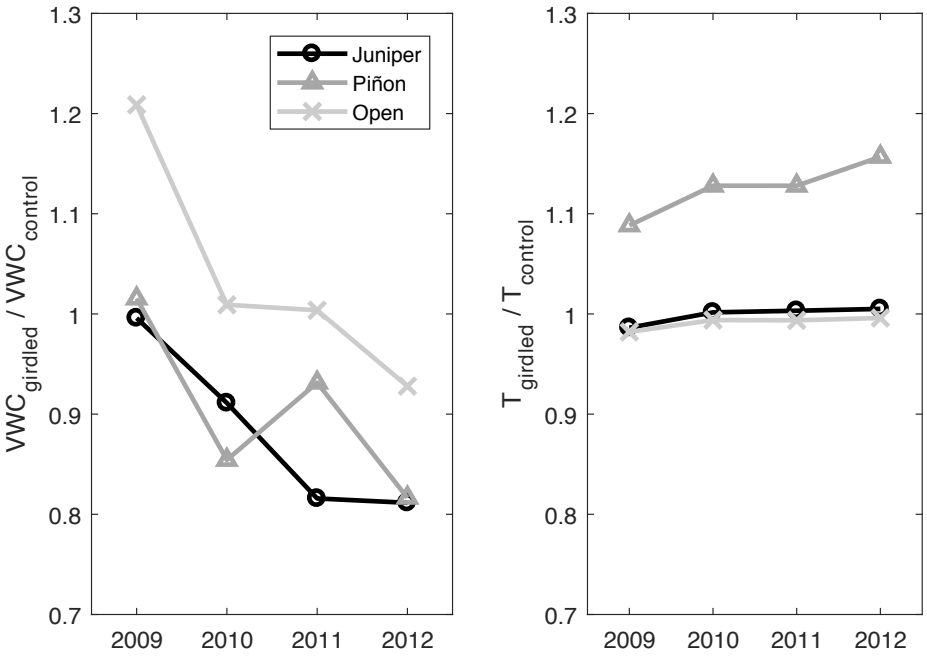

Figure 2.1: Comparisons of depth-averaged soil volumetric water content (VWC) and soil temperature (T) at the girdled and control sites after mortality from 2009-2012. Each point describes the slope of the linear regression between the two sites for that year, under juniper canopies, piñon canopies, and open areas.

Table 2.2: R^2 values for linear regressions of soil volumetric water content at the girdled and control sites from 2009-2012 for different cover types (under piñon canopy, under juniper canopy, and in an open area).

Year	Cover type	R^2
2009	Piñon	0.646
	Juniper	0.836
	Open	0.797
2010	Piñon	0.856
	Juniper	0.906
	Open	0.930
2011	Piñon	0.896
	Juniper	0.787
	Open	0.728
2012	Piñon	0.203
	Juniper	0.823
	Open	0.570

Table 2.3: R^2 values for linear regressions of soil temperature at the girdled and control sites from 2009-2012 for different cover types (under piñon canopy, under juniper canopy, and in an open area).

Year	Cover type	R^2
2009	Piñon	0.954
	Juniper	0.894
	Open	0.933
2010	Piñon	0.991
	Juniper	0.995
	Open	0.995
2011	Piñon	0.991
	Juniper	0.995
	Open	0.993
2012	Piñon	0.949
	Juniper	0.972
	Open	0.990

2.3.2 Leaf-level response to simulated mortality

Juniper and small piñon in both the girdled and control plots exhibited similar seasonal patterns of A_{max} over the course of the year, with the highest A_{max} rates occurring during the wettest and relatively cool times of the year (April and October) (Fig. 2.2). We observed very little evidence of competitive release in leaf-level photosynthetic responses in either species. Photosynthetic activity in juniper did not significantly differ between the girdled and control plots on any day over the course of the year of measurements (Fig. 2.2). In the remaining small piñon in the girdled plot, photosynthetic activity was similar to the control plot trees on all but two measurement days, suggesting if any competitive release occurred in small piñon, it was limited, and only occurred during the summer (July 11, 2012, July 21, 2012, Fig. 2.2).

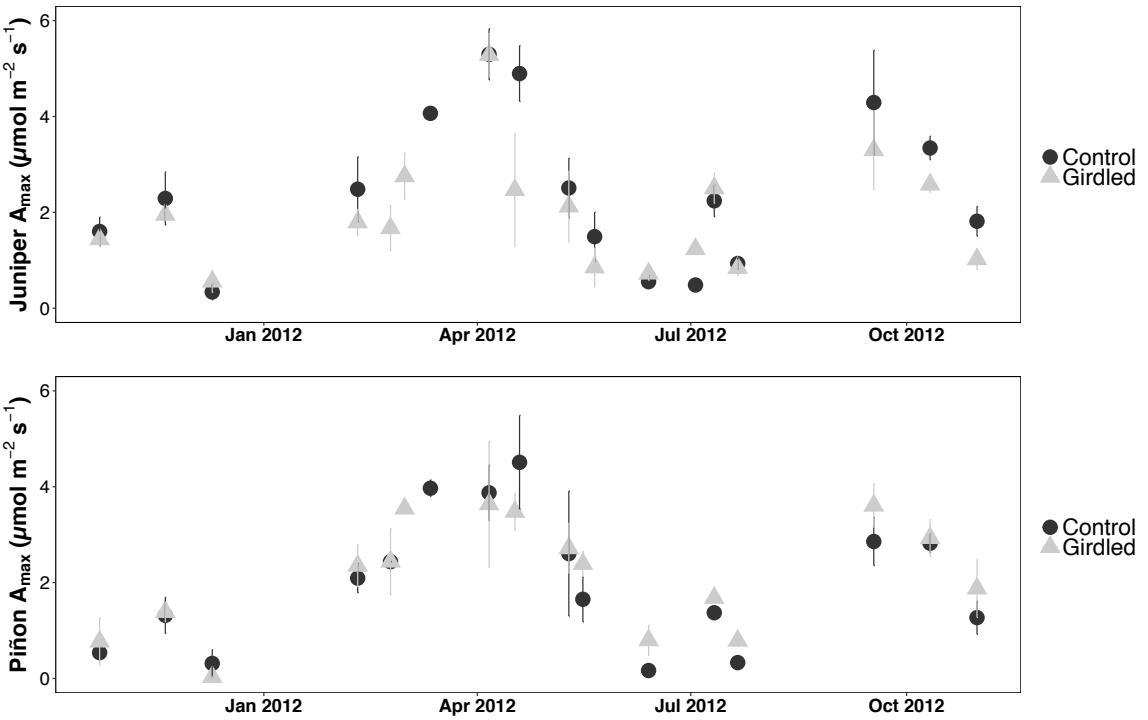

Figure 2.2: Photosynthetic activity (represented by A_{max}) for juniper and small piñon in the control and girdled plots. Points represent the mean +/- SE. During two days (July 11, 2012 and July 21, 2012), the A_{max} rates on plot were higher than off plot for small piñon only ($p = 0.0174$ and $p = 0.00889$, respectively).

We also did not observe any evidence of competitive release in photosynthetic capacity in either species in the girdled plot following the girdling. Because all V_{cmax} measurements were made under well-watered conditions (corresponding to the conditions of highest A_{max} in Fig. 2.2), we compared all of the V_{cmax} measurements together. In small piñon, the mean photosynthetic capacities measured at the girdled plot were not significantly different from the mean capacities measured at the control plot (Fig. 2.3). We did observe a significant difference between the photosynthetic capacities in juniper between the two plots (Fig. 2.3), but the direction of the difference was not what we expected. The decrease, rather than increase, of photosynthetic capacity of juniper in the

girdled plot relative to the control plot suggests that instead of benefiting from competitive release, these trees were detrimentally affected by the girdling instead.

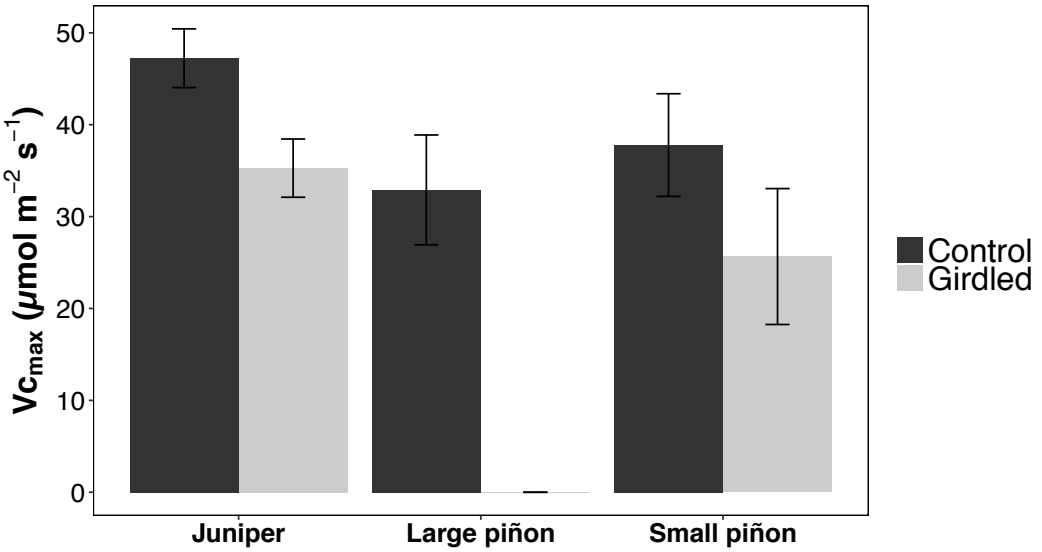

Figure 2.3: Photosynthetic capacity (represented by Vc_{max}) for juniper, small piñon and large piñon in the girdled and control plots. Mean +/- SE. Vc_{max} in juniper at the control plot was significantly higher than in the girdled plot ($p = 0.0124$).

2.3.3 Cavitation vulnerability response to simulated mortality

Both hydraulic conductivity and vulnerability to cavitation did not differ between trees at the girdled and control plots for either species (Fig. 2.4 – 2.6), suggesting that no acclimation in hydraulic architecture occurred in the remaining trees following piñon mortality. We found no significant difference in K_s (the hydraulic conductivity before air injection), P_{50} (the pressure at which 50% of hydraulic conductivity was lost), or in the air entry threshold P_e (the pressure at which runaway cavitation begins) between the girdled and control plot in piñon or juniper (Fig. 2.4 and 2.6). Both P_{50} and P_e were significantly less negative in piñon than in juniper, both at the girdled plot and the control plot (Fig. 2.6).

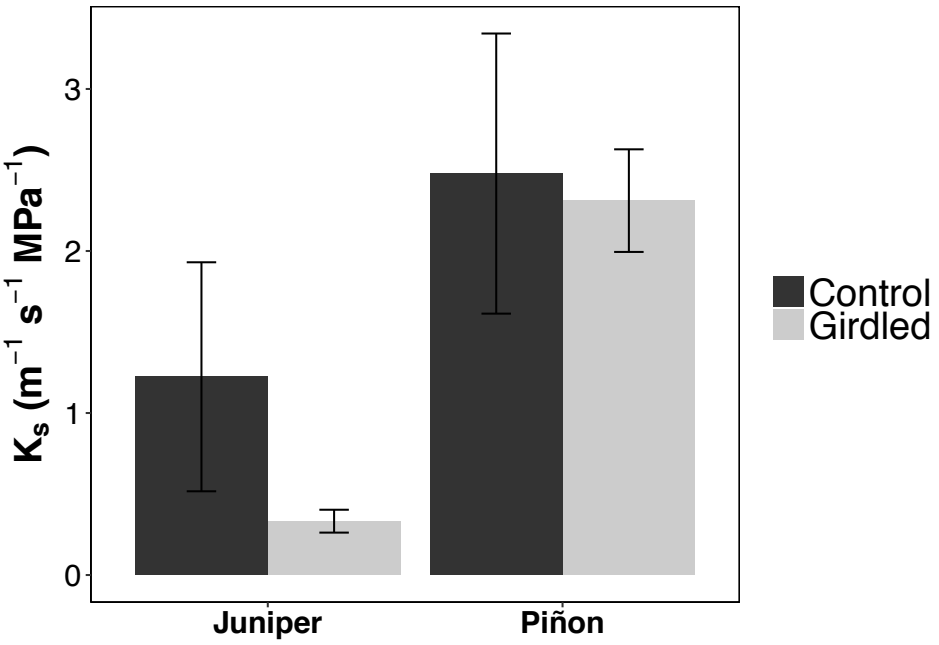

Figure 2.4: Sapwood-area specific hydraulic conductivity (K_s) for juniper and piñon in the girdled and control plots. Bars represent mean +/- standard error. K_s values were not significantly different between species or treatments ($p > 0.05$).

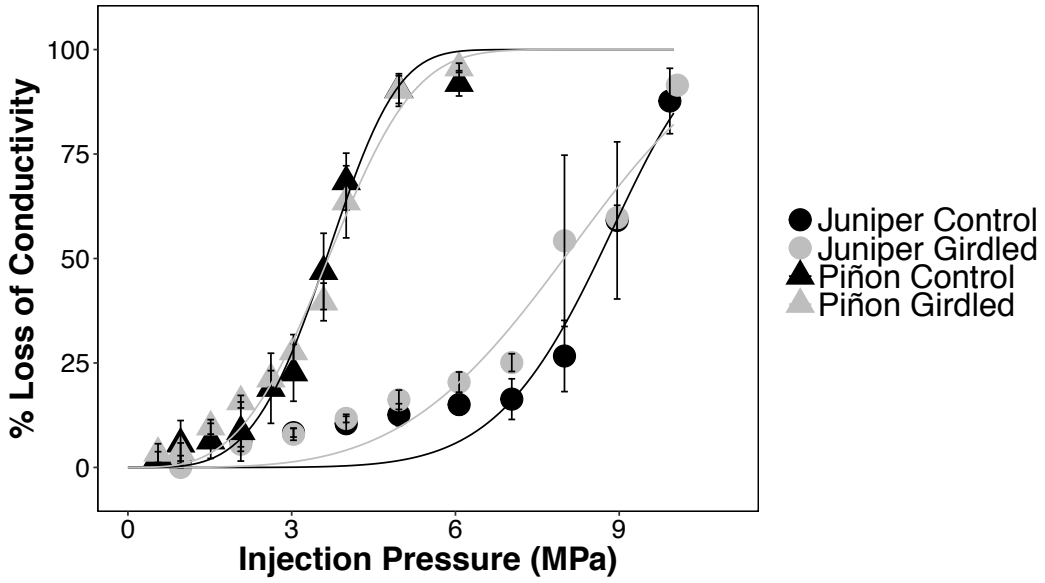

Figure 2.5: Vulnerability curves showing the % loss of conductivity for piñon and juniper in the girdled and control plots over a range of injection pressures. Points represent mean +/- standard error; lines represent the fitted Weibull function for each species and treatment

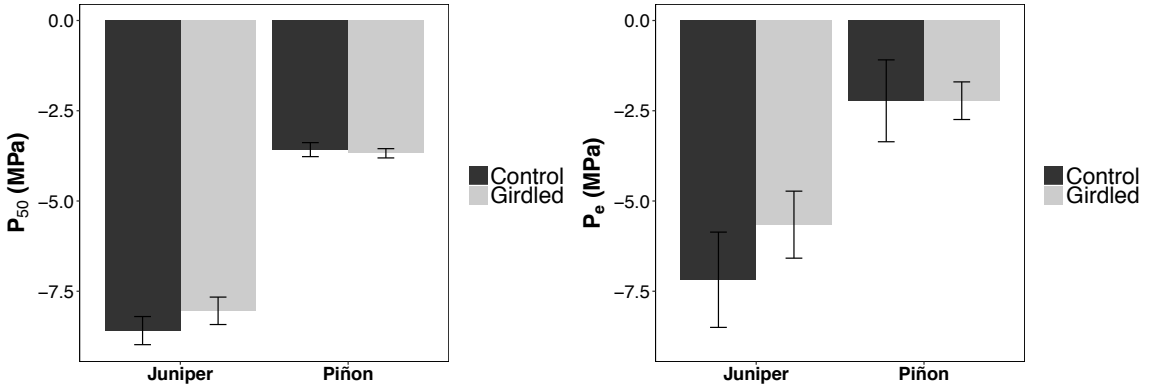

Figure 2.6: Water potential at which 50% of conductivity is lost (P_{50}, left), and the air entry threshold (P_e, right) for juniper and piñon in the girdled and control plots. Bars represent mean +/- standard error. P_{50} values were significantly less negative in piñon than juniper at both the girdled and control plots ($p < 0.005$ for both). P_e values were significantly less negative in piñon than juniper at both the girdled and control plots ($p < 0.005$ for both).

2.3.4 Changes in biomass at the girdled site

After the girdling in 2009, both live foliar and total piñon biomass decreased in both 2011 and 2012 (Fig. 2.7), indicating no recovery of piñon biomass in the years after mortality. Juniper live foliar and total biomass remained the same between 2009 and 2012, and slightly decreased in 2013 (Fig. 2.7).

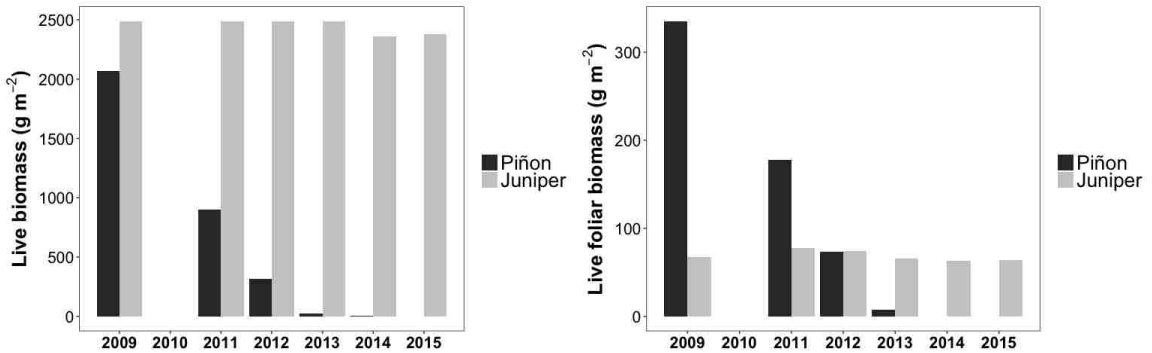

Figure 2.7: Total live and live foliar biomass for piñon and juniper at the girdled site from 2009-2012.

2.4 Discussion

As global climate changes, we expect to see an increase in the frequency and intensity of extreme drought (Overpeck and Udall 2010, Dai 2013), and widespread tree mortality (Breshears et al. 2005, Allen et al. 2010, Carnicer et al. 2011, Peng et al. 2011, Anderegg et al. 2016b), with large potential consequences for ecosystem structure and function (Rich et al. 2008, Royer et al. 2011, Lloret et al. 2012, Anderegg et al. 2016b, Morillas et al. 2017). One factor that will help determine the extent to which ecosystem structure and function are altered post-mortality is understanding how long it will take for these biomes to recover to their pre-disturbance state (Lloret et al. 2012, Anderegg et al. 2016b) or shift to a new vegetative state (Allen and Breshears 1998, Mueller et al. 2005). By imposing piñon mortality through girdling in a piñon-juniper woodland, we were able to simulate natural mortality that occurred in the Southwest US after the turn of the century and quantify organismal-level responses of surviving trees. We found very little evidence of competitive release in the remaining trees two years post-mortality. The lack of response may have been due to the open canopy structure of our system, which allowed soil evaporation to increase, limiting the amount of water available to the remaining tree competitors. It also may have been due to the severe drought that prevailed during our measurements. We suggest that the hotter and drier soil conditions in the two years following mortality were unfavorable for recovery of the system through competitive release or seedling recruitment. The observed lack of competitive release may have important implications for the recovery of these biomes, perhaps leading to a vegetation shift toward a juniper-dominated ecosystem.

2.4.1 Why didn't we observe competitive release in this system?

Although we predicted that the death of large piñon at the girdled site would have afforded the surviving trees greater access to resources such as nutrients, water, and light (Rich et al. 2008, Adams et al. 2010, Royer et al. 2011, Lloret et al. 2012, Anderegg et al. 2016b), soil conditions were both drier and hotter following mortality (Fig. 2.1, Morillas et al. 2017). Consistent with this measured decrease in water availability, we found very little evidence of competitive release in leaf or tree-level measurements in remaining juniper and small piñon following the mortality event. In addition, the lack of increase in either foliar or total biomass of the remaining trees (Fig. 2.7), or in gross primary productivity (GPP) at the girdled site following the girdling (Krofcheck et al. 2015) do not support competitive release. The decrease in photosynthetic capacity in juniper at the girdled site relative to the control site suggests that piñon mortality may even have had a detrimental effect on carbon sequestration. Morillas et al. (2017) also documented decreased sap flow in remaining juniper and small piñon in the girdled plot supporting a decrease in overall physiological activity in the remaining trees following piñon mortality.

Neither cavitation vulnerability nor conductivity changed in the remaining trees as soil water availability decreased following mortality in our study. In a nearby PJ woodland, Hudson et al. (2018) observed an increase in K_s in response to increased water availability, but no change in either K_s or vulnerability to cavitation under ambient or prolonged drought treatment. Taken together, these results suggest that K_s in these trees may be more sensitive than cavitation vulnerability to soil water availability, but K_s is more sensitive to an increase in soil water availability than drought.

We expected our system to respond to the imposed piñon mortality in an analogous manner to other tree-thinning studies (e.g. Simard et al. 2004, Pretzsch 2005, Schuler 2006, Martínez-Vilalta et al. 2007, Ward 2008), with increased growth rates in the remaining trees. However, most of these studies are from more mesic ecosystems with dense canopy cover. We suggest that the sparse canopy cover, typical of semi-arid biomes in general, reduced the potential for competitive release in our site. When mortality occurs, canopy loss increases the amount of light penetrating to the bare ground (Royer et al. 2011), which can, in turn, increase the amount of soil evaporation in those areas (Raz-Yaseef et al. 2010). The resulting increase in soil evaporation should be higher in ecosystems with sparser canopies (Raz-Yaseef et al. 2010). In this scenario, increased soil evaporation in response to canopy loss should decrease soil water availability, as we observed (Fig. 2.1, Morillas et al. 2017), contrary to our predictions of increased water availability. This decrease in soil water availability following canopy loss, and the resulting lack of competitive release, may be more common in semi-arid ecosystems where soil evaporation makes up a large part of the ecosystem water budget and the amount of water available for plant growth is already limiting (Raz-Yaseef et al. 2010, Morillas et al. 2017). At the girdled site, for example, 80% of evapotranspiration before girdling was already from non-canopy components, including soil (Morillas et al. 2017).

The drought that occurred in 2011 and 2012 may also have complicated any competitive release response to mortality (Anderegg et al. 2016b, Morillas et al. 2017). While some acclimation effects such as changes in photosynthetic capacity and/or cavitation vulnerability would be unlikely to have occurred immediately following

mortality in 2010, we might have been more likely to see an acclimation response in photosynthetic activity (as observed in response to different precipitation regimes by Limousin et al. (2013)) soon after mortality if soil water availability was higher.

Although we only focused on measuring competitive release in piñon and juniper, understory species (e.g. perennial forbs and grasses and annual forbs) may also have been able to take advantage of any temporary increases in water availability in the ecosystem (Huxman et al. 2005, Rich et al. 2008, Krofcheck et al. 2014, Morillas et al. 2017), particularly since their root systems are typically shallower than trees. We did observe an increased density of understory vegetation under dead piñon canopies during the wet 2010 monsoon season (Krofcheck et al. 2014), suggesting that increasing transpiration from understory species may be another factor that potentially decreased soil water availability and thus competitive release for the two tree species (Morillas et al. 2017).

2.4.2 Ecosystem consequences of mortality without competitive release

Absence of competitive release may hinder the potential recovery of piñon-juniper woodlands following severe drought and mortality. Many factors can affect ecosystem recovery from mortality disturbance, including spatial distribution of the mortality, climate following the mortality, and the size and functional role of the dead trees (Anderegg et al. 2016b). The severe drought that followed our imposed mortality event (Morillas et al. 2017) affected overall ecosystem water availability and likely, the opportunities for competitive release and seedling recruitment as well (Lloret et al. 2012, Stevens-Rumann et al. 2017). In addition, increased soil temperatures under dead piñon canopies relative to the control site with an intact piñon canopy (Fig. 2.1) could also

inhibit seedling recruitment (Adams et al. 2017a). Without the presence of increased seed source, recruitment, and increased growth in the remaining trees, recovery of the ecosystem will occur more slowly (Lloret et al. 2012, Anderegg et al. 2016b, Stevens-Rumann et al. 2017). In addition, following drought, we observed mortality of most of the remaining piñon at the girdled site, consistent with the suggestions of Mueller et al. (2005) that previous mortality in a piñon-juniper woodland may make that ecosystem more susceptible to additional mortality.

Our imposed mortality event (similar to the natural piñon mortality that occurred throughout the southwest in the early 2000's) removed only the large piñon trees (Mueller et al. 2005, Floyd et al. 2009). Large trees have a disproportionate effect on carbon storage for ecosystems and thus their mortality will affect carbon fluxes in ecosystems far more than the mortality of smaller trees (Slik et al. 2013, Anderegg et al. 2016b). Large trees may also function as both source plants and nurse plants for piñon seedlings, which establish at higher rates next to already established trees (Landis and Bailey 2005). The disproportionate loss of large trees could therefore provide an additional impairment to seedling recruitment.

The many impediments to seedling recruitment discussed above, and lack of a competitive release effect, increase the potential for a vegetation shift to occur in disturbed woodlands following large-scale piñon mortality (Allen and Breshears 1998, Mueller et al. 2005, Allen et al. 2010, Anderegg et al. 2016b, Stevens-Rumann et al. 2017). For example, without recruitment and regrowth of piñon, disturbed PJ woodlands ecosystems may transition to juniper-dominated woodlands or savannas. While juniper are considered more "drought-tolerant" species due to their anisohydric hydraulic

strategy (McDowell et al. 2008), the loss of diversity in a juniper-dominated ecosystem may make any subsequent disturbance harder to recover from (Anderegg et al. 2016b).

2.4.3 Conclusion

We observed very little evidence of competitive release following piñon mortality in a piñon-juniper woodland, in contrast to other studies in more mesic systems. We suggest that due to the semi-arid and sparse canopy nature of our system, the expected increase in plant water availability may not consistently occur post-mortality in these biomes, as much of this water is lost from soil evaporation or used by understory vegetation. It is possible that drought conditions shortly after the imposed mortality may have delayed the recovery trajectory by further impairing the possibility of a competitive release response. The conditions in piñon-juniper woodlands following mortality, including the loss of large trees that will reduce both nurse plants and the availability of new seeds, and hotter, drier soils under dead piñon canopies, may trigger a vegetation shift toward an ecosystem dominated by juniper.

Chapter 3

The sensitivity of semi-arid woody species to atmospheric drought and its dependence on both water availability and hydraulic strategy.

3.1 Introduction

In coming decades, global climate change is expected to increase the severity, duration, and spatial extent of drought (Overpeck and Udall 2010, Crausbay et al. 2017). These changes are predicted to increase the frequency of extreme drought, impacting ecosystem functioning (Jentsch et al. 2007), triggering plant mortality (Williams et al. 2013), and increasing landscape heterogeneity (Allen and Breshears 1998, Breshears et al. 2005, Allen et al. 2010, Peng et al. 2011, Anderegg et al. 2012). The severity and ecosystem impacts of drought will be determined by the interaction between two components of drought: soil moisture drought driven by changes in precipitation and measured as soil water content or potential (ψ_s), and atmospheric drought driven by increased atmospheric evaporative demand associated with warming temperatures and measured as vapor pressure deficit (VPD). Both components of drought can impact the function of ecosystems and individual trees, with effects ranging from diminished physiological function to widespread tree mortality (McDowell et al. 2008, Breshears et al. 2013, Eamus et al. 2013, Williams et al. 2013, Novick et al. 2016). Predictions of future precipitation, and hence soil moisture drought, are more uncertain than the effect of future temperatures on atmospheric drought (Burke and Brown 2008, Greve et al. 2014, Novick et al. 2016). Moreover, the progressive warming of the atmosphere will

likely lead to more frequent short-term decoupling of the two drought components as high VPD occurs even when soil moisture is high (Novick et al. 2016). It is therefore crucial to have a framework to predict not only the sensitivity of species and ecosystems to both components of drought, but also the potential interactions between them.

The hydraulic strategy of the dominant species in an ecosystem is one factor that may contribute to the relative sensitivities of ecosystems to the components of drought. Studies of drought responses have commonly identified tree species as isohydric or anisohydric. Isohydric species have been viewed as having tighter stomatal control during soil moisture drought, as evidenced by a relatively constant leaf water potential (ψ_l) over a wide range of ψ_s and VPD. Anisohydric species, on the other hand, continue to transpire as the soil dries, and stomata allow ψ_l to further decrease as drought progresses (Franks et al. 2007, McDowell et al. 2008, Domec and Johnson 2012, Martínez-Vilalta et al. 2014). Recent studies, however, have suggested that instead of two distinct categories of hydraulic strategy, a continuum of isohydric-to-anisohydric behavior is more appropriate (Klein 2014, Martínez-Vilalta et al. 2014). Furthermore, there is a growing body of evidence that suggests that isohydric-to-anisohydric behavior may not be as dependent on differences in stomatal control as previously thought, and instead, that soil-xylem hydraulics may play an important role in the observed patterns of stomatal regulation of transpiration (e.g. Martínez-Vilalta et al. 2014, Skelton et al. 2015, Garcia-Forner et al. 2016, Garcia-Forner et al. 2017, Martínez-Vilalta and Garcia-Forner 2017).

The relative impacts of atmospheric drought (high VPD) and soil moisture drought (low soil water potential, ψ_s) on the responses of plants with different hydraulic strategies can be explored using the supply-loss framework described in Sperry and Love

(2015) and Sperry et al. (2016). The supply component of the framework describes the extraction of water from the soil and transport to the transpiring canopy through the soil and plant as described by the whole-system hydraulic conductance of the plant (k) and canopy pressure (P). Transpiration (E) for a given value of P (i.e. the water supply function) can be calculated by integrating k through all the components of the soil-plant-atmosphere continuum. Along this supply function, E increases with decreasing P up to a critical point where the variation of E with respect to P approaches zero (i.e. $dE/dP = 0$) and the plant has reached its hydraulic limit (referred to as E_{crit} and P_{crit}). E can no longer increase above this critical point without inducing hydraulic failure (Sperry et al. 2002). As soil water potential (ψ_s) decreases (i.e. the pre-dawn P becomes more negative), the resulting supply function is progressively limited by a smaller k, because a more negative P is required to drive the transpiration stream along the soil-plant-atmosphere continuum. As a result, E_{crit} decreases as ψ_s decreases, eventually reaching zero when $\psi_s = P_{crit}$.

Stomatal regulation of E is determined by the loss function and its connection with the supply function in response to VPD and ψ_s (Sperry and Love 2015, Sperry et al. 2016). This suggests that the stomatal regulation of E is mainly governed by the soil-xylem hydraulics. For a given VPD, E decreases along the loss function with decreasing ψ_s. As VPD increases, E increases along the supply function but eventually saturates due to stomatal regulation, at which point further increases in VPD do not increase E (Sperry and Love 2015). Importantly, this framework primarily incorporates atmospheric drought at a short time scale, where high VPD can occur with low ψ_s, rather than at a longer time scale, where prolonged high VPD will decrease ψ_s over time (Breshears et al. 2013).

Based on the framework proposed by Sperry and Love (2015), the differences in cavitation vulnerability dictate the differences in how isohydric and anisohydric species respond to ψ_s and VPD. Isohydric plants are typically more vulnerable to cavitation than anisohydric plants. When compared with isohydric plants, anisohydric plants have supply functions where the dE/dP approaches zero at more negative values of P and loss functions that are less steep and converge on a single loss function at higher values of VPD. Accordingly, anisohydric plants have a relatively static stomatal sensitivity to VPD and ψ_s, while stomatal responses for isohydric plants can vary significantly with changing VPD and ψ_s (Sperry and Love 2015 Fig. 3).

To examine the responses of co-occurring isohydric and anisohydric species, we studied long-term tree water use in a piñon-juniper woodland, an ideal model system because the two dominant tree species exhibit very different hydraulic strategies. Piñon-juniper woodlands are one of the largest ecosystems in the Western US (West 1999), and have already experienced substantial mortality as a result of drought (Breshears et al. 2005, McDowell et al. 2008, Allen et al. 2010, Gaylord et al. 2013). Piñon (*Pinus sp.*) lies on the isohydric end of the spectrum and has xylem that is more vulnerable to cavitation, while juniper (*Juniperus sp.*) lies on the anisohydric end of the spectrum and has xylem that is more resistant to cavitation (Liebrecht chapter 2, Linton et al. 1998, McDowell et al. 2008). We used a 7-year time series of measured tree-level sap flow (J_s) and calculated canopy conductance (G_S) from a piñon-juniper woodland to examine the relative impacts of atmospheric and soil moisture drought, and interactions between them, on tree physiology. We also used the framework of Sperry and Love (2015) to

examine how the two dominant species respond to these two components of drought across the long-term range of variability in environmental conditions.

Adopting the framework proposed by Sperry and Love (2015), we hypothesized that the sensitivity of trees to these drought conditions would be dependent on their hydraulic strategy (isohydric vs. anisohydric), as dictated by soil-xylem hydraulics. Specifically, we predicted:

1) When soil moisture is abundant (ψ_s is high), juniper will increase J_s in response to increasing VPD with a larger slope than piñon, due to a less sensitive stomatal response.
2) Both piñon and juniper will decrease sap flow (J_s) and canopy conductance (G_s) in response to decreasing ψ_s, as predicted by the loss function. Isohydric piñon will decrease J_s and G_s with a more negative slope.
3) When ψ_s is low during soil moisture drought, both species will maintain a constant J_s rate in response to increasing VPD as the stomata close to prevent additional decreases in ψ_l.
4) Piñon canopy conductance (G_s) will decrease with a more negative slope than juniper G_s as VPD increases when ψ_s is high, but will decrease with a similar slope to juniper when ψ_s is low.

3.2 Methods

3.2.1 Study site

Our 4 ha study site is located on a mesa (elevation 2100 m) at 34.438450° N, -106.237694°W, just south of Mountainair, NM (Fig. 3.1). The site has two dominant tree

species, *Juniperus monosperma* (juniper) and *Pinus edulis* (piñon), with a mean canopy height of 2.8 m. The dominant understory vegetation includes the perennial C4 grass *Bouteloua gracilis* and the perennial shrub *Gutierrezia sarothrae*, as well as several cactus species and annual forbs.

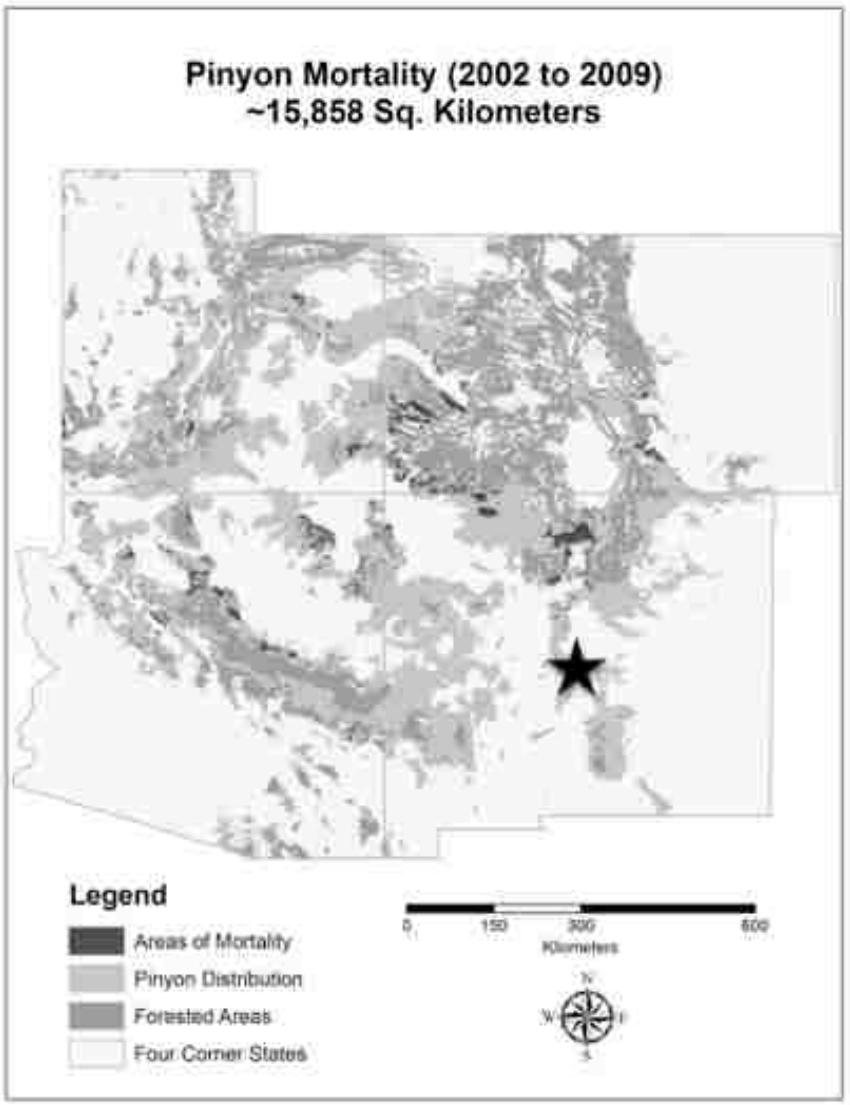

Figure 3.1. The extent of piñon-juniper woodlands and piñon mortality from 2002 to 2009 (from NAU-DIRENet) with our study site marked as the black star.

This site is characterized as semi-arid, with a 30-year mean annual precipitation (1981-2010, http://www.prism.oregonstate.edu) of 385.69 mm, 48% of which occurs

during the monsoon season (July-September), and 10% occurring during the shoulder season of October. Winter precipitation is primarily in the form of snow, in irregular events. The mean 30-year temperature was 10.6 °C, with a mean winter temperature (December-March) of 2.15 °C and a mean summer temperature (June-August) of 20.3 °C. During the study period (2010-2016), the site experienced typical monthly temperatures compared to the 30-year mean (Fig. 3.2). Of the seven years, only 2015 received more precipitation than the 30-year mean, and overall, the site had 13.6% less precipitation than the 30-year mean. In all years except 2015, the maximum vapor pressure deficit (VPD) was higher than the 30-year mean, an average of 21.6% higher across all years (Fig. 3.2). The site is fairly flat (< 3% slope), with soils of Turkey Springs stony loam, and a petrocalcic "caliche" layer (Morillas et al. 2017) from a soil depth of about 40 to about 80 cm.

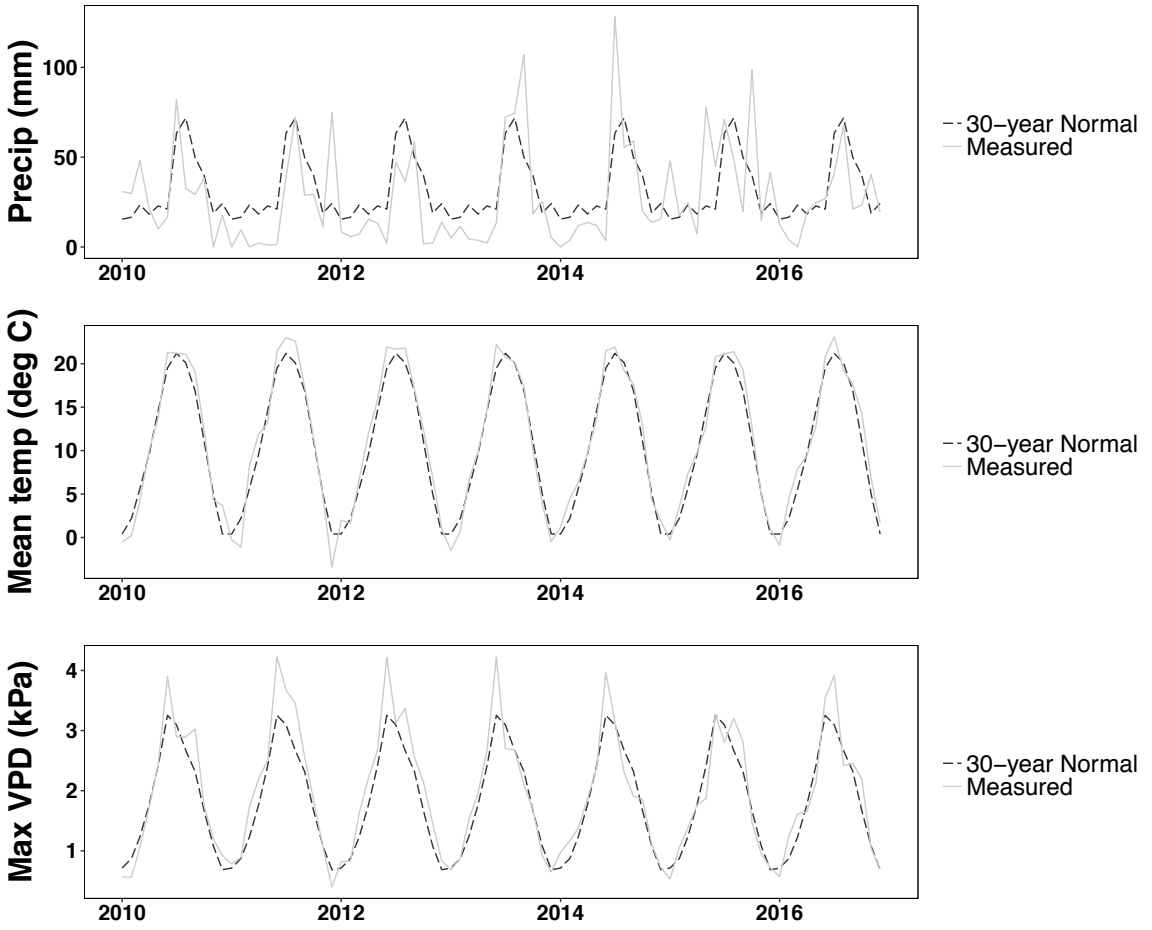

Figure 3.2. Monthly precipitation, mean temperature, and maximum VPD, over the 7 years of the study and the 30-year climate normal from 1981-2010. PRISM data from http://www.prism.oregonstate.edu.

3.2.2 Sap flow measurements

We measured sap flow every minute, compiled in 30-minute averages from five juniper (ranging from 12-45 cm root crown diameter) and five piñon (ranging from 14-24 cm diameter at breast height) at the study site, from 2010-2016. Sap flow was measured using modified 10 mm Granier heat dissipation sensors (Granier 1987) built at the University of New Mexico, with an additional reference thermocouple pair, as described by Plaut et al. (2013). These sensors, in addition to the typical heated and unheated

probes, have additional pair of probes, both unheated, installed 5 cm away horizontally from the first two probes, to account for temperature gradients in the stem (Goulden and Field 1994), which is very important in the high light conditions (Pangle et al. 2012, Plaut et al. 2013), present in our study site. We installed two sets of sensors into the outermost sapwood of each tree, both at >1 m above the ground, and covered them with reflective insulation both for protection and to help mitigate the high light conditions. We recorded average temperature differences between the heated and reference probes every 30 minutes using a CR23X data logger (Campbell Scientific, Logan, Utah, USA), and applied real-time corrections for temperature gradients in the stem that might confound the measurement (Goulden and Field 1994). We replaced the sensors every 1-2 years, after installation, in August 2011, July 2012, July 2013, and March 2014.

We filtered data for instrument failure and noise, as well as for minimum temperatures below -2 Celsius. We estimated sap flow J_s (g m^{-2} s^{-1}) at each 30 minute interval according to Granier (1987). We averaged the sap flow values for the two sensors at each tree so we had one set of sap flow values for each of the five trees. For the purposes of this analysis, we only used sap flow data from April-September (the growing season) of each year. We gap filled any short missing periods (less than half a day) using a spline function, averaged all of the 30 minute sap flow values for each day, and converted to a daily J_s (kg m^{-2} day^{-1}).

3.2.3 Climate metrics

We measured soil water content below three piñon and below three juniper at 5, 10 and 30 cm soil depth using CS610 soil moisture sensors (Campbell Scientific, Logan,

Utah, USA), starting in 2008. We were unable to measure at deeper soil levels due to the "caliche" layer. In 2015, using co-located TM229-SMM soil water matric potential sensors (ICT International, Armidale, Australia), we measured soil water potential at 10 and 30 cm and used an exponential equation to compare soil water content and soil water potential. We used that equation ($SWP = -19.798*e^{(-37.29*SWC)}$) to convert soil water content from previous years to soil water potential values. We calculated integrated soil water potential across the different soil layers for each 30-minute interval. We used the 5 cm value of soil water potential to approximate the soil water potential of the soil column from 0-7.5 cm, the 10 cm value to approximate from 7.5-22.5 cm, and the 30 cm value to approximate from 22.5-40 cm. We used this integrated daily soil water potential value for all subsequent analyses.

We used HMP60 probes (Vaisala, Helsinki, Finland) placed at a height of 10 m to measure temperature and relative humidity, and calculated VPD at 30-minute intervals from 2008-2016. For our analysis, we used the mid-day average VPD value for each day. We looked at the correlation of VPD and soil water potential on different timescales from hourly to seasonal, and determined that the correlation between the two was fairly low (< 0.4) on the daily timescale (Fig. 3.3). This demonstrated decoupling on the time scale used for our study justifies studying the response to each metric separately in our analysis.

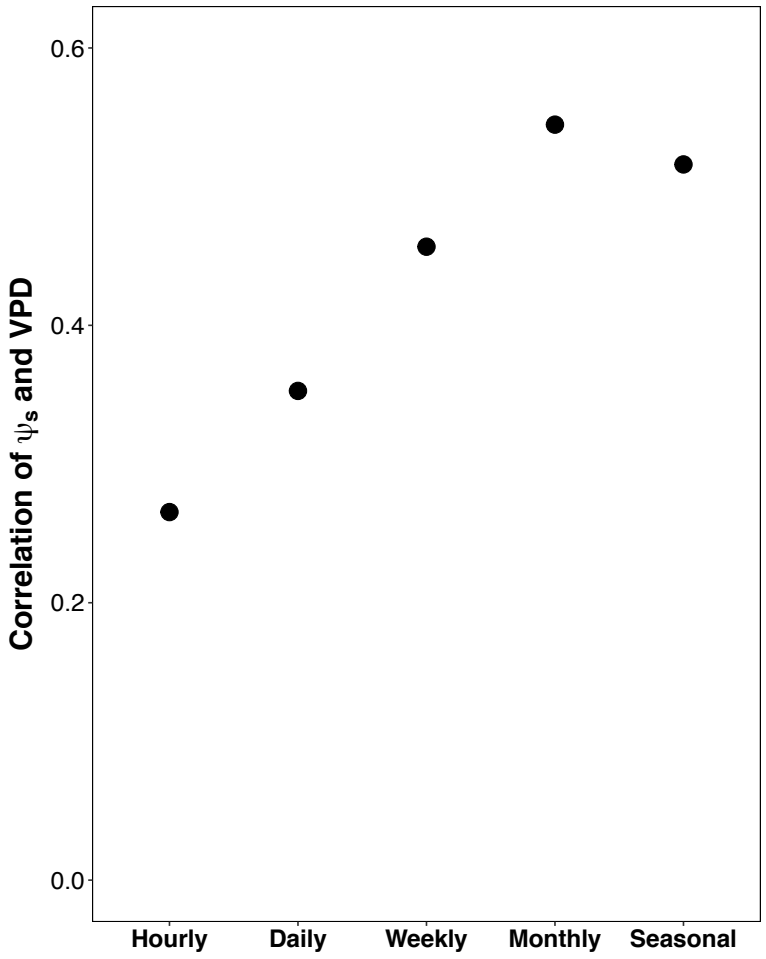

Figure 3.3. Correlation coefficients of VPD (kPa) and integrated soil water potential (MPa) over different time scales at our site.

3.2.4 Statistical analysis

We used RStudio for all data analysis (version 1.1.423). To analyze sap flow response to VPD, we separated data into five categories based on soil water potential. To choose categories of equal size, we calculated percentiles of the full range of measured soil water potential (0-20%, 20-40%, 40-60%, 60-80%, and 80-100%), which resulted in the following categories: 1) extremely dry (< -2.24 MPa), 2) very dry (between -2.24 MPa and -1.88 MPa), 3) moderately dry (between -1.88 MPa and -1.15 MPa), 4) moderately wet (between -1.15 MPa and -0.49 MPa), and 5) wet (> -0.49 MPa). Within

each category, we binned data by VPD, creating VPD bins that were 0.2 kPa wide. For data in each category, we described the response of sap flow to VPD by fitting linear mixed effects models for each species using the nlme package (Pinheiro et al. 2014). We used daily sap flow as the response variable, maximum daily VPD as the fixed effect, and the tree number as a random effect. We used an ANOVA to compare models with and without interaction between the soil water potential category and VPD to determine whether there was a significant difference between the responses in different categories within each species. In addition, we used ANOVAs to compare models with and without interaction between the species and VPD to determine whether there was a significant difference between the responses of the two species within each soil water potential category. We also compared species responses by using pairwise comparisons to compare the daily sap flow of the two species within each bin.

To analyze sap flow response to soil moisture drought, we followed a similar process. We first separated data into three categories based on VPD. As suggested by Novick et al. (2016), we removed any days with VPD < 1 from our analysis. We chose the categories to highlight the effect of extreme VPD, using percentiles of our range of VPD (0-50%, 50-90%, and 90-100%). This division resulted in the following categories: 1) low VPD (between 1 and 2.06 MPa), 2) moderate VPD (between 2.06 and 3.01 kPa) and 3) high VPD (> 3.01 kPa). Within each category, we binned data by soil water potential, creating bins that were 0.2 MPa wide. For data in each category, we described the response of sap flow to soil water potential by fitting exponential mixed effects models for each species using daily sap flow as the response variable, average daily soil water potential as the fixed effect, and the tree number as a random effect. We used an

ANOVA to compare models with and without interaction between the VPD category and soil water potential to determine whether there was a significant difference between the responses in different categories within each species. In addition, we used ANOVAs to compare models with and without interaction between the species and soil water potential to determine whether there was a significant difference between the responses of the two species within each VPD category. We also compared species responses by using pairwise comparisons to compare the daily sap flow of the two species within each bin.

To analyze the combined effects high VPD and low soil moisture on the two species, we adapted the methods of Novick et al. (2016) and (Oren et al. 1999) to look at the relative sensitivities of canopy conductance (G_s) to VPD and soil water potential. We calculated canopy conductance from sap flow and VPD for each 30-minute interval according to Oren et al. (1998), assuming that leaf area (LA) to sapwood area (SA) ratios remained constant over the time of the study (0.195 m^2 LA/cm^2 SA for piñon, 0.236 m^2 LA/cm^2 SA for juniper). We calculated a daily mean canopy conductance from the 30-minute data and binned this data by soil water potential and VPD. For the soil water potential bins, we used percentiles of the full range of measured soil water potential, with bins of 0-20%, 20-40%, 40-60%, 60-80%, and 80-100%. Within each soil water potential bin, we further binned by VPD, with each VPD bin having a width of 0.2 kPa. Following Novick et al. (2016), we did not use any data with a VPD below 1. Additionally, we did not include in our analysis any VPD bin that did not have at least 5 data points within it. We averaged data within each VPD bin and following Oren et al. (1999) and Novick et al. (2016) fitted data within each soil water potential bin to the equation:

$$G_s = G_{s,ref} - m \ln(VPD) \quad (1)$$

We compared the effect of soil water potential on each species by looking at how the intercept ($G_{s,ref}$) of Eq. 1 varied across different soil water potentials. We compared the effect of VPD on each species by looking at how the slope (m) of Eq. 1 varied across different soil water potentials.

3.3 Results

3.3.1 Piñon and juniper sap flow responses to soil moisture drought and high VPD

In both species, daily sap flow decreased exponentially as ψ_s decreased (Fig 3.4, Table 3.1). In piñon, VPD did not alter the nature of the decline in J_s with ψ_s ($p = 0.118$; Fig. 3.4A). In contrast, the rate of decrease of J_s in juniper as soil water availability decreased was steeper at higher VPD ($p = 0.0004$, Fig. 3.4B).

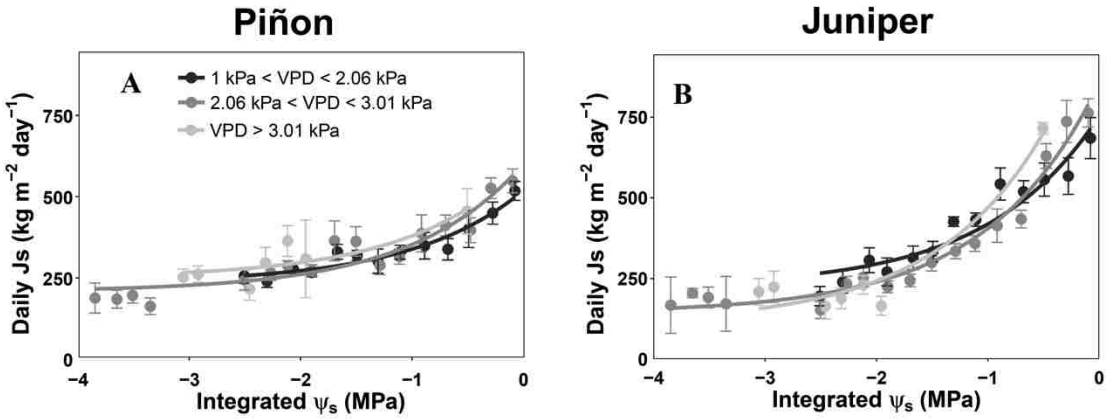

Figure 3.4. Daily J_s in response to changes in ψ_s, separated based on VPD in Piñon (A) and Juniper (B).

Table 3.1. Equations for piñon and juniper daily J_s (kg m^{-2} day^{-1}) response to changing VPD (kPa) and integrated soil water potential (ψ_s) (MPa).

Piñon equations fit with the form: daily J_s = m*VPD + b				
Category	m	b	p-value	R^2
ψ_s < -2.24 MPa	-8.81	245	0.454	0.072
- 2.24 MPa < ψ_s < -1.88 MPa	13.4	242	0.478	0.065
-1.88 MPa < ψ_s < -1.15 MPa	28.2	263	0.172	0.219
-1.15 MPa < ψ_s < -0.49 MPa	-18.1	391	0.565	0.058
ψ_s > -0.49 MPa	-7.82	515	0.739	0.015
Juniper equations fit with the form: daily J_s = m*VPD + b				
Category	m	b	p-value	R^2
ψ_s < -2.24 MPa	-20.3	253	0.189	0.205
- 2.24 MPa < ψ_s < -1.88 MPa	-38.5	331	0.157	0.233
-1.88 MPa < ψ_s < -1.15 MPa	-54.1	431	3.7e-3*	0.673
-1.15 MPa < ψ_s < -0.49 MPa	-62.9	598	0.085	0.415
ψ_s > -0.49 MPa	70.2	547	7.19e-4*	0.779
Piñon equations fit with the form: daily J_s = m*exp(ψ_s) + b				
Category	m	b	p-value	R^2
1 kPa < VPD < 2.06 kPa	286	234	8.91e-8*	0.932
2.06 kPa < VPD < 3.01 kPa	394	208	2.59e-8*	0.881
VPD > 3.01 kPa	353	250	0.012*	0.749
Juniper equations fit with the form: daily J_s = m*exp(ψ_s) + b				
Category	m	b	p-value	R^2
1 kPa < VPD < 2.06 kPa	532	224	8.63e-7*	0.898
2.06 kPa < VPD < 3.01 kPa	713	144	8.04e-13*	0.970
VPD > 3.01 kPa	974	112	3.50e-4*	0.937

Juniper daily J_s was also more sensitive to VPD, but the response was dependent on soil water availability (Fig. 3.4D, Table 3.1, p = 7.55e-5). In relatively wet soils (ψ_s > -0.49 MPa), daily J_s increased significantly in response to increasing VPD (Fig. 3.5B, p = 7.19e-4). Daily J_s did decrease slightly at ψ_s between -1.88 and -1.15 MPa (Fig. 3.5B, p = 0.0037), but overall, higher VPD had little to no effect during dry ψ_s conditions. Piñon J_s did not change with VPD at any ψ_s (Fig. 3.5A, Table 3.1).

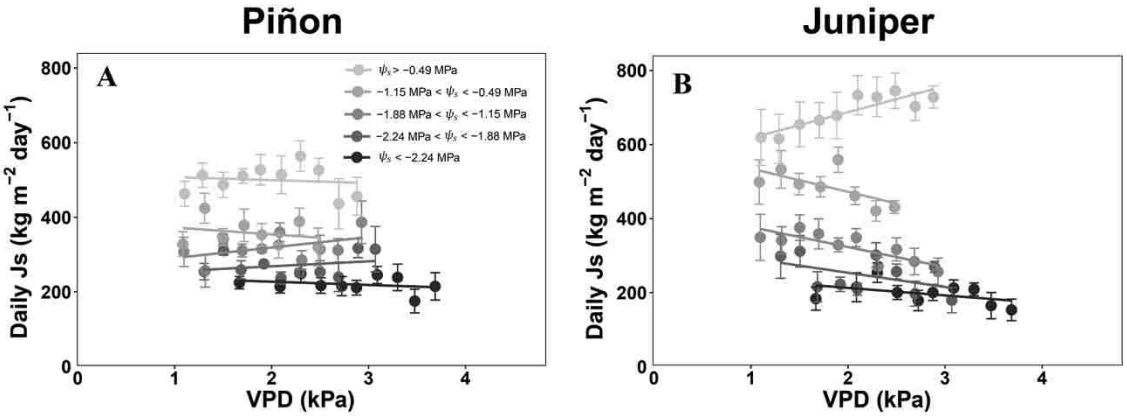

Figure 3.5. Daily J_s in response to changes in VPD, separated based on ψ_s in Piñon (A) and Juniper (B).

3.3.2 Comparing piñon vs. juniper sap flow responses to soil moisture drought and high VPD

Regardless of VPD, juniper daily J_s rates were significantly higher than piñon J_s at the wettest ψ_s values (Fig. 3.6) and decreased with a steeper slope in response to decreasing ψ_s compared to piñon (Table 3.2). J_s rates were similar in both species at very negative ψ_s, indicating that when soil moisture drought was strong enough, the two species responded similarly. However, piñon daily J_s rates plateaued to their minimum value at a slightly less negative ψ_s than juniper, particularly in high VPD conditions (Fig. 3.6).

Table 3.2. Comparing piñon and juniper daily J_s (kg m^{-2} day^{-1}) within different categories of VPD (kPa).

Piñon and juniper daily J_s comparisons		
VPD category	ψ_s category	p-value
1 kPa < VPD < 2.06 kPa	-2.6 MPa < ψ_s < -2.4 MPa	0.272
	-2.4 MPa < ψ_s < -2.2 MPa	0.998
	-2.2 MPa < ψ_s < -2 MPa	0.541
	-2 MPa < ψ_s < -1.8 MPa	0.937
	-1.8 MPa < ψ_s < -1.6 MPa	0.761
	-1.6 MPa < ψ_s < -1.4 MPa	0.788
	-1.4 MPa < ψ_s < -1.2 MPa	0.016*
	-1.2 MPa < ψ_s < -1 MPa	0.045*
	-1 MPa < ψ_s < -0.8 MPa	2.50e-4*
	-0.8 MPa < ψ_s < -0.6 MPa	5.90e-4*
	-0.6 MPa < ψ_s < -0.4 MPa	2.82e-3*
	-0.4 MPa < ψ_s < -0.2 MPa	0.022*
	ψ_s > -0.2 MPa	1.40e-3*
2.06 kPa < VPD < 3.01 kPa	-4 MPa < ψ_s < -3.8 MPa	0.760
	-3.8 MPa < ψ_s < -3.6 MPa	0.698
	-3.6 MPa < ψ_s < -3.4 MPa	0.935
	-3.4 MPa < ψ_s < -3.2 MPa	0.895
	-2.6 MPa < ψ_s < -2.4 MPa	0.098
	-2.4 MPa < ψ_s < -2.2 MPa	0.523
	-2.2 MPa < ψ_s < -2 MPa	0.499
	-2 MPa < ψ_s < -1.8 MPa	0.321
	-1.8 MPa < ψ_s < -1.6 MPa	0.022*
	-1.6 MPa < ψ_s < -1.4 MPa	0.201
	-1.4 MPa < ψ_s < -1.2 MPa	0.344
	-1.2 MPa < ψ_s < -1 MPa	0.374
	-1 MPa < ψ_s < -0.8 MPa	0.574
	-0.8 MPa < ψ_s < -0.6 MPa	0.628
	-0.6 MPa < ψ_s < -0.4 MPa	4.35e-6*
	-0.4 MPa < ψ_s < -0.2 MPa	2.90e-5*
	ψ_s > -0.2 MPa	2.03e-5*
VPD > 3.01 kPa	-3.2 MPa < ψ_s < -3 MPa	0.475
	-3 MPa < ψ_s < -2.8 MPa	0.534
	-2.6 MPa < ψ_s < -2.4 MPa	0.366
	-2.4 MPa < ψ_s < -2.2 MPa	0.064
	-2.2 MPa < ψ_s < -2 MPa	0.017*
	-2 MPa < ψ_s < -1.8 MPa	0.049*
	-0.6 MPa < ψ_s < -0.4 MPa	3.20e-5*

Piñon and juniper modeled fit comparison	
VPD category	p-value
1 kPa < VPD < 2.06 kPa	3.81e-4*
2.06 kPa < VPD < 3.01 kPa	4.20e-7*
VPD > 3.01 kPa	1.63e-3*

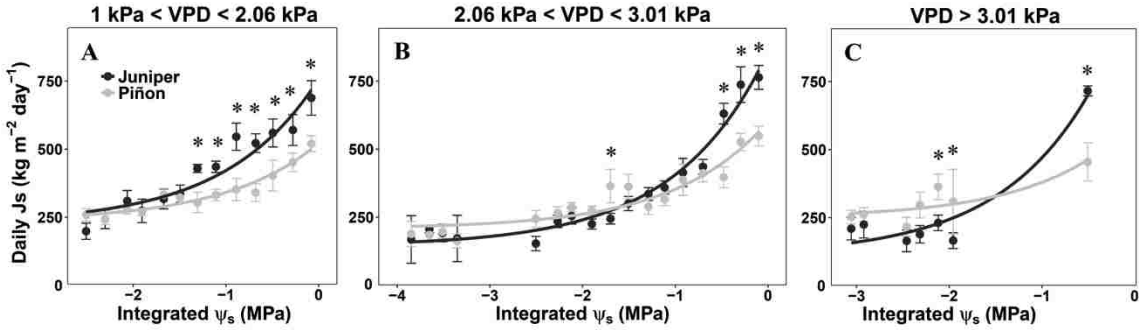

Figure 3.6. Species-specific daily J_s in response to changes in ψ_s in three different VPD categories (A-C). Asterisks indicate a significant difference between the species for each point.

For most ψ_s conditions, both piñon and juniper J_s rates did not respond to increasing VPD (Fig. 3.7B, D, and E). However, when ψ_s was very high (> -0.49 MPa), J_s in juniper increased with increasing VPD, while J_s in piñon did not change (Fig. 3.7A, Table 3.3). Additionally, during conditions of ψ_s between -1.88 and -1.15 MPa, J_s in juniper slightly decreased with increasing VPD, but J_s in piñon did not change (Fig. 3.7C, Table 3.3). Juniper J_s rates were higher than piñon J_s in most VPD conditions when ψ_s was above -1.15 MPa (Fig. 3.7A, B, Table 3.3). Thus, when the soil was wet, juniper was performing at a higher level of physiological function than piñon. However, when the soil was dry (< -1.15 MPa), there were no differences between juniper and piñon J_s rates for most VPD conditions (Fig. 3.7C-E, Table 3.3).

Table 3.3. Comparing piñon and juniper daily J_s (kg m^{-2} day^{-1}) within different categories of integrated soil water potential (ψ_s) (MPa).

Piñon and juniper daily Js comparisons		
ψ_s category	VPD category	p-value
ψ_s < -2.24 MPa	1.6 kPa < VPD < 1.8 kPa	0.270
	2 kPa < VPD < 2.2 kPa	0.992
	2.2 kPa < VPD < 2.4 kPa	0.889
	2.4 kPa < VPD < 2.6 kPa	0.656
	2.6 kPa < VPD < 2.8 kPa	0.324
	2.8 kPa < VPD < 3 kPa	0.768
	3 kPa < VPD < 3.2 kPa	0.375
	3.2 kPa < VPD < 3.4 kPa	0.423
	3.4 kPa < VPD < 3.6 kPa	0.785
	3.6 kPa < VPD < 3.8 kPa	0.123
- 2.24 MPa < ψ_s < -1.88 MPa	1.2 kPa < VPD < 1.4 kPa	0.304
	1.4 kPa < VPD < 1.6 kPa	0.983
	1.6 kPa < VPD < 1.8 kPa	0.310
	1.8 kPa < VPD < 2 kPa	0.216
	2 kPa < VPD < 2.2 kPa	0.510
	2.2 kPa < VPD < 2.4 kPa	0.293
	2.4 kPa < VPD < 2.6 kPa	0.928
	2.6 kPa < VPD < 2.8 kPa	0.316
	2.8 kPa < VPD < 3 kPa	0.265
	3 kPa < VPD < 3.2 kPa	7.10e-3*
-1.88 MPa < ψ_s < -1.15 MPa	1 kPa < VPD < 1.2 kPa	0.410
	1.2 kPa < VPD < 1.4 kPa	0.100
	1.4 kPa < VPD < 1.6 kPa	0.477
	1.6 kPa < VPD < 1.8 kPa	0.324
	1.8 kPa < VPD < 2 kPa	0.781
	2 kPa < VPD < 2.2 kPa	0.808
	2.2 kPa < VPD < 2.4 kPa	0.763
	2.4 kPa < VPD < 2.6 kPa	0.965
	2.6 kPa < VPD < 2.8 kPa	0.562
	2.8 kPa < VPD < 3 kPa	8.30e-3*
-1.15 MPa < ψ_s < -0.49 MPa	1 kPa < VPD < 1.2 kPa	1.71e-3*
	1.2 kPa < VPD < 1.4 kPa	0.041*
	1.4 kPa < VPD < 1.6 kPa	6.69e-3*
	1.6 kPa < VPD < 1.8 kPa	0.043*
	1.8 kPa < VPD < 2 kPa	2.00e-4*
	2 kPa < VPD < 2.2 kPa	0.011*
	2.2 kPa < VPD < 2.4 kPa	0.537
	2.4 kPa < VPD < 2.6 kPa	0.037*
ψ_s > -0.49 MPa	1 kPa < VPD < 1.2 kPa	0.027*
	1.2 kPa < VPD < 1.4 kPa	0.143
	1.4 kPa < VPD < 1.6 kPa	0.018*
	1.6 kPa < VPD < 1.8 kPa	0.028*
	1.8 kPa < VPD < 2 kPa	0.032*
	2 kPa < VPD < 2.2 kPa	2.30e-3*
	2.2 kPa < VPD < 2.4 kPa	0.020*
	2.4 kPa < VPD < 2.6 kPa	2.20e-3
	2.6 kPa < VPD < 2.8 kPa	2.40e-4*
	2.8 kPa < VPD < 3 kPa	1.80e-4*

Piñon and juniper modeled fit comparison	
ψ_s category	p-value
ψ_s < -2.24 MPa	0.534
- 2.24 MPa < ψ_s < -1.88 MPa	0.108
-1.88 MPa < ψ_s < -1.15 MPa	2.60e-3*
-1.15 MPa < ψ_s < -0.49 MPa	0.315
ψ_s > -0.49 MPa	8.96e-4*

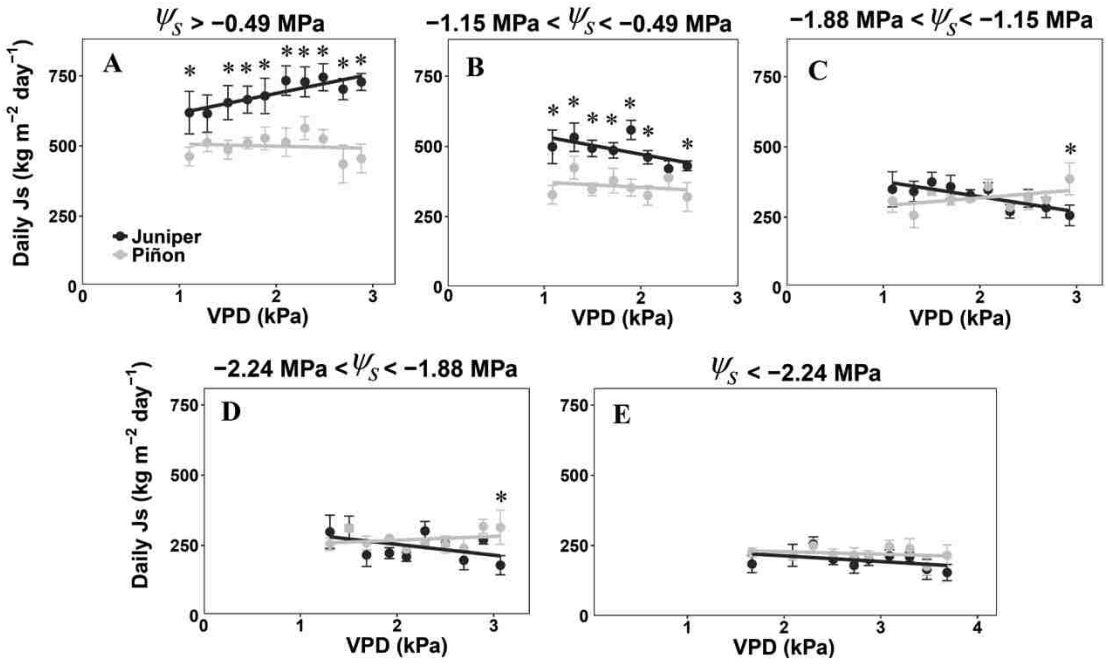

Figure 3.7. Species-specific daily J_s in response to changes in VPD in five different ψ_s categories (A-E). Asterisks indicate a significant difference between the species for each point.

3.3.3 Sensitivity of canopy conductance to high VPD and soil moisture drought

Piñon and juniper stomatal dynamics in response to both VPD and ψ_s were very similar. In both species, G_s decreased exponentially as VPD increased across all ψ_s conditions (Fig. 3.8A, B, Table 3.4). This decrease in G_s in both species was most pronounced in wetter soils (> -0.24 MPa), which suggests that the effects of high VPD on G_s are minimal as soil moisture decreases.

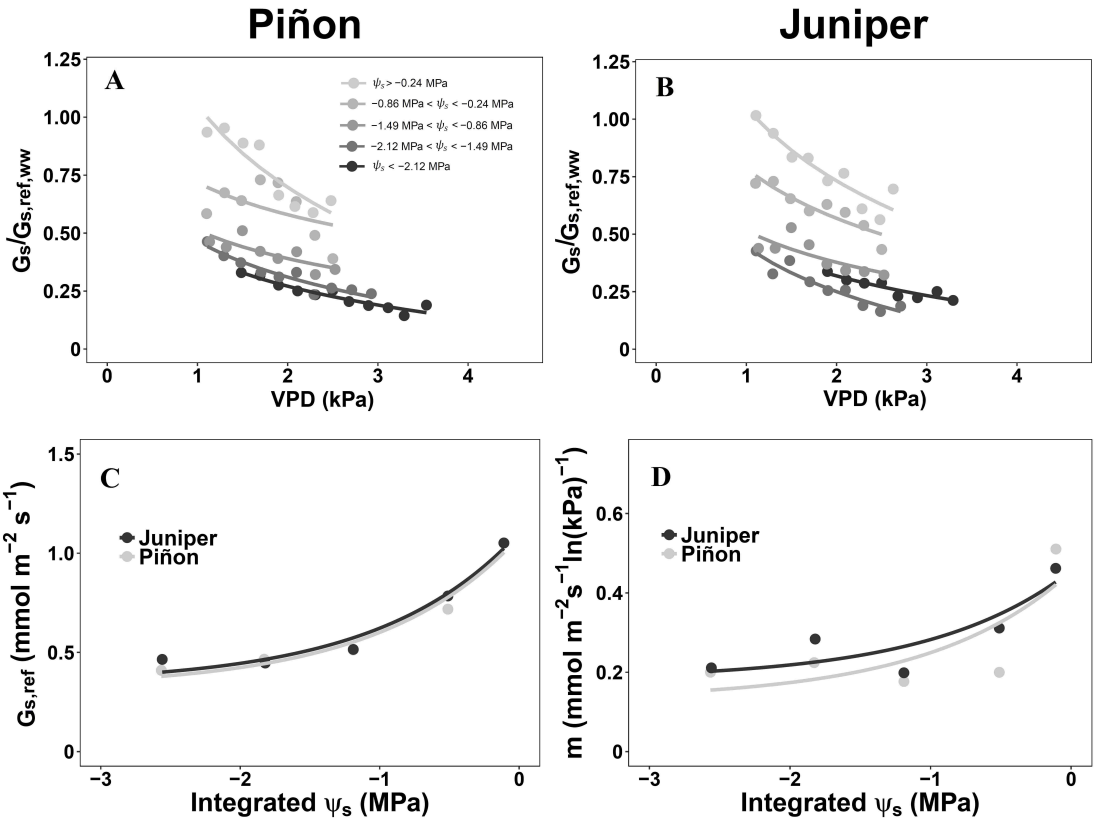

Figure 3.8. Calculated ratio of canopy conductance (G_s) to a well-watered reference ($G_{s,ref,ww}$) in response to VPD, separated based on ψ_s in Piñon (A) and Juniper (B), with points fit to Eq. 1. Species-specific $G_{s,ref}$ in response to ψ_s (C). Species-specific m in response to ψ_s (D).

The reference conductance values ($G_{s,ref}$) were consistently similar in both species across the full range of ψ_s (Fig. 3.8C). $G_{s,ref}$, as the y-intercept of Eq. 2, helps describe the sensitivity of G_s to ψ_s. The similarity in $G_{s,ref}$ between species suggests that the maximum leaf-specific G_s that each species can achieve under the various ψ_s conditions are the same. The sensitivity of $G_{s,ref}$ to decreasing ψ_s (soil moisture drought) (Fig. 3.8C, Table 3.4) was also very similar in both species, which indicates that G_s in both species is limited by ψ_s, and that the magnitude of that limitation is the same.

Table 3.4. Piñon and juniper canopy conductance (G_s) (mmol CO_2 m^{-2} leaf area s^{-1}) response to VPD (kPa) and sensitivity to VPD and integrated soil water potential (ψ_s) (MPa).

Piñon equations fit with the form: $G_s = G_{s,ref} - m*\ln(VPD)$			
ψ_s category	$G_{s,ref}$	m	p-value
ψ_s < -2.12 MPa	0.410	0.200	4.68e-6*
-2.12 MPa < ψ_s < -1.49 MPa	0.466	0.224	1.29e-5*
-1.49 MPa < ψ_s < -0.86 MPa	0.513	0.177	0.017*
-0.86 MPa < ψ_s < -0.24 MPa	0.718	0.200	0.218
ψ_s > -0.24 MPa	1.05	0.511	1.52e-3*

Juniper equations fit with the form: $G_s = G_{s,ref} - m*\ln(VPD)$			
ψ_s category	$G_{s,ref}$	m	p-value
ψ_s < -2.12 MPa	0.465	0.211	1.16e-3*
-2.12 MPa < ψ_s < -1.49 MPa	0.446	0.284	1.06e-4*
-1.49 MPa < ψ_s < -0.86 MPa	0.515	0.199	0.027*
-0.86 MPa < ψ_s < -0.24 MPa	0.785	0.312	1.26e-3*
ψ_s > -0.24 MPa	1.05	0.462	2.02e-4*

Modeled fits with the form: $G_{s,ref} = a*\exp(\psi_s) + b$				
Species	a	b	p-value	R^2
Piñon	0.762	0.321	2.46e-3*	0.968
Juniper	0.762	0.342	2.48e-3*	0.968

Modeled fits with the form: $m = a*\exp(\psi_s) + b$				
Species	a	b	p-value	R^2
Piñon	0.324	0.130	0.116	0.615
Juniper	0.275	0.181	5.01e-2	0.771

Comparing piñon and juniper modeled fits for $G_{s,ref}$ and m	
Parameter	p-value
$G_{s,ref}$	0.999
m	0.783

The slope of Eq. 2 (m) describes the sensitivity of G_s to VPD. The similarity in m values between the two species across the full range of ψ_s (Fig. 3.8D) suggests that leaf-specific G_s in both species is similarly sensitive to VPD. In addition, m in both species is similarly sensitive to decreasing ψ_s (soil moisture drought) (Fig. 3.8D, Table 3.4), which indicates that both species are regulating ψ_l similarly in response to soil moisture drought.

3.4 Discussion

We set out to compare the responses of the two dominant species in a piñon-juniper woodland to test for differences between the response of an isohydric species (piñon) and an anisohydric species (juniper) to long-term variation in low soil water potential (ψ_s) associated with soil moisture drought and vapor pressure deficit (VPD) between leaves and the atmosphere. Our seven-year time series of sap flux (J_s), coupled with measurements of soil and atmospheric conditions, spanned sufficient variation in both ψ_s and VPD to characterize how each species responded. Using the conceptual framework of Sperry and Love (2015), we were able to explain some of the observed behavior of piñon and juniper to low ψ_s and high VPD on a daily time scale. For example, juniper J_s increased in response to increasing VPD more steeply than piñon J_s when ψ_s was high, but both juniper and piñon maintained constant J_s rates in response to increasing VPD when ψ_s was low, as predicted by the framework. While the framework explained some species differences, it also pointed out some important limitations of the classically defined dichotomy of isohydry vs. anisohydry.

3.4.1 Does hydraulic strategy accurately predict species responses to these components of drought?

We predicted that hydraulic strategy (isohydry vs. anisohydry) would influence the sensitivity of piñon and juniper to atmospheric and soil moisture drought. Following the framework proposed by Sperry and Love (2015), we predicted that piñon transpiration rates (as represented in this study by J_s) would decrease faster in response to soil moisture drought (low ψ_s) than juniper, given that it is considered an isohydric

species and should close its stomata at a lower ψ_s to avoid E_{crit}. We further predicted that when ψ_s became very low, J_s rates in the two species would be similarly low. Although J_s rates did converge between the two species when ψ_s was low, as expected, J_s rates in juniper declined more steeply than J_s in piñon in response to decreasing ψ_s, contrary to what the framework predicted. This steeper response was a result of juniper J_s rates being higher than piñon J_s at high ψ_s and similar to piñon J_s at low ψ_s. The relatively low J_s rates in piñon when ψ_s was high could have been due to higher rates of chronic embolism in piñon, as previously demonstrated by Garcia-Forner et al. (2016). Alternatively, piñon could have hydraulically isolated its roots from the soil to prevent water loss, which has been observed in several isohydric species, including piñon (Limousin et al. 2009, Plaut et al. 2013, Mackay et al. 2015).

We also predicted that juniper and piñon J_s rates would be differentially sensitive to high VPD based on their differing hydraulic strategies. As we predicted, when ψ_s was high, J_s in juniper increased with VPD. When ψ_s was low, both species maintained constant rates of J_s across a range of VPD, which was also consistent with our prediction, likely because their stomata were maximally regulating to prevent decreases in ψ_l. Surprisingly, piñon J_s rates remained constant with increasing VPD even when ψ_s was high, contrary to what we predicted from the Sperry and Love (2015) framework. This suggests that even under high ψ_s conditions, piñon stomata were closing in response to increasing VPD to regulate decreases in ψ_l. Juniper, on the other hand, appeared to maintain higher stomatal conductance at high ψ_s, although regulation of J_s in response to increasing VPD was evident as ψ_s became more negative. Juniper J_s rates were constant as VPD increased at all but the highest ψ_s conditions, while we had expected this

convergence between loss functions to occur at a more negative ψ_s. Such a high ψ_s threshold for increasing stomatal regulation suggests that while juniper are operating according to the anisohydric classification in the absence of soil moisture drought, they are operating closer to the isohydric classification in the presence of soil moisture drought. This further suggests that the isohydric-to-anisohydric behavior for juniper can shift in response to environmental conditions such as ψ_s. Other examples of plants that seem to change classification in response to shifting climatic conditions have been documented, particularly in the well-studied realm of *Vitis vinifera* cultivars (Franks et al. 2007, Zhang et al. 2011, Domec and Johnson 2012).

Hydraulic strategy was also a poor predictor of canopy conductance in piñon and juniper in response to both atmospheric and soil moisture drought. Leaf-specific canopy conductance in both species responded similarly to both high VPD and low ψ_s, regardless of hydraulic strategy. Both $G_{s,ref}$ and m decreased in response to ψ_s similarly in both species, indicating similar ψ_s limitations to G_s in both species and similar regulations of ψ_l in response to decreases in ψ_s in both species, respectively. These similarities suggest that the differences in soil-plant hydraulics lead to differences in transpiration between the species, rather than a difference in stomatal regulation. The observed similarity in stomatal dynamics between these two species is not without precedent (Garcia-Forner et al. 2016), and there are several possible explanations. As suggested by Garcia-Forner et al. (2016), piñon and juniper may have different root distributions so that they may not experience the same ψ_s even when their rooting system are located within the same soil column. Additionally, piñon may have lower leaf-specific hydraulic conductance than juniper under both wet and dry conditions (Hudson

et al. 2018, but see Sperry et al. 2016), which may explain why juniper transpires at higher rates at high ψ_s without having a larger canopy conductance. At low ψ_s, the convergence of stomatal dynamics matches the convergence of transpiration rates in the two species, and can be explained by both species regulating similarly to avoid transpiration passing E_{crit} (Sperry and Love 2015).

The convergence of both canopy conductance and transpiration rates we observed between an isohydric and anisohydric species under relatively wet ψ_s, as suggested by Sperry and Love (2015) and Sperry et al. (2016) lends further support to changing the way we define hydraulic strategies (Klein 2014, Martínez-Vilalta et al. 2014, Skelton et al. 2015, Garcia-Forner et al. 2017, Martínez-Vilalta and Garcia-Forner 2017). The classic definitions of isohydry and anisohydry that depend on the presence of tighter or looser stomatal control in response to drought conditions (Tardieu and Simonneau 1998) may not be accurate, and an alternative method of defining isohydry and anisohydry is needed, one that includes hydraulic architecture (e.g. Martínez-Vilalta et al. 2014, Skelton et al. 2015, Garcia-Forner et al. 2016, Martínez-Vilalta and Garcia-Forner 2017).

3.4.2 In semi-arid biomes, decreased soil water potential has a larger overall influence on sap flow than increases in VPD.

Although we expected increased VPD in conjunction with dry soil to further decrease transpiration relative to just dry soil (Eamus et al. 2013), there was very little evidence of this in our ecosystem, at least on the daily time scale we employed (Fig. 3.3). Under conditions of low ψ_s, J_s in both species was not sensitive to increasing VPD. Both species appeared to be maximally regulating their transpiration rates such that additional

increases in VPD had no further effect. In terms of stomatal dynamics, canopy conductance in both species slightly decreased with increasing VPD, even when ψ_s was low. However, the calculated sensitivity to VPD (m) was smaller than when ψ_s was high. This result is not surprising in the context of the work of Novick et al. (2016), who found similarly low m values across the driest sites in the range of biomes they studied. Our m values were smaller than that reported for a semi-arid sagebrush shrub (*Artemisia tridentata*) (Naithani et al. 2012), which had a more mesic m value, which suggests that there might be large variability across different species and/or functional types in semi-arid biomes, particularly if those species, like sagebrush, have access to deeper soil moisture (Naithani et al. 2012).

Previous studies have suggested that increased atmospheric drought should detrimentally affect ecosystems through physiological stress, decreased transpiration rates, and tree mortality (Breshears et al. 2013, Eamus et al. 2013, Williams et al. 2013). While our data do not suggest any evidence for further decreases in transpiration in the dominant species in our system when low ψ_s is accompanied by high VPD, this does not preclude increased physiological stress or tree mortality if these conditions persist. At the daily time scale, VPD and ψ_s are largely decoupled, while at a longer time scale they are much more correlated (Fig. 3.3). In response to long-term elevated VPD, soil evaporation will increase, decreasing the ψ_s of the ecosystem further (Breshears et al. 2013), which will then result in lower transpiration rates, according to the supply-loss framework. Furthermore, according to the chronic stress hypothesis (Sperry and Love 2015), plants that experience chronically high loss of hydraulic conductance due to cavitation (which is likely to occur when ψ_s is low) are at a higher risk of mortality.

3.4.3 How do these responses help us predict how semi-arid ecosystems will respond to climate change in the future?

Due to the trade-off between water loss and carbon uptake, any decreases in tree-level transpiration rates in response to soil moisture and/or high VPD could decrease ecosystem carbon uptake (McDowell et al. 2008). Future climate scenarios for both the Southwestern US (Overpeck and Udall 2010, Gutzler and Robbins 2011, Dai 2013) and other areas globally (Crausbay et al. 2017) predict increases in both atmospheric and soil moisture drought. Our observations indicate that semi-arid ecosystems are likely to become less productive both in terms of water use and carbon uptake under future drought, regardless of the hydraulic strategies of the dominant species. However, differences in the dominant species could affect how semi-arid ecosystems respond to periods of high VPD without concurrent low ψ_s. Anisohydric species such as juniper may be able to increase transpiration (and carbon uptake) in response to high VPD as long as soil water availability is not limiting, making ecosystems with a larger fraction of anisohydric species more productive under these conditions than ecosystems with more isohydric species such as piñon.

Over the past few decades, tree mortality has become widespread, especially in semi-arid biomes (Allen et al. 2010) and it been suggested that isohydric species are more likely to succumb to mortality (Skelton et al. 2015). Thus, if mortality continues, semi-arid ecosystems could become more dominated by anisohydric species, which would result in ecosystems that would fluctuate more widely in productivity between periods of combined high VPD and low ψ_s and periods of high VPD and high ψ_s. This scenario is likely to be the case for piñon-juniper woodlands, which have experienced substantial

piñon mortality since the turn of the century (Breshears et al. 2005, McDowell et al. 2008). The combination of decreased plant biomass contributing to carbon uptake and high ecosystem sensitivity to combined high VPD and low ψ_s will likely lead to a decrease in the carbon sink associated with piñon-juniper woodlands, which make up a large percentage of land mass in North America (West 1999). This reduction could have important consequences for carbon dynamics in the Western US.

3.4.4 Conclusion

In piñon-juniper woodlands, we found that soil moisture drought over a 7 year period explained most of the decrease in plant physiological function on a daily time scale, rather than high VPD. We were able to explain only some of the responses of isohydric and anisohydric species to both high VPD and low ψ_s using the supply-loss framework for transpiration (Sperry and Love 2015, Sperry et al. 2016). We provided additional evidence of shifting isohydric-to-anisohydric behavior in response to varying environmental conditions such as ψ_s, and additional evidence that the definition of hydraulic strategy based on stomatal regulation is outdated. The difference between isohydric and anisohydric behavior is most likely dictated by soil-xylem hydraulics, as well as soil water status (ψ_s) and atmospheric drought (VPD). Finally, we predicted that if current climate patterns continue, piñon-juniper woodlands (and potentially other semi-arid biomes) are likely to experience wide fluctuations in productivity in response to the presence or absence of soil moisture drought.

Chapter 4

Integration of tree and ecosystem scale flux measurements to examine the consequences of severe drought on ecosystem function and mortality in a semi-arid woodland.

4.1 Introduction

Ecosystems respond to drought both directly and indirectly on a variety of spatial and temporal scales (Frank et al. 2015, von Buttlar et al. 2018). Drought decreases physiological function in plants, leading to lower photosynthesis and ecosystem productivity (Williams et al. 2010, Zhao and Running 2010, Rodrigues et al. 2011, Gatti et al. 2014, Frank et al. 2015, von Buttlar et al. 2018), and mortality in some cases (McDowell et al. 2008, Allen et al. 2010, Carnicer et al. 2011, Peng et al. 2011, Anderegg et al. 2013, Anderegg et al. 2016b). Drought may also have legacy effects that impact the years following drought, including predisposition of trees to insect attack (Raffa et al. 2008, Gaylord et al. 2013), reduced growth, and changes in vegetation cover (Anderegg et al. 2015b, Frank et al. 2015). These legacy effects can hinder ecosystem recovery from drought (Anderegg et al. 2015b, Schwalm et al. 2017), complicating ecosystem-level modeling of drought effects (Anderegg et al. 2015b). In addition, legacy effects may be more severe in already-dry areas (Anderegg et al. 2015b) or in areas where the recovery period was interrupted by additional drought (Schwalm et al. 2017). As the prevalence of

extreme droughts increases (Overpeck and Udall 2010, Dai 2013), frequent droughts and longer recovery times may prevent full ecosystem recovery (Schwalm et al. 2017).

One well-documented impact of more extreme droughts is climate driven tree mortality across the globe (Allen et al. 2010). In the Southwestern US, tree mortality occurred in response to droughts in the 1950's (Allen and Breshears 1998) and at the turn of the century (Breshears et al. 2005). The mechanistic causes of drought-induced mortality are still the subject of much research, but mortality is widely attributed to a complex interplay between physiological stress to drought (e.g. carbon starvation and/or hydraulic failure) and biotic agents such as insects (McDowell et al. 2008, Gaylord et al. 2013, Anderegg et al. 2015a). Evidence of hydraulic failure in the literature is fairly common, while evidence of carbon starvation is more rare (Anderegg et al. 2012, Anderegg et al. 2016a, Adams et al. 2017b). Although the frequency of these climate-driven mortality events is expected to increase, we still know very little about the physiological thresholds of species and ecosystems to drought, and the consequences of drought-induced mortality on ecosystem function on longer time scales. Quantifying these responses is crucial for understanding how drought will specifically alter carbon, water, and energy dynamics and ecosystem resilience.

Although the prevalence of long-term ecosystem monitoring networks such as FLUXNET and AmeriFlux has increased our knowledge of drought effects on ecosystem-level carbon fluxes globally (e.g. Ciais et al. 2005, Xiao et al. 2011), many studies focus on immediate effects rather than legacy effects (Frank et al. 2015, von Buttlar et al. 2018). Long-term data sets that include ecosystem measurements both before and after climate driven tree mortality are also rare (Anderegg et al. 2016b). Here

we use one such long-term data set (seven years, 2010-2016) with intensive measurements of tree and ecosystem level fluxes in a piñon-juniper woodland spanning pre-treatment (2010), a severe drought (2011-2013), widespread mortality (2013) of piñon (*Pinus edulis*) and the subsequent recovery (2013-2016). We previously evaluated the tree-level responses of this woodland to decreased soil water availability (soil moisture drought) and increased VPD (atmospheric drought) (Liebrecht, chapter 3). In this study, we extend this work to the ecosystem scale in order to examine if these tree level responses can help explain the observed increase in mortality and decrease in ecosystem function during and after the drought, which will have implications for ecosystem recovery.

As part of our long-term experiment, we have a wide range of data available, including a suite of climate metrics that allow us to categorize drought, tree level sap flux measurements that allow us to quantify physiological stress, and ecosystem level carbon flux measurements that allow us to quantify ecosystem response to extreme drought and mortality over several years following the events. Furthermore, we have detailed annual biomass measurements of both dominant tree species, piñon and juniper (*Juniperus monosperma*), as well as seasonal biomass measurements of understory vegetation. By combining our biomass measurements with tree and ecosystem level flux measurements, we can resolve how the different components of the ecosystem respond to drought and mortality. We will also use the changes post-mortality in the different ecosystem components to explain ecosystem-level responses.

From the seven years of intensive measurements at our site, we will quantify: 1) the extent of physiological stress on piñon, juniper and ecosystem function to see if

drought may help explain observed patterns of mortality in 2013, 2) how mortality altered the contributions of ecosystem components to overall ecosystem productivity, and 3) how mortality altered piñon, juniper and overall ecosystem function.

4.2 Methods

4.2.1 Site description

Our study site is located at 34.438450° N, -106.237694° W, near Mountainair, NM. The site occupies 4 ha on top of a mesa at an elevation of 2100 m. It is dominated by two tree species, *Pinus edulis* (piñon) and *Juniperus monosperma* (juniper). In addition to the two tree species, there are a variety of understory species including perennial species such as the C4 grass *Bouteloua gracilis*, the shrub *Gutierrezia sarothrae*, various cactus species in the *Opuntia* genus, *Yucca baccata*, and annual ephemeral forbs that proliferate during the monsoon season (July-September). Widespread natural piñon mortality occurred at the site in 2013. The site is characterized by a semi-arid climate with a seasonal monsoon (the North American Monsoon). Over the 30 years prior to our study (1981-2010), the site had a mean annual precipitation of 385.69 mm, 48% of which occurred during the monsoon season (http://www.prism.oregonstate.edu). During the winter, precipitation comes mostly in the form of irregular snow events. The 30-year mean temperature for the site was 10.6 °C (2.15 °C in the winter, 20.3 °C in the summer). The site is relatively flat, with less than a 3% slope. The soil is a Turkey Springs stony loam. At a soil depth of about 40 to 80 cm (heterogeneous throughout the site) there is a petrocalcic “caliche” layer (Morillas et al. 2017). Our study ran from 2010-2016. We defined years as hydrological year rather than

calendar year, with each year designated from October 1 – Sept 30 (e.g. HY 2010 runs from Oct 1, 2009 - Sept 30, 2010).

4.2.2 Climate measurements

We measured soil water content at 30-minute intervals starting in 2008, using CS610 soil moisture sensors (Campbell Scientific, Logan, Utah, USA), at three depths below three piñon, three juniper, and in three open areas (5, 10 and 30 cm). In 2015, we installed TM229-SMM soil water matric potential sensors (ICT International, Armidale, Australia) near the existing soil moisture sensors at 10 and 30 cm depth to establish an exponential relationship between measured soil water content (SWC) and soil water potential (SWP). We used the resulting equation ($SWP = -19.798*e^{(-37.29*SWC)}$) to convert the measured soil water content to soil water potential values for the time period of the study (2010-2016). We integrated soil water potential over the different layers of the soil for each 30-minute interval using the 5 cm value to approximate the soil water potential from 0-7.5 cm, the 10 cm value to approximate the soil water potential from 7.5-22.5 cm and the 30 cm value to approximate the soil water potential from 22.5-40 cm. All analyses used the daily mean integrated soil water potential.

We measured temperature and relative humidity for the site using HMP60 probes (Vaisala, Helsinki, Finland) placed at a height of 10 m and calculated vapor pressure deficit (VPD) from 30-minute averages of temperature and relative humidity. For this analysis, we used the maximum VPD for each day.

We calculated the evaporative stress index (ESI) on a daily interval as an additional metric to describe the dryness of our site over the study period (2010-2016).

ESI is calculated as 1 – the ratio of actual to potential evapotranspiration (Otkin et al. 2014, Wolf et al. 2016). We estimated potential evapotranspiration from the eddy covariance tower data using the Penman-Monteith equation (Monteith 1965, Droogers and Allen 2002), and calculated ESI using those estimates and our measured daily evapotranspiration values, as detailed below.

4.2.3 Ecosystem-level fluxes

We measured ecosystem-level water and carbon fluxes starting in 2008 using the eddy covariance (EC) method. The EC system includes a LI-7500 open-path infrared gas analyzer (LiCor, Lincoln, Nebraska, USA) and a CSAT-3 sonic anemometer (Campbell Scientific, Logan, Utah, USA) mounted at 9 m to measure carbon and water fluxes for the site. The fluxes were initially collected at 10 Hz using a CR5000 data logger (Campbell Scientific, Logan, Utah, USA), and were later converted to 30-minute data. We used the 30-minute data to calculate integrated daily totals for evapotranspiration (ET) and net ecosystem exchange (NEE), as described by Anderson-Teixeira et al. (2011). We estimated ecosystem respiration (RE) following the methods of Reichstein et al. (2005) and combined RE with NEE to estimate gross primary productivity (GPP).

4.2.4 Tree level sap fluxes

Starting in April 2009, we measured sap flow in 30-minute intervals in five juniper and five piñon at the study site. We used 10 mm Granier heat dissipation sensors (Granier 1987) that incorporated an extra pair of reference thermocouples, as described by Goulden and Field (1994) and Plaut et al. (2013). These sensors were built at the

University of New Mexico, and included an extra probe-pair, installed 5 cm adjacent to the first probe pair, to account for temperature gradients along the measured stem associated with solar heating in our open canopy system. We installed two sensors in each tree, in the outermost sapwood more than 1 m from the ground. All sensors were covered with reflective insulation to protect them from weather and rodents and to minimize temperature changes due to high solar radiation. Using a CR23X data logger (Campbell Scientific, Logan, Utah, USA), we recorded average temperature differences between the heated and reference probes at 30 minute intervals, and applied real-time temperature corrections (Goulden and Field 1994). Over the six-year period, we replaced sensors every 1-2 years, in August 2011, July 2012, July 2013, and March 2014.

We filtered data for minimum temperatures below -2 Celsius, as well as for instrument noise and failure. At each 30 minute interval we estimated sap flow J_s (g m^{-2} s^{-1}) according to Granier (1987). For the purposes of this analysis, we gap-filled any short missing periods (less than half a day) using a spline function, averaged the values from all sensors for each species, and calculated the total daily rate for each species, in g m^{-2} day^{-1}.

We calculated canopy conductance G_s (mmol CO_2 m^{-2} s^{-1}) from sap flow and VPD at each 30 minute interval following the methods of Oren et al. (1998), assuming that our leaf area to sapwood area ratios remained constant over the time period of the study (0.195 m^2 LA/cm^2 SA for piñon, 0.236 m^2 LA/cm^2 SA for juniper) (Pangle et al. 2015). We calculated the total daily rate for each species in mol CO_2 m^{-2} day^{-1}.

4.2.5 Choosing drought thresholds

To quantify the extent of physiological stress on tree and ecosystem function, we developed a method to separate the data into drought and non-drought periods using drought thresholds. To determine these thresholds, we used the results of our previous work (Liebrecht, chapter 3), where we had determined that soil moisture drought had a larger impact on piñon and juniper physiological function than atmospheric drought due to high VPD. We determined the loss of function across a range of soil water potential values using daily sap flow rates for piñon and juniper, created bins of soil water potential that were 0.2 MPa wide and averaged the sap flow rates for each species within each bin. We fit an exponential function to daily sap flow vs. soil water potential for each species, and then calculated the sap flow rate predicted by that relationship at a soil water potential of 0 (our maximum rate) and the sap flow rate predicted by that relationship at the lowest soil water potential (our minimum rate) for each species. Across the range of soil water potentials from 0 to our minimum soil water potential, we estimated the sap flow rates predicted by our fitted relationship and then normalized those rates with the maximum and minimum rates to range from zero to one. We then calculated the loss of J_s by subtracting the normalized sap flow rate from 1 and chose our soil water potential threshold by calculating the soil water potential at which 80% of J_s function was lost. We performed this analysis several times using different VPD thresholds.

4.2.6 Biomass measurements

We measured the extent of piñon mortality each year and changes in piñon, juniper and herbaceous biomass over the full time period of the study to estimate the

contribution of each component to ecosystem fluxes. To quantify the extent of piñon mortality, we performed a site-wide mortality survey each winter, starting in January 2014 after the mortality was first observed in summer 2013. The site was divided into 16 50m x 50m squares, and within each square, each dead tree was tagged. In subsequent years, already tagged dead trees were not included in the survey. At each dead tree we measured the root crown diameter and height of the tree and looked for evidence of bark beetles. For years prior to 2017, diameter at breast height was measured in piñon instead of root crown diameter, and was later converted to root crown diameter using the relationship derived by Chojnacky et al. (2013). We used allometric relationships from Grier et al. (1992) (see also Liebrecht, chapter 2) to calculate the total biomass of the newly dead trees for each year.

We non-destructively surveyed piñon and juniper biomass each year between June and October within 4-6 circular plots (each with a 10 m radius) across the site (4 plots prior to 2013, 6 plots from 2013 on). Within each plot, we measured the height, root crown diameter (RCD), and canopy diameters of all the trees. Just as in the mortality survey, prior to 2017 diameter at breast height was measured in piñon instead of RCD, and was later converted (Chojnacky et al. 2013). We used allometric relationships from a nearby piñon-juniper woodland (Pangle et al. 2015) to calculate sapwood area (SA) for each measured tree ($SA = 0.8112*RCD^{1.7341}$, $R^2 = 0.9687$ for piñon, $SA = 0.8227*RCD^{1.3903}$, $R^2 = 0.9148$ for juniper), and calculated the ratio of sapwood area per species to ground area per plot. We used the plot average to estimate site-level sapwood area/ground area for each year. We assumed a constant leaf area/sapwood area ratio (0.195 m^2 LA/cm^2 SA for piñon, 0.236 m^2 LA/cm^2 SA for juniper) (Pangle et al. 2015)

for the whole time period, and used those ratios to estimate the leaf area/ground area ratio for each species for each year.

We destructively harvested herbaceous biomass during the spring and fall of each year, along two perpendicular 80 m transects. Every 10 m along each transect, we threw a 0.25 m^2 quadrat under a tree (covered) and in an open area and harvested all grass and annual forb species whose basal stem was located within the quadrat. The plant material from each quadrat was dried and weighed, and averaged to get an estimate for the whole site in covered and open areas (in g C m^2).

4.2.7 Integrating tree and ecosystem fluxes to estimate contributions of different components to GPP

To determine the relative contributions of piñon ($f_{c,P}$) and juniper ($f_{c,J}$) to the gross primary productivity (GPP) of the site, we scaled carbon uptake from piñon and juniper using canopy conductance (G_s) for each species using the equation $f_c = c_a * G_s * A_l * (1 - c_i/c_a)$, where c_a is the atmospheric concentration of CO_2 (which was measured by the eddy covariance tower), A_l is the leaf area (calculated above), and c_i is the CO_2 concentration at the site of photosynthesis inside the leaf. We estimated c_i/c_a ratios for piñon and juniper as between 0.4-0.7 using gas exchange measurements made at the same site in 2013 and 2014. Assuming c_i/c_a decreased linearly as soil water potential decreased (Dang et al. 1997, Mielke et al. 2000, Xu and Baldocchi 2003), we used a linear relationship to approximate c_i/c_a daily across this range of c_i/c_a values using measured soil water potential.

We assumed that total ecosystem GPP equals the sum of f_c from piñon ($f_{c,P}$), juniper ($f_{c,J}$) and the understory vegetation ($f_{c,U}$), and calculated the contribution from the understory ($f_{c,U}$) as GPP – $f_{c,P}$ – $f_{c,J}$ on a daily time scale. Each component was divided by daily GPP, and averaged by season to get one number per component for spring of each year (April-June) and summer of each year (July-September). The growing season was split into spring and summer to separate the effects of winter-derived precipitation (spring) and monsoon-derived precipitation (summer).

4.2.8 Data analysis

We used RStudio for all data analysis (version 1.1.423). To examine climate conditions across the seven years of our study, we performed kernel density estimation using the ks package (Duong 2007) to look at the frequency of different combinations of VPD and soil water potential for each year.

To compare contributions to GPP over the period of the study, we used pairwise comparisons to compare contributions from all three components (piñon, juniper, and understory) to each other and across years in the spring, and then in the summer.

To analyze the impact of drought on tree and ecosystem-level carbon fluxes, we used only data from the growing season (April-September). Within this period, we classified the days of each year where VPD was above our chosen VPD threshold and integrated soil water potential was more negative than our chosen SWP threshold as drought days. All days where both thresholds were not exceeded were considered non-drought days. We performed pairwise comparisons to compare daily NEE, GPP, and RE across years and drought vs. non-drought days, as well as pairwise comparisons to

compare G_s in piñon and juniper across years and drought vs. non-drought days. Additionally, we looked at the effect of the number of days the thresholds were exceeded each year on tree and ecosystem-level carbon fluxes. We counted the number of drought days and performed linear regressions of the average annual GPP, NEE, RE, $G_{s,P}$ and $G_{s,J}$ values for each year vs. the number of drought days for each year.

To analyze the effects of mortality on tree and ecosystem-level carbon fluxes, we averaged the daily GPP, NEE, RE, $G_{s,P}$ and $G_{s,J}$ values before mortality (2010-2012) and after mortality (2014-2016) and used pairwise comparisons to compare GPP, NEE, and RE before and after mortality and to compare G_s in piñon and juniper before and after mortality.

4.3 Results

4.3.1 Climate conditions during the study

The seven years of our study covered a range of climate conditions, with the wettest conditions occurring in the first year of the study, 2010 (Fig. 4.1 and 4.2). The following three years, 2011-2013, were hot and dry overall (Fig. 4.2), with long periods when the ratio of actual evapotranspiration (AET) to potential evapotranspiration (PET) was low (high ESI, Fig. 4.1). The next two years, 2014 and 2015, were relatively wet across the growing season, with a low frequency of days with very low soil water potential and high VPD (Fig. 4.2) and shorter periods where the ratio of AET to PET was low. The final year, 2016, was drier than the previous two with a very dry monsoon season, but on average was wetter than 2011-2013 (Fig. 4.1 and 4.2).

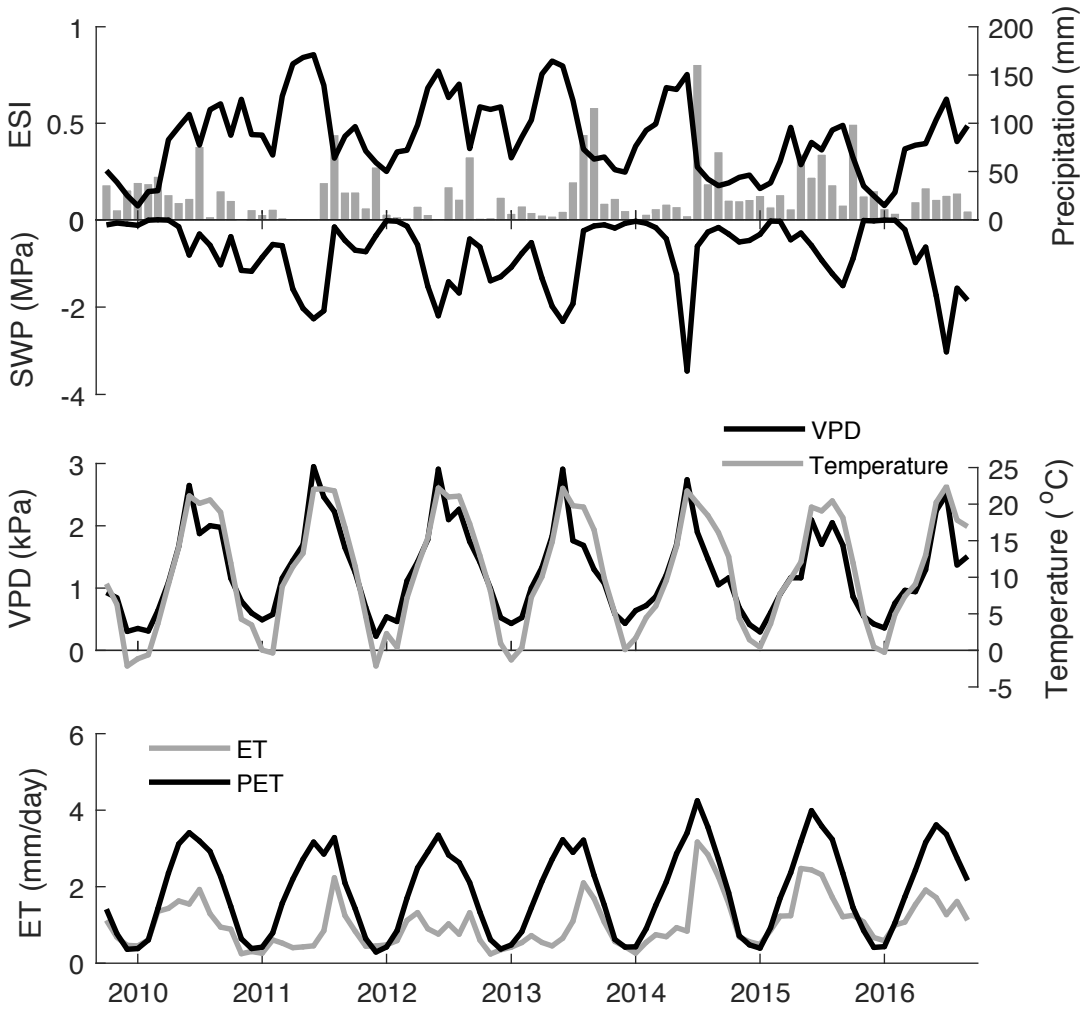

Figure 4.1: Monthly-averaged climate conditions at our site over the seven years of the study, including the evaporative stress index (ESI), integrated soil water potential (SWP), precipitation, vapor pressure deficit (VPD), temperature, evapotranspiration (ET) and potential evapotranspiration (PET).

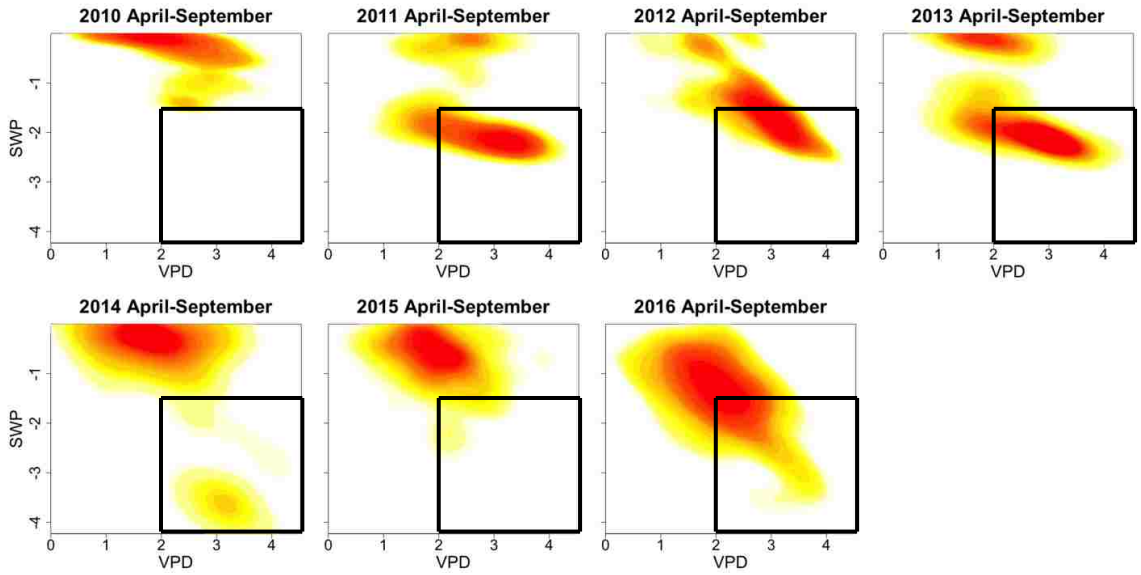

Figure 4.2: Kernel density estimates of different combinations of integrated soil water potential (SWP) and VPD at our site over the seven years of the study. A redder color indicates a higher frequency of days falling into that climate space.

4.3.2 Drought thresholds

Both species lost 80% of J_s at approximately -1.5 MPa (Fig. 4.3). We used this as our soil water potential threshold to separate the study period into days where the trees were physiologically stressed (drought) or not. This 80% decline at -1.5 MPa was consistent at VPD thresholds of either 1 or 2 kPa, matching our previous findings that decreased soil water potential has a larger impact than VPD on tree J_s in this system (Liebrecht, chapter 3). We chose a VPD threshold of 2 kPa to ensure that our drought category represented both atmospheric and soil moisture drought, as opposed to soil moisture drought (low soil water potential) alone.

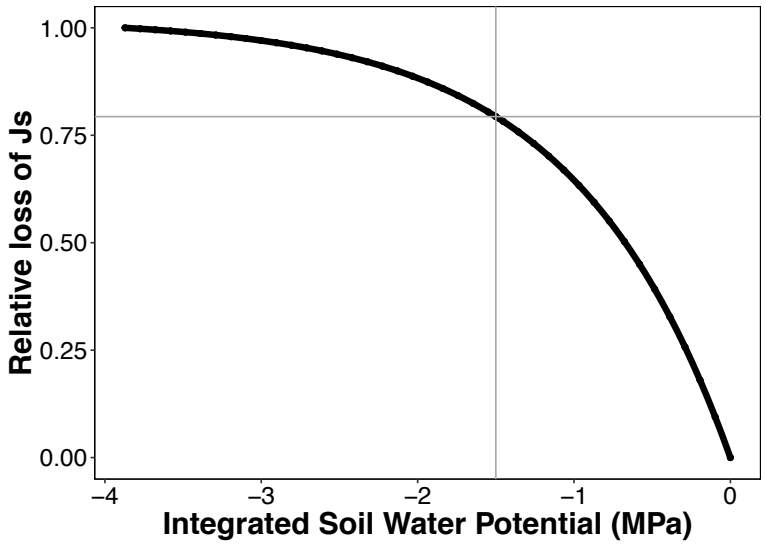

Figure 4.3: Loss of J_s as soil water potential decreases. A soil water potential of -1.5 MPa results in an 80% loss of J_s.

The frequency of days beyond the combined VPD and soil water potential thresholds during the growing season of each year indicated a severe drought from 2011-2013 that was both preceded by and followed by relative wet periods (Fig. 4.4). During the first year of the study, 2010, there were no days that were beyond the drought thresholds, while between 2011 and 2013 there were 70 or more days beyond the drought thresholds during the growing season of each year. 2014 and 2015 were also relatively wet years, with only 37 and 18 days, respectively that exceeded the drought thresholds. 2016 was more of an intermediate year in terms of drought, with 60 days beyond the drought thresholds. 2011, 2013, and 2014 had more drought days occurring in the spring than in the summer (Fig. 4.4), while 2015 and 2016 had more drought days occurring in the summer (Fig. 4.4).

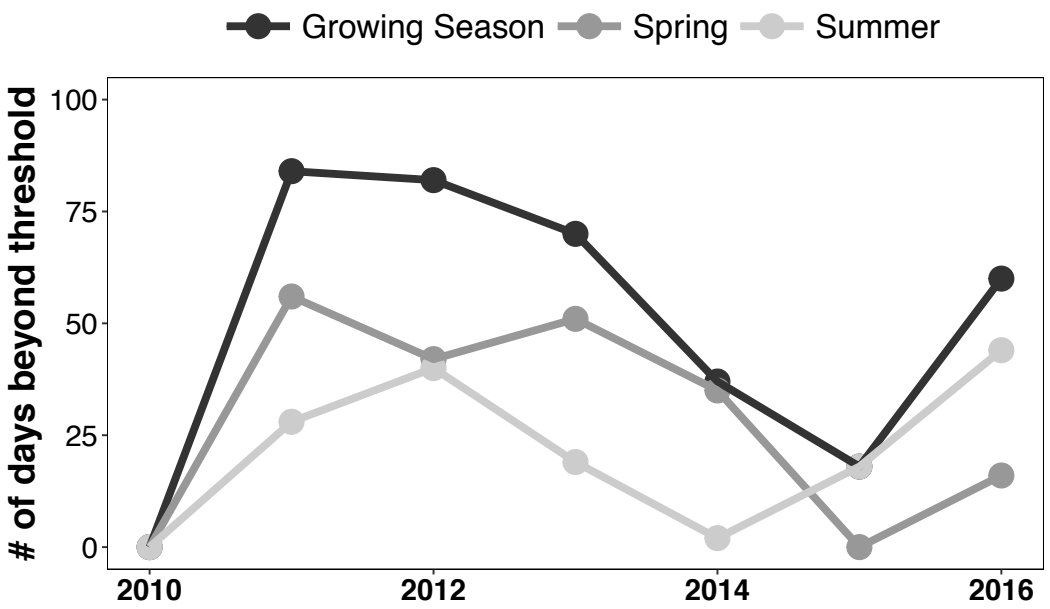

Figure 4.4: The number of days exceeding the SWP and VPD thresholds each year during the growing season, spring, and summer.

4.3.3 Effects of exceeding drought thresholds at the tree and ecosystem level

Both tree and ecosystem level function decreased when the combined VPD and soil water potential threshold was exceeded. We used 2010 as a reference point for normal tree and ecosystem function (as indicated by the horizontal lines in Fig. 4.5), because there were no days in 2010 that exceeded the drought thresholds (Fig. 4.5). In all other years, mean daily G_s rates in both species were significantly lower on days that exceeded the drought thresholds compared to non-drought days (Fig. 4.5). At the ecosystem scale, mean daily NEE and GPP were also both significantly lower on days when the drought threshold was exceeded compared to non-drought days in all but one year (Fig. 4.5). Mean daily RE was significantly lower on drought days, but only from 2011-2014 (Fig. 4.5).

Annual G_s rates in both piñon and juniper, and annual GPP and RE decreased significantly as the number of days beyond the drought threshold increased per year (Fig. 4.6). While annual NEE became less negative (indicating less carbon sequestration) as the number of drought days per year increased, this relationship was not significant at the 95% confidence level (Fig. 4.6).

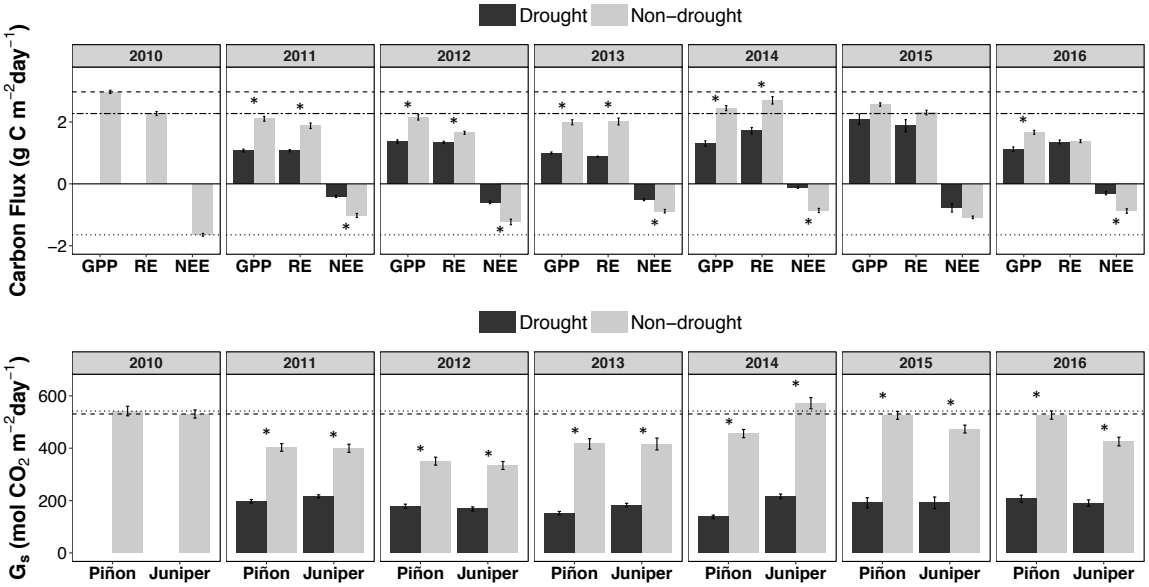

Figure 4.5: Mean daily gross primary productivity (GPP), ecosystem respiration (RE), net ecosystem exchange (NEE), and piñon and juniper canopy conductance (G_s) during drought days (beyond the drought thresholds) and non-drought days for each year of the study. Each bar represents mean +/- standard error. Asterisks denote significant differences between drought and non-drought days (see Table 4.1 for p-values). The horizontal lines on the figure indicate the values of all parameters in 2010, which had no drought days.

Table 4.1: Pairwise comparisons between drought and non-drought days for NEE, GPP, RE, piñon G_s and juniper G_s. Asterisks denote significance at the 95% confidence level.

Parameter	Year	P-value
NEE	2011	9.59e-10*
	2012	1.99e-10*
	2013	3.72e-4*
	2014	2.73e-9
	2015	0.165
	2016	7.38e-7
GPP	2011	1.94e-18*
	2012	9.73e-12*
	2013	4.33e-16*
	2014	5.90e-15*
	2015	0.0689
	2016	4.81e-5*
RE	2011	7.16e-9*
	2012	0.0225*
	2013	6.91e-15*
	2014	1.70e-8*
	2015	0.164
	2016	0.892
Piñon G_s	2011	3.63e-13*
	2012	5.91e-10*
	2013	4.29e-19*
	2014	1.73e-19*
	2015	5.08e-8*
	2016	2.99e-21*
Juniper G_s	2011	5.26e-10*
	2012	9.60e-9*
	2013	3.29e-14*
	2014	7.66e-22*
	2015	1.15e-5*
	2016	9.35e-12*

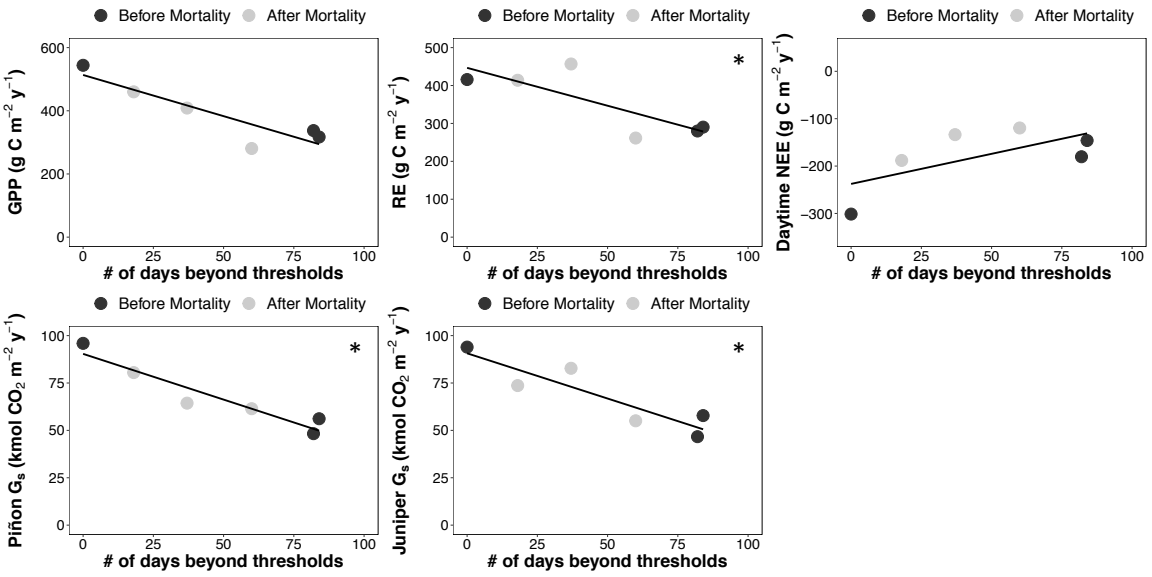

Figure 4.6: Changes in annual net ecosystem exchange (NEE), gross primary productivity (GPP), ecosystem respiration (RE), and piñon and juniper canopy conductance (G_s) as a function of the number of days beyond the drought threshold in each year. Each point represents one year. Asterisks denote a significant relationship between the parameter and the number of days beyond the drought threshold (see Table 4.2 for equation parameters, p-values and R^2 values).

Table 4.2: Linear regressions between annual fluxes and number of days beyond the drought threshold for NEE, GPP, RE, piñon G_s and juniper G_s. Asterisks denote significance at the 95% confidence level.

Parameter	Slope	Intercept	p-value	R^2
NEE	1.27	-237.6	0.152	0.439
GPP	-2.61	513.4	0.0129*	0.775
RE	-2.00	446.7	0.05*	0.655
Piñon G_s	-482.6	90372.2	0.00351*	0.905
Juniper G_s	-477.2	90665.4	0.0134*	0.817

4.3.4 Description of mortality

Widespread piñon mortality was first evident in the summer of 2013. Our first mortality survey in January 2014 indicated that more than 50% of the mortality happened

in 2013. Total mortality recorded in 2014 was 1649 piñon and 1 juniper, which accounted for 36 Mg C of dead biomass (Fig. 4.7). Mortality continued in 2014 and 2015 with 605 and 72 new dead piñon and juniper, respectively (~12 Mg C in new dead biomass) recorded in the 2015 survey, and 530 and 31 dead piñon and juniper, respectively (~11 Mg newly dead biomass) recorded in the 2016 survey (Fig. 4.7). Mortality after the 2016 survey was minor (Fig. 4.7). Piñon mortality overall was much higher than juniper mortality. We observed small holes in the surveyed piñon trunks that we attributed to *Ips confusus* (piñon ips beetle) in 97.6% of the dead piñon surveyed in 2014, and in 82.9% of the dead piñon surveyed from 2014-2018. However, we could not determine whether the beetles attacked the tree before or after mortality occurred.

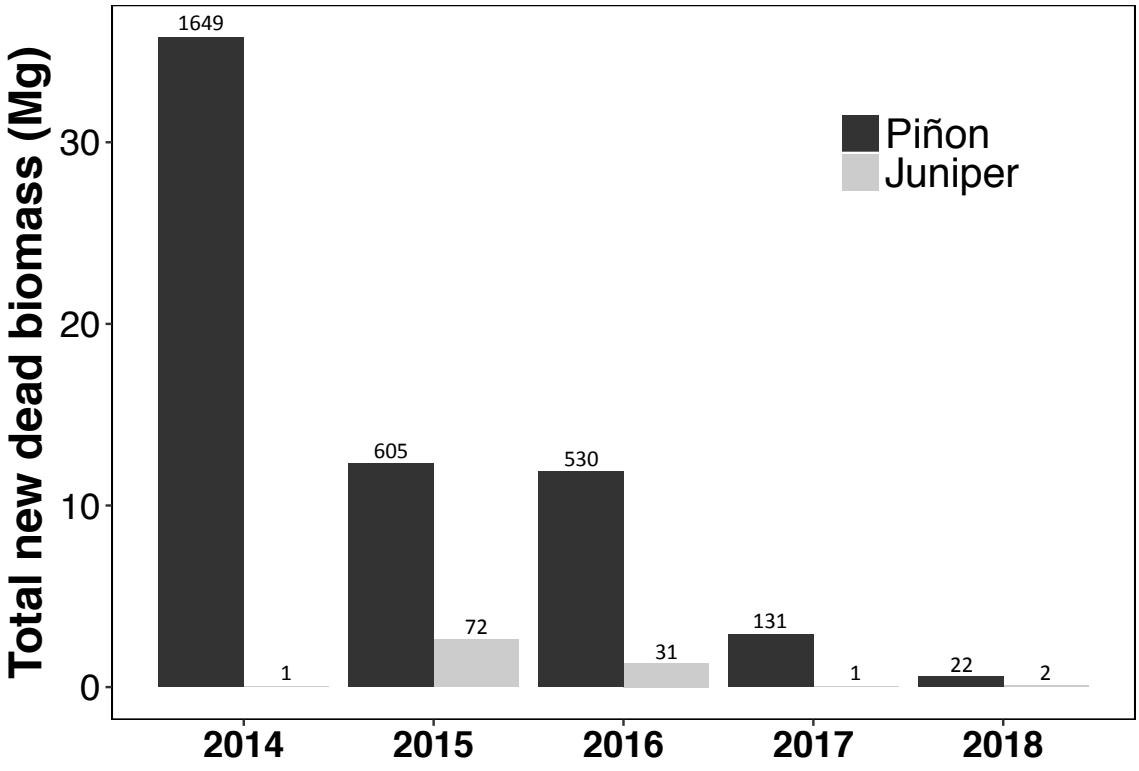

Figure 4.7: Mortality of piñon and juniper from 2014 onwards. The number above each bar corresponds to the number of dead trees documented.

4.3.5 Relative contributions from different ecosystem components

The relative contributions to total GPP of the dominant components of the ecosystem (piñon, juniper, and understory vegetation) changed in response to the mortality event (Fig. 4.8). Before piñon mortality, piñon and juniper contributed similarly to total GPP (< 6% difference between species) during both parts of the growing season (spring and summer) (Fig. 4.8). After mortality, the contribution from piñon in both spring and summer decreased by more than half due to the loss of live piñon trees and remained stable (Fig. 4.8). The contribution from juniper to spring GPP increased relative to piñon just prior to mortality (7% higher than piñon in 2013) and continued to increase following mortality (27% higher than piñon in 2016) (Fig. 4.8). Post-mortality, the contribution from juniper to summer GPP increased initially in 2014, but then decreased back to pre-mortality levels (Fig. 4.8).

The understory contribution to total GPP was variable from year to year before the mortality event but increased following mortality, particularly in the summer (Fig. 4.8). This increase in the understory contribution to GPP was particularly evident in 2015, a relatively wet year with few days beyond the drought threshold, when the understory contributed 67% of total GPP in the summer. Herbaceous understory biomass also increased following mortality in 2013, supporting this increase in the understory contribution to GPP (Fig. 4.9).

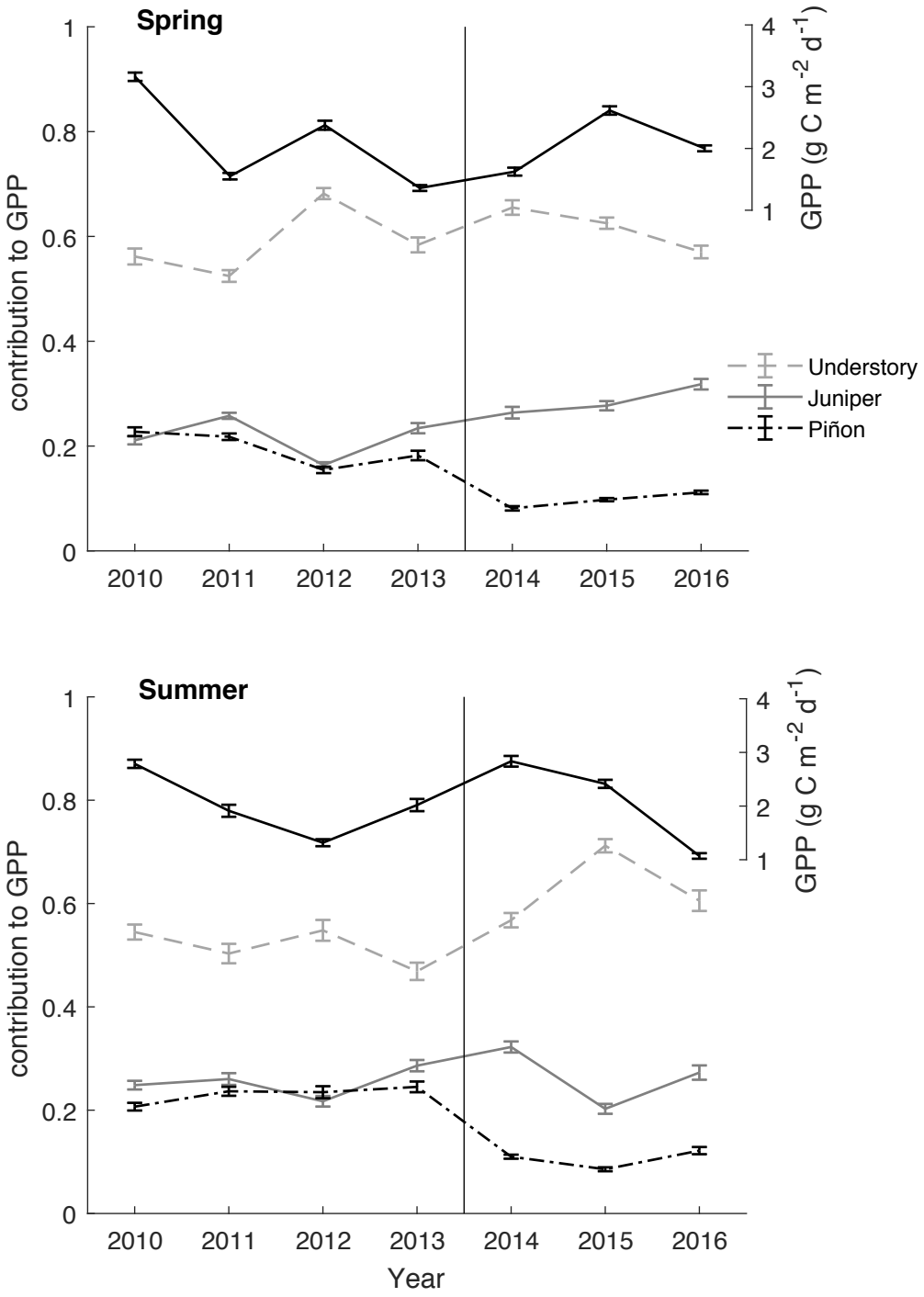

Figure 4.8: Overall GPP and relative contributions to GPP from piñon, juniper, and understory vegetation over the seven years of the study, separated by season (spring and summer). Each point indicates the mean contribution for that season and year +/- standard error. The vertical gray line indicates the onset of mortality. The results of statistical analysis comparing the contributions between components and years can be found in Tables 4.3 and 4.4.

Table 4.3: Pairwise comparisons of piñon, juniper and understory vegetation contributions to total GPP in spring, from 2010-2016. Asterisks denote significance at the 95% confidence level.

Comparing between years			
Years	Juniper	Piñon	Understory
2010 vs. 2011	7.4e-4*	0.49	7.3e-3*
2011 vs. 2012	< 1e-5*	< 1e-5*	< 1e-5*
2012 vs. 2013	< 1e-5*	0.045*	< 1e-5*
2013 vs. 2014	0.032*	< 1e-5*	< 1e-5*
2014 vs. 2015	0.35	0.24	0.036*
2015 vs. 2016	4.0e-3*	0.33	1.2e-4*
2010 vs. 2016	< 1e-5*	< 1e-5*	0.54

Comparing between components							
Components	2010	2011	2012	2013	2014	2015	2016
Juniper vs. Piñon	0.24	3.7e-3*	0.50	1.4e-4*	< 1e-5*	< 1e-5*	< 1e-5*
Juniper vs. Understory	< 1e-5*	< 1e-5*	< 1e-5*	< 1e-5*	< 1e-5*	< 1e-5*	< 1e-5*
Piñon vs. Understory	< 1e-5*	< 1e-5*	< 1e-5*	< 1e-5*	< 1e-5*	< 1e-5*	< 1e-5*

Table 4.4: Pairwise comparisons of piñon, juniper and understory vegetation contributions to total GPP in summer, from 2010-2016. Asterisks denote significance at the 95% confidence level.

Comparing between years			
Years	Juniper	Piñon	Understory
2010 vs. 2011	0.51	0.10	0.022*
2011 vs. 2012	0.020*	0.92	0.016*
2012 vs. 2013	2.5e-4*	0.58	2.7e-5*
2013 vs. 2014	0.061	< 1e-5*	< 1e-5*
2014 vs. 2015	< 1e-5*	0.21	< 1e-5*
2015 vs. 2016	7.5e-4*	0.083	< 1e-5*
2010 vs. 2016	0.23	2.8e-5*	2.8e-3*

Comparing between components							
Components	2010	2011	2012	2013	2014	2015	2016
Juniper vs. Piñon	0.019*	0.20	0.34	0.031*	< 1e-5*	< 1e-5*	< 1e-5*
Juniper vs. Understory	< 1e-5*	< 1e-5*	< 1e-5*	< 1e-5*	< 1e-5*	< 1e-5*	< 1e-5*
Piñon vs. Understory	< 1e-5*	< 1e-5*	< 1e-5*	< 1e-5*	< 1e-5*	< 1e-5*	< 1e-5*

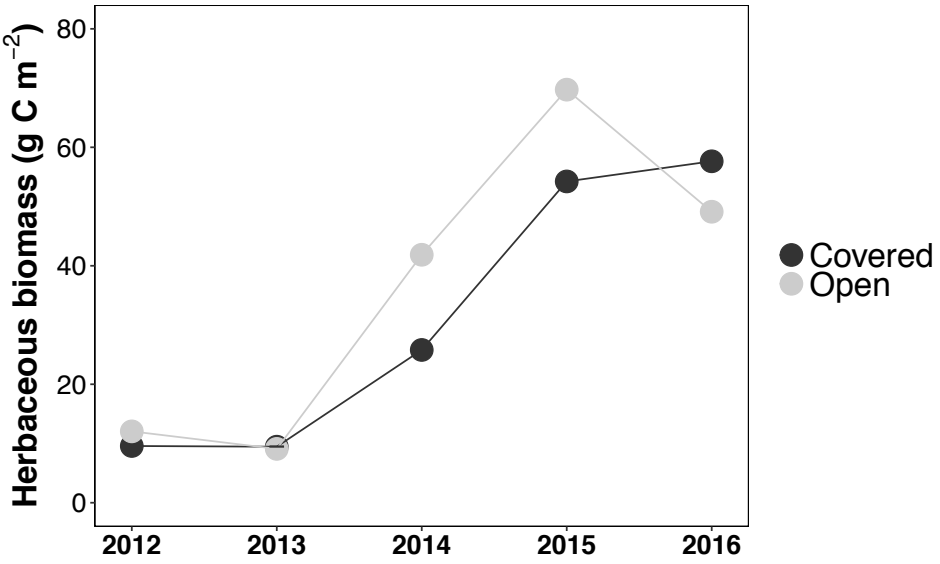

Figure 4.9: Herbaceous biomass destructively harvested under tree canopies (covered) and in open areas from 2012 to 2016.

4.3.6 Effects of mortality on tree and ecosystem level carbon fluxes

In the years after the largest number of piñon died (2014-2016), mean daily net ecosystem exchange (NEE) was significantly less negative (indicating that the ecosystem was sequestering less carbon) than before mortality (2010-2012) (Fig. 4.10). Although daily GPP did not change after mortality (Fig. 4.10), daily RE increased significantly (Fig. 4.10), suggesting that the increase in NEE of the ecosystem after mortality was driven by the increase in RE rather than a decrease in GPP. Both piñon and juniper mean daily G_s rates increased by about 12% after mortality (Fig. 4.10).

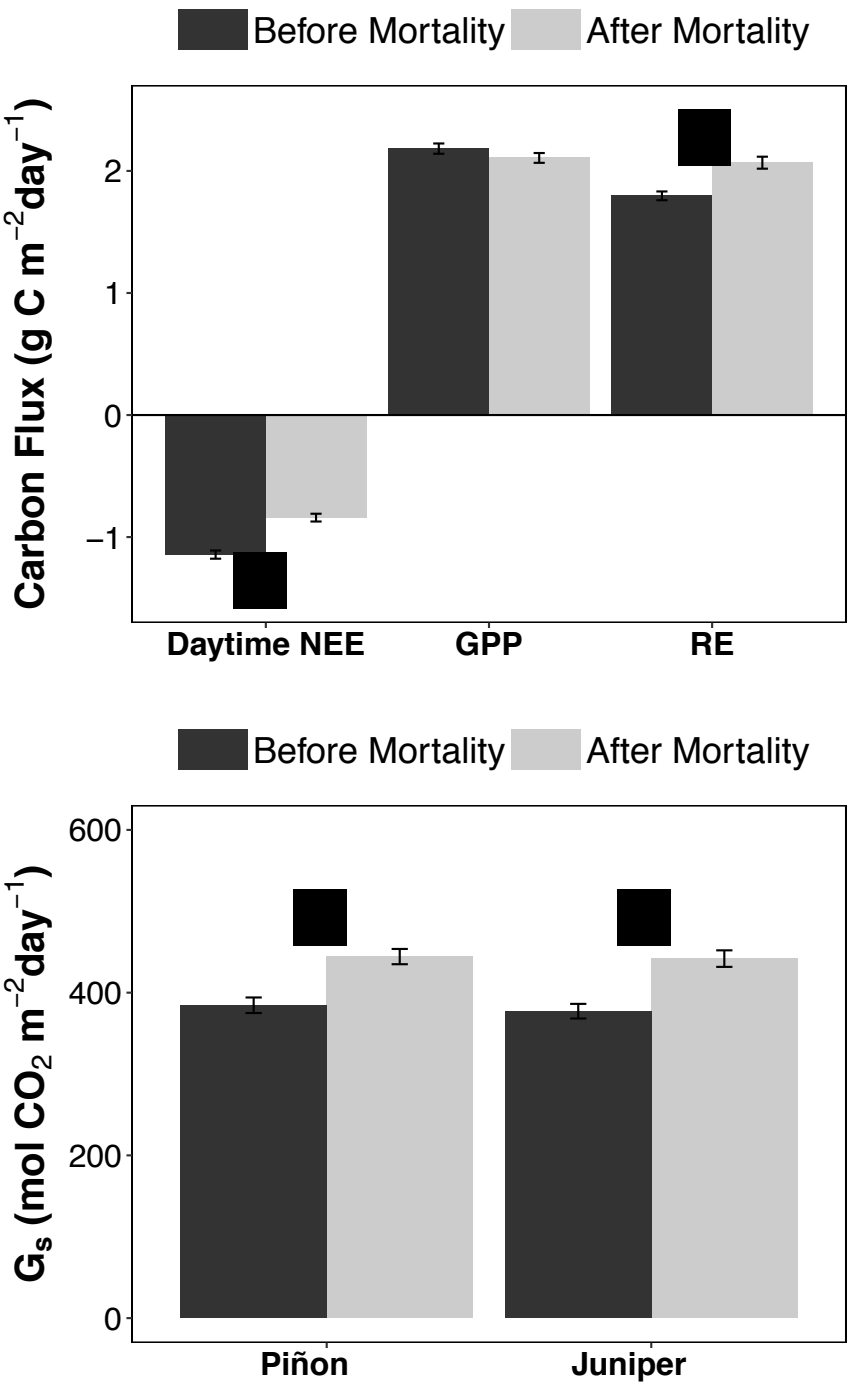

Figure 4.10: Average daily net ecosystem exchange (NEE), gross primary productivity (GPP), ecosystem respiration (RE), and piñon and juniper canopy conductance (G_s) before and after piñon mortality. Each bar represents mean +/- standard error. Asterisks denote a significant difference between before and after mortality (p-values can be found in Table 4.5).

Table 4.5: Pairwise comparisons between before and after mortality for NEE, GPP, RE, piñon G_s and juniper G_s. Asterisks denote significance at the 95% confidence level.

Parameter	p-value
NEE	4.80e-8*
GPP	0.168
RE	9.70e-7*
Piñon G_s	2.30e-5*
Juniper G_s	3.70e-6*

4.4 Discussion

Jentsch et al. (2007) and Heimann and Reichstein (2008) both highlighted the importance of quantifying ecosystem responses to extreme climate events (e.g. droughts and/or mortality episodes), in addition to climate trends. Because the frequency of these events is increasing, documenting the responses to these events is crucial to determine relative impacts and inform predictive models and management decisions (Crausbay et al. 2017). Dryland ecosystems, including semi-arid woodlands such as piñon-juniper woodlands, cover 45% of global land surface and are a large contributor to interannual variability in the strength of the global carbon sink (Poulter et al. 2014, Ahlström et al. 2015). Increasing our ability to quantify the impact of legacy effects of drought and mortality on ecosystem recovery in these biomes is vital to both predicting ecosystem function as droughts become more frequent, and enhancing global models of ecosystem responses to extreme events (Frank et al. 2015, Anderegg et al. 2016b, Berner et al. 2017, von Buttlar et al. 2018). Our seven-year study of a piñon-juniper woodland included both a period of drought and a natural mortality event followed by several wet years, allowing us to quantify both immediate and legacy effects of drought on the ecosystem. In our system, we found that the three consecutive years of drought decreased productivity at

both the tree and ecosystem scales and was followed by the widespread mortality of piñon. During two very wet years after the drought ended, the productivity of the surviving juniper and understory vegetation increased, helping to offset the loss of productivity due to the mortality.

4.4.1 Physiological drought thresholds can quantify and explain changes in ecosystem productivity.

The response of ecosystem productivity to drought is challenging to quantify using time series of ecosystem carbon fluxes and climate conditions. Identifying drought thresholds allowed us to quantitatively assign daily data to drought and non-drought conditions across our long-term record, which helped to resolve the effects of drought on a finer temporal scale (daily as opposed to seasonal or yearly). Both tree level function (G_s) and ecosystem function (productivity and overall carbon uptake) were lower on days that exceeded the drought threshold compared to non-drought days (Fig. 4.5). This suggests that decreased tree level G_s in both piñon and juniper drove the overall ecosystem response. Decreased GPP in response to drought is supported in many other ecosystems globally (e.g. Reichstein et al. 2002, Ciais et al. 2005, Zhao and Running 2010, Xiao et al. 2011, Gatti et al. 2014).

The effects of drought on ecosystem respiration (RE) were less straightforward than the effects on GPP. Decreased GPP due to drought or mortality is frequently associated with a concurrent decrease in autotrophic respiration, due to diminished substrate availability (Ciais et al. 2005, Berryman et al. 2013, Frank et al. 2015, Ballantyne et al. 2017, von Buttlar et al. 2018). Heterotrophic (soil microbial) respiration,

on the other hand, may increase, decrease, or not change in response to drought due to the competing influences of high temperature and lack of soil moisture (Ciais et al. 2005, Frank et al. 2015, Ballantyne et al. 2017, von Buttlar et al. 2018). Heterotrophic respiration may also increase following mortality due to dead biomass inputs to the system (Frank et al. 2015, Anderegg et al. 2016b), which may change the microbial communities in the soil under dead trees (Warnock et al. 2016) and decrease carbon limitation of litter respiration (Berryman et al. 2013). From 2011-2014, mean daily RE was lowest on days that exceeded drought thresholds, as expected. In 2015 and 2016, mean daily RE was similar on drought and non-drought days. This was likely due to the tradeoff of increased decomposition of litter fall and snag fall from the dead piñon (Berryman et al. 2013) and reduced water availability (Ciais et al. 2005, Ruehr et al. 2012).

As expected, mean daily net ecosystem exchange (NEE) was less negative during drought days than non-drought days in all years except for 2015, which decreased carbon uptake for the ecosystem (Anderson-Teixeira et al. 2011, Rodrigues et al. 2011, Schwalm et al. 2012, Ma et al. 2016). This difference was most likely driven by decreases in GPP, rather than an increase in RE, since no increase in RE was observed in any of the years of the study. This decrease in mean daily NEE in response to drought has important implications for the future of piñon-juniper woodlands. Severe droughts are predicted to increase (Overpeck and Udall 2010, Dai 2013, Crausbay et al. 2017), and based on these measured responses to drought, we can expect that these ecosystems will become either a weaker carbon sink or possibly a carbon source (Ciais et al. 2005, Schwalm et al. 2012, Frank et al. 2015, Ma et al. 2016, Schwalm et al. 2017, von Buttlar et al. 2018).

4.4.2 Using thresholds to explain the relationship between drought and piñon mortality.

In addition to reduced carbon fluxes, drought also commonly triggers large scale mortality (Frank et al. 2015). The linkage we observed between drought and natural piñon mortality can be explored by looking at changes in sap-flow estimated canopy conductance (G_s) of piñon and juniper. In the three consecutive years that included high numbers of drought days (2011-2013, Fig. 4.4), both piñon and juniper daily G_s rates were low, indicating both species were physiologically stressed (Fig. 4.5). Our G_s data do not provide direct evidence that piñon was more physiologically stressed than juniper. It has previously been suggested that the differing hydraulic strategies of piñon and juniper (isohydry and anisohydry, respectively) can help predict the mechanism of mortality in each species, and that juniper's anisohydric strategy makes it more susceptible to hydraulic failure (McDowell et al. 2008). However, recent work in a piñon-juniper woodland (Garcia-Forner et al. 2016) found that piñon actually had more chronic damage to their hydraulic machinery than juniper during periods of drought. In addition, hot and dry conditions during these years could have increased background levels of the piñon-specific bark beetle *Ips confusus* (Logan et al. 2003, Raffa et al. 2008, Bentz et al. 2010). While juniper was also physiologically stressed by drought during these years, mortality was likely low because it has fewer pathogens that drive large scale mortality events (Floyd et al. 2009).

4.4.3 Integration of tree and ecosystem fluxes can show increases in productivity contributions from non-piñon components post-mortality.

Eddy covariance measurements provide a good estimate of ecosystem-scale fluxes, but are unable to resolve the contributions of individual ecosystem components to the overall flux. In our site, growing season mean daily GPP did not change before and after mortality, despite the huge loss of live biomass from piñon mortality (Fig. 4.10). By integrating tree level flux measurements with eddy covariance data, we observed that the relative contributions of the different ecosystem components (piñon, juniper, and understory vegetation) to GPP changed after the mortality event, with either juniper or understory vegetation contributions increasing, depending on the season. As expected, the relative contribution from piñon decreased starting in 2014, due to the severely reduced live biomass of piñon trees. In the spring, the contribution from juniper increased post-mortality. However, there was no similar increase in juniper contribution in the summer. Although juniper can use both winter-derived precipitation such as snowmelt and monsoon precipitation (Williams and Ehleringer 2000, West et al. 2007, Limousin et al. 2013), their contribution may not increase in summer because of the abundance of understory species competing for monsoon precipitation.

The contribution from understory vegetation to GPP, on the other hand, stayed relatively the same during the spring, but increased in the summer following piñon mortality. This increased contribution was supported by an increase in herbaceous biomass in the years following mortality (Fig. 4.9). A similar increase in understory vegetation was observed in a manipulated piñon mortality study by Krofcheck et al. (2014), where an increase in annual forbs was observed under dead piñon canopies post-mortality. The higher contributions of understory vegetation in summer relative to spring are supported by phenological patterns in the Chihuahuan desert that indicate C3 species

active during the spring are typically less abundant than the C4 grasses and forbs active during the summer monsoon period (Kemp 1983). In addition to the established perennial species at our site (e.g. *Bouteloua gracilis, Yucca baccata, Gutierrezia sarothrae*), some annual species can also take advantage of monsoon precipitation (Báez et al. 2013). In general, NDVI values in this region are higher during summer (Weiss et al. 2004, Krofcheck et al. 2014), providing evidence that understory species regularly take advantage of monsoon precipitation, and can explain the observed increase in understory contributions to summer GPP.

After mortality, compensatory processes such as competitive release can help facilitate ecosystem recovery in many biomes (Anderegg et al. 2016b). Competitive release can occur if increased light, nutrient, and water availability post-mortality due to lower competition sets up conditions for increased growth and productivity of surviving trees and increased recruitment (Lloret et al. 2012) or increased herbaceous response (Rich et al. 2008). However, whether or not this release effect occurs may be dependent upon the climate conditions following mortality (Liebrecht, chapter 2, Anderegg et al. 2016b, Stevens-Rumann et al. 2017), with wet conditions allowing for release, and dry conditions possibly preventing release from occurring. We previously studied competitive release in a piñon-juniper woodland with simulated drought-induced mortality. Surviving piñon and juniper did not show any changes in photosynthetic rate or cavitation vulnerability after mortality (Liebrecht, chapter 2), and GPP decreased post-mortality (Krofcheck et al. 2015), indicating that remaining trees were not taking advantage of released resources. However, that study took place during the severe drought years of 2011-2012.

In this study, the changing contributions from juniper and understory vegetation appear to offset overall ecosystem loss of GPP from the mortality. Mean daily GPP did not decrease after mortality, which was surprising, given reported decreases in net primary productivity in response to mortality in other ecosystems (Anderegg et al. 2013). Although we don't have direct evidence, this offset in GPP loss can potentially be explained by competitive release (Rich et al. 2008, Lloret et al. 2012) for juniper in the spring, and understory vegetation in the summer (Fig. 4.9), in relatively wet years following mortality (2014-2015).

While mean daily GPP did not change post-mortality, mean daily RE did increase, probably due to the combination of additional inputs of dead biomass from the mortality and the wet years immediately following mortality (Ruehr et al. 2012). The overall decrease in carbon sequestration following mortality (less negative NEE) suggests that the juniper and understory offsets to GPP we observed were not enough to offset the increase in respiration.

4.4.4 Conclusion

Over a seven-year study in a piñon-juniper woodland, we observed drought-induced reductions in GPP at both the tree and ecosystem level. After three years of severe drought (2011-2013), widespread piñon mortality occurred due to a combination of drought-induced physiological stress at the tree level and increased insect activity in the ecosystem. While overall carbon sequestration of the ecosystem decreased post-mortality, this decrease was due mostly to increased respiration (presumably due to increased decomposition rates) rather than a decrease in GPP. Juniper and understory

vegetation increased their relative contributions to GPP post-mortality, which suggests these species may have experienced competitive release. Although a release effect was not seen at the ecosystem level in a nearby manipulated piñon-juniper woodland post-mortality in a previous study (Krofcheck et al. 2015), that mortality event was followed by drought conditions. The observed increased contributions of the remaining components of the ecosystem following mortality in relatively wet conditions highlights the importance of climate for post-mortality ecosystem trajectories (Anderegg et al. 2016b, Schwalm et al. 2017, Stevens-Rumann et al. 2017) and suggests that the availability of soil water may determine whether these disturbed ecosystems ultimately recover or shift to a new stable state.

Chapter 5

Conclusion

As semi-arid ecosystems such as piñon-juniper (PJ) woodlands become hotter and drier (Overpeck and Udall 2010, Dai 2013), it becomes crucial to quantify the effects of drought (including mortality) on tree and ecosystem function. The way that trees and ecosystems respond to these extreme events, in combination with climate, may influence their recovery trajectory, and determine whether or not they can recover at all, or instead change to an alternate stable state (Allen and Breshears 1998, Schwalm et al. 2017). In this dissertation, I combined leaf and tree level measurements (chapters 2 and 3) with ecosystem level carbon fluxes (chapter 4) to quantify species and ecosystem level effects of both drought and mortality and show that climate after a mortality event can impact ecosystem recovery (chapter 2 and 4).

In chapter 2, I looked for evidence of competitive release in a PJ woodland after more than 1600 large piñon were girdled to simulate drought-induced mortality. I made leaf-level gas exchange and root cavitation vulnerability measurements to determine whether the remaining trees (both piñon and juniper) acclimated to conditions of increased resource availability post-mortality. I found very little evidence of competitive release by looking at either of these parameters. However, my measurements were made during a severe drought, and I suggest that because of the interaction between drought and a low canopy density, my assumption that there was more available water in the ecosystem post-mortality was not supported, due to a combination of increased soil

evaporation and increased water use by understory vegetation (Morillas et al. 2017). Competitive release has mostly been observed in wetter, denser forests, and my results suggested that it may not be as prevalent in semi-arid biomes. This has implications for succession of these biomes following large-scale disturbances, particularly as more frequent droughts are forecast in the coming decades.

In chapter 3, I investigated the role of hydraulic strategy in piñon and juniper responses to two different kinds of drought, soil moisture drought (low soil moisture), and atmospheric drought (high evaporative demand). I used an existing framework (Sperry and Love 2015, Sperry et al. 2016) to explain how sap flow and stomatal conductance in the two species would respond to the two different drought types. Over the time period of the study, I found that while juniper was impacted more by atmospheric drought than piñon was, this difference was only seen in the absence of soil moisture drought. When soil moisture drought was present, both species behaved similarly, decreasing their transpiration substantially. My results provide additional evidence to the proposed hypothesis that hydraulic function is more of a continuum than discrete categories, and that plants can change hydraulic strategies under different climatic conditions (Klein 2014, Martínez-Vilalta et al. 2014). I also observed that both piñon and juniper had similar stomatal conductance in the face of drought conditions of both types, which suggests that defining hydraulic strategy by different types of stomatal regulation may be an outdated method, which is also supported by the work of Garcia-Forner et al. (2016) and Martínez-Vilalta and Garcia-Forner (2017).

In chapter 4, I built on my findings from chapter 3 and integrated sap flow and eddy covariance measurements to examine how the effects of drought extend from tree to

ecosystem scales, and how this drought may have led to a natural piñon mortality event. In addition, I quantified the effects of this mortality event on overall carbon uptake in the ecosystem. I found that in all but the wettest years of the study, drought conditions led to a decrease in both tree-level and ecosystem-level function, decreasing the carbon uptake of the site as a whole. I also found that mortality led to decreased carbon uptake of the site, mostly due to increased ecosystem respiration. The contributions from different components of the ecosystem also changed post-mortality; the decreased contribution from piñon was mostly offset by increased contributions from juniper in the spring and understory vegetation during the summer monsoon, particularly during the wetter years of 2014 and 2015. While I cannot fully explain the mortality at my site, it was preceded by very dry conditions, and the years before the drought (2011-2013) showed the greatest number of days exceeding the climate thresholds of all the years.

If extreme droughts become more common in semi-arid biomes such as piñon-juniper woodlands, the trees will become more physiologically stressed, as shown in chapters 3 and 4, which will decrease overall ecosystem carbon uptake, as shown in chapter 4, and potentially lead to piñon mortality. The different recovery trajectories post-mortality suggested by chapters 2 and 4 highlight the importance of climate conditions post-mortality in determining the ecosystem response. If drought conditions follow the mortality event (chapter 2), competitive release may not occur, hindering ecosystem recovery. On the other hand, if wet conditions follow the mortality event (chapter 4), increases in juniper and understory productivity may help offset ecosystem losses in productivity, facilitating ecosystem recovery, as suggested by Anderegg et al. (2016b). This dissertation underlines the complex interplay between drought and mortality, and the

importance of future climate in determining ecosystem recovery trajectories from these disturbances.

Moving forward, the frameworks and techniques that I used can potentially be applied to other ecosystems. The framework that I used in chapter 3, which helps explain how plant species with different hydraulic strategies will respond to different types of drought, can be applied to other plant species in the future. In chapter 4, I developed new methods to analyze flux data that allowed me to observe the effects of drought on multiple scales. These methods included using climate thresholds to partition between drought and non-drought conditions and integrating tree and ecosystem level fluxes to determine the relative contributions of different ecosystem components to total ecosystem productivity. These methods provide a starting point for amassing data that can be used to improve ecosystem modeling of drought and mortality responses.

References

Adams, H., A. Macalady, D. Breshears, C. Allen, N. Stephenson, S. Saleska, T. Huxman, and N. McDowell. 2010. Climate-induced tree mortality: earth system consequences. Eos **91**.

Adams, H. D., G. A. Barron-Gafford, R. L. Minor, A. A. Gardea, L. P. Bentley, D. J. Law, D. D. Breshears, N. G. McDowell, and T. E. Huxman. 2017a. Temperature response surfaces for mortality risk of tree species with future drought. Environmental Research Letters **12**:115014.

Adams, H. D., C. H. Luce, D. D. Breshears, C. D. Allen, M. Weiler, V. C. Hale, A. Smith, and T. E. Huxman. 2012. Ecohydrological consequences of drought‐and infestation‐triggered tree die‐off: insights and hypotheses. Ecohydrology **5**:145-159.

Adams, H. D., M. J. Zeppel, W. R. Anderegg, H. Hartmann, S. M. Landhäusser, D. T. Tissue, T. E. Huxman, P. J. Hudson, T. E. Franz, and C. D. Allen. 2017b. A multi-species synthesis of physiological mechanisms in drought-induced tree mortality. Nature ecology & evolution **1**:1285.

Ahlström, A., M. R. Raupach, G. Schurgers, B. Smith, A. Arneth, M. Jung, M. Reichstein, J. G. Canadell, P. Friedlingstein, and A. K. Jain. 2015. The dominant role of semi-arid ecosystems in the trend and variability of the land CO2 sink. Science **348**:895-899.

Allen, C. D., and D. D. Breshears. 1998. Drought-induced shift of a forest–woodland ecotone: rapid landscape response to climate variation. Proceedings of the National Academy of Sciences **95**:14839-14842.

Allen, C. D., A. K. Macalady, H. Chenchouni, D. Bachelet, N. McDowell, M. Vennetier, T. Kitzberger, A. Rigling, D. D. Breshears, and E. H. Hogg. 2010. A global overview of drought and heat-induced tree mortality reveals emerging climate change risks for forests. Forest ecology and management **259**:660-684.

Anderegg, W. R., J. A. Berry, D. D. Smith, J. S. Sperry, L. D. Anderegg, and C. B. Field. 2012. The roles of hydraulic and carbon stress in a widespread climate-induced forest die-off. Proceedings of the National Academy of Sciences **109**:233-237.

Anderegg, W. R., J. A. Hicke, R. A. Fisher, C. D. Allen, J. Aukema, B. Bentz, S. Hood, J. W. Lichstein, A. K. Macalady, and N. McDowell. 2015a. Tree mortality from drought, insects, and their interactions in a changing climate. New Phytologist **208**:674-683.

Anderegg, W. R., J. M. Kane, and L. D. Anderegg. 2013. Consequences of widespread tree mortality triggered by drought and temperature stress. Nature Climate Change **3**:30-36.

Anderegg, W. R., T. Klein, M. Bartlett, L. Sack, A. F. Pellegrini, B. Choat, and S. Jansen. 2016a. Meta-analysis reveals that hydraulic traits explain cross-species patterns of drought-induced tree mortality across the globe. Proceedings of the National Academy of Sciences **113**:5024-5029.

Anderegg, W. R., J. Martinez-Vilalta, M. Cailleret, J. J. Camarero, B. E. Ewers, D. Galbraith, A. Gessler, R. Grote, C.-y. Huang, and S. R. Levick. 2016b. When a tree dies in the forest: scaling climate-driven tree mortality to ecosystem water and carbon fluxes. Ecosystems **19**:1133-1147.

Anderegg, W. R., C. Schwalm, F. Biondi, J. J. Camarero, G. Koch, M. Litvak, K. Ogle, J. D. Shaw, E. Shevliakova, and A. Williams. 2015b. Pervasive drought legacies in forest ecosystems and their implications for carbon cycle models. science **349**:528-532.

Anderson-Teixeira, K. J., J. P. Delong, A. M. Fox, D. A. Brese, and M. E. Litvak. 2011. Differential responses of production and respiration to temperature and moisture drive the carbon balance across a climatic gradient in New Mexico. Global Change Biology **17**:410-424.

Báez, S., S. L. Collins, W. T. Pockman, J. E. Johnson, and E. E. Small. 2013. Effects of experimental rainfall manipulations on Chihuahuan Desert grassland and shrubland plant communities. Oecologia **172**:1117-1127.

Ballantyne, A., W. Smith, W. Anderegg, P. Kauppi, J. Sarmiento, P. Tans, E. Shevliakova, Y. Pan, B. Poulter, and A. Anav. 2017. Accelerating net terrestrial carbon uptake during the warming hiatus due to reduced respiration. Nature Climate Change **7**:148.

Bentz, B. J., J. Régnière, C. J. Fettig, E. M. Hansen, J. L. Hayes, J. A. Hicke, R. G. Kelsey, J. F. Negrón, and S. J. Seybold. 2010. Climate change and bark beetles of the western United States and Canada: direct and indirect effects. BioScience **60**:602-613.

Bernacchi, C. J., E. L. Singsaas, C. Pimentel, A. R. Portis, and S. P. Long. 2001. Improved temperature response functions for models of Rubisco-limited photosynthesis. Plant Cell and Environment **24**:253-259.

Berner, L. T., B. E. Law, and T. W. Hudiburg. 2017. Water availability limits tree productivity, carbon stocks, and carbon residence time in mature forests across the western US. Biogeosciences **14**:365.

Berryman, E., J. D. Marshall, T. Rahn, M. Litvak, and J. Butnor. 2013. Decreased carbon limitation of litter respiration in a mortality-affected piñon–juniper woodland. Biogeosciences **10**:1625-1634.

Breshears, D. D., H. D. Adams, D. Eamus, N. McDowell, D. J. Law, R. E. Will, A. P. Williams, and C. B. Zou. 2013. The critical amplifying role of increasing atmospheric

moisture demand on tree mortality and associated regional die-off. Frontiers in plant science **4**:266.

Breshears, D. D., N. S. Cobb, P. M. Rich, K. P. Price, C. D. Allen, R. G. Balice, W. H. Romme, J. H. Kastens, M. L. Floyd, and J. Belnap. 2005. Regional vegetation die-off in response to global-change-type drought. Proceedings of the National Academy of Sciences of the United States of America **102**:15144-15148.

Burke, E. J., and S. J. Brown. 2008. Evaluating uncertainties in the projection of future drought. Journal of Hydrometeorology **9**:292-299.

Carnicer, J., M. Coll, M. Ninyerola, X. Pons, G. Sanchez, and J. Penuelas. 2011. Widespread crown condition decline, food web disruption, and amplified tree mortality with increased climate change-type drought. Proc Natl Acad Sci U S A **108**:1474-1478.

Chojnacky, D. C., L. S. Heath, and J. C. Jenkins. 2013. Updated generalized biomass equations for North American tree species. Forestry **87**:129-151.

Ciais, P., M. Reichstein, N. Viovy, A. Granier, J. Ogée, V. Allard, M. Aubinet, N. Buchmann, C. Bernhofer, and A. Carrara. 2005. Europe-wide reduction in primary productivity caused by the heat and drought in 2003. Nature **437**:529.

Clifford, M. J., M. E. Rocca, R. Delph, P. L. Ford, and N. S. Cobb. 2008. Drought induced tree mortality and ensuing Bark beetle outbreaks in Southwestern pinyon-juniper woodlands.

Cochard, H., P. Cruiziat, and M. T. Tyree. 1992. Use of Positive Pressures to Establish Vulnerability Curves - Further Support for the Air-Seeding Hypothesis and Implications for Pressure-Volume Analysis. Plant physiology **100**:205-209.

Crausbay, S. D., A. R. Ramirez, S. L. Carter, M. S. Cross, K. R. Hall, D. J. Bathke, J. L. Betancourt, S. Colt, A. E. Cravens, and M. S. Dalton. 2017. Defining ecological drought for the 21st century. Bulletin of the American Meteorological Society.

Dai, A. 2013. Increasing drought under global warming in observations and models. Nature Climate Change **3**:52-58.

Dang, Q.-L., H. A. Margolis, M. R. Coyea, M. Sy, and G. J. Collatz. 1997. Regulation of branch-level gas exchange of boreal trees: roles of shoot water potential and vapor pressure difference. Tree physiology **17**:521-535.

Domec, J.-C., and B. L. Gartner. 2001. Cavitation and water storage capacity in bole xylem segments of mature and young Douglas-fir trees. Trees **15**:204-214.

Domec, J.-C., and D. M. Johnson. 2012. Does homeostasis or disturbance of homeostasis in minimum leaf water potential explain the isohydric versus anisohydric behavior of Vitis vinifera L. cultivars? Tree physiology **32**:245-248.

Droogers, P., and R. G. Allen. 2002. Estimating reference evapotranspiration under inaccurate data conditions. Irrigation and drainage systems **16**:33-45.

Duong, T. 2007. ks: Kernel density estimation and kernel discriminant analysis for multivariate data in R. Journal of Statistical Software **21**:1-16.

Eamus, D., N. Boulain, J. Cleverly, and D. D. Breshears. 2013. Global change‐type drought‐induced tree mortality: vapor pressure deficit is more important than temperature per se in causing decline in tree health. Ecology and evolution **3**:2711-2729.

Feild, T. S., P. J. Hudson, L. Balun, D. S. Chatelet, A. A. Patino, C. A. Sharma, and K. McLaren. 2011. The Ecophysiology of Xylem Hydraulic Constraints by "Basal" Vessels in Canella Winterana (Canellaceae). International Journal of Plant Sciences **172**:879-888.

Floyd, M. L., M. Clifford, N. S. Cobb, D. Hanna, R. Delph, P. Ford, and D. Turner. 2009. Relationship of stand characteristics to drought-induced mortality in three Southwestern piñon-juniper woodlands. Ecological Applications **19**:1223-1230.

Frank, D., M. Reichstein, M. Bahn, K. Thonicke, D. Frank, M. D. Mahecha, P. Smith, M. Velde, S. Vicca, and F. Babst. 2015. Effects of climate extremes on the terrestrial carbon cycle: concepts, processes and potential future impacts. Global Change Biology **21**:2861-2880.

Franks, P. J., P. L. Drake, and R. H. Froend. 2007. Anisohydric but isohydrodynamic: seasonally constant plant water potential gradient explained by a stomatal control mechanism incorporating variable plant hydraulic conductance. Plant, cell & environment **30**:19-30.

Garcia-Forner, N., H. D. Adams, S. Sevanto, A. D. Collins, L. T. Dickman, P. J. Hudson, M. J. Zeppel, M. W. Jenkins, H. Powers, and J. Martínez-Vilalta. 2016. Responses of two semiarid conifer tree species to reduced precipitation and warming reveal new perspectives for stomatal regulation. Plant, cell & environment **39**:38-49.

Garcia-Forner, N., C. Biel, R. Savé, and J. Martínez-Vilalta. 2017. Isohydric species are not necessarily more carbon limited than anisohydric species during drought. Tree physiology **37**:441-455.

Gatti, L., M. Gloor, J. Miller, C. Doughty, Y. Malhi, L. Domingues, L. Basso, A. Martinewski, C. Correia, and V. Borges. 2014. Drought sensitivity of Amazonian carbon balance revealed by atmospheric measurements. Nature **506**:76.

Gaylord, M. L., T. E. Kolb, W. T. Pockman, J. A. Plaut, E. A. Yepez, A. K. Macalady, R. E. Pangle, and N. G. McDowell. 2013. Drought predisposes piñon–juniper woodlands to insect attacks and mortality. New Phytologist **198**:567-578.

Gleason, S. M., M. Westoby, S. Jansen, B. Choat, U. G. Hacke, R. B. Pratt, R. Bhaskar, T. J. Brodribb, S. J. Bucci, and K. F. Cao. 2016. Weak tradeoff between xylem safety and xylem ‐ specific hydraulic efficiency across the world's woody plant species. New Phytologist **209**:123-136.

Goulden, M., and C. Field. 1994. Three methods for monitoring the gas exchange of individual tree canopies: ventilated-chamber, sap-flow and Penman-Monteith measurements on evergreen oaks. Functional Ecology:125-135.

Granier, A. 1987. Evaluation of transpiration in a Douglas-fir stand by means of sap flow measurements. Tree physiology **3**:309-320.

Greve, P., B. Orlowsky, B. Mueller, J. Sheffield, M. Reichstein, and S. I. Seneviratne. 2014. Global assessment of trends in wetting and drying over land. Nature geoscience **7**:716-721.

Grier, C. C., K. J. Elliott, and D. G. McCullough. 1992. Biomass distribution and productivity of Pinus edulis—Juniperus monosperma woodlands of north-central Arizona. Forest ecology and management **50**:331-350.

Gutzler, D. S., and T. O. Robbins. 2011. Climate variability and projected change in the western United States: regional downscaling and drought statistics. Climate Dynamics **37**:835-849.

Harley, P. C., R. B. Thomas, J. F. Reynolds, and B. R. Strain. 1992. Modeling Photosynthesis of Cotton Grown in Elevated Co2. Plant Cell and Environment **15**:271-282.

Heimann, M., and M. Reichstein. 2008. Terrestrial ecosystem carbon dynamics and climate feedbacks. Nature **451**:289.

Hudson, P., J. Limousin, D. Krofcheck, A. Boutz, R. Pangle, N. Gehres, N. McDowell, and W. Pockman. 2018. Impacts of long ‐ term precipitation manipulation on hydraulic architecture and xylem anatomy of piñon and juniper in Southwest USA. Plant, Cell & Environment **41**:421-435.

Huxman, T. E., B. P. Wilcox, D. D. Breshears, R. L. Scott, K. A. Snyder, E. E. Small, K. Hultine, W. T. Pockman, and R. B. Jackson. 2005. Ecohydrological implications of woody plant encroachment. Ecology **86**:308-319.

Jentsch, A., J. Kreyling, and C. Beierkuhnlein. 2007. A new generation of climate-change experiments: events, not trends. Frontiers in Ecology and the Environment **5**:365-374.

Kemp, P. R. 1983. Phenological patterns of Chihuahuan Desert plants in relation to the timing of water availability. The Journal of Ecology:427-436.

Klein, T. 2014. The variability of stomatal sensitivity to leaf water potential across tree species indicates a continuum between isohydric and anisohydric behaviours. Functional Ecology **28**:1313-1320.

Krofcheck, D. J., J. U. Eitel, C. D. Lippitt, L. A. Vierling, U. Schulthess, and M. E. Litvak. 2015. Remote sensing based simple models of GPP in both disturbed and undisturbed Piñon-Juniper woodlands in the Southwestern US. Remote Sensing **8**:20.

Krofcheck, D. J., J. U. Eitel, L. A. Vierling, U. Schulthess, T. M. Hilton, E. Dettweiler-Robinson, R. Pendleton, and M. E. Litvak. 2014. Detecting mortality induced structural and functional changes in a piñon-juniper woodland using Landsat and RapidEye time series. Remote Sensing of Environment **151**:102-113.

Landis, A. G., and J. D. Bailey. 2005. Reconstruction of age structure and spatial arrangement of pinon–juniper woodlands and savannas of Anderson Mesa, northern Arizona. Forest ecology and management **204**:221-236.

Limousin, J., S. Rambal, J. Ourcival, A. Rocheteau, R. Joffre, and R. Rodríguez‐Cortina. 2009. Long‐term transpiration change with rainfall decline in a Mediterranean Quercus ilex forest. Global Change Biology **15**:2163-2175.

Limousin, J.-M., C. P. Bickford, L. T. Dickman, R. E. Pangle, P. J. Hudson, A. L. Boutz, N. Gehres, J. L. Osuna, W. T. Pockman, and N. G. McDowell. 2013. Regulation and acclimation of leaf gas exchange in a piñon–juniper woodland exposed to three different precipitation regimes. Plant, Cell & Environment **36**:1812-1825.

Linton, M., J. Sperry, and D. Williams. 1998. Limits to water transport in Juniperus osteosperma and Pinus edulis: implications for drought tolerance and regulation of transpiration. Functional Ecology **12**:906-911.

Lloret, F., A. Escudero, J. M. Iriondo, J. Martínez‐Vilalta, and F. Valladares. 2012. Extreme climatic events and vegetation: the role of stabilizing processes. Global Change Biology **18**:797-805.

Logan, J. A., J. Regniere, and J. A. Powell. 2003. Assessing the impacts of global warming on forest pest dynamics. Frontiers in Ecology and the Environment **1**:130-137.

Ma, X., A. Huete, J. Cleverly, D. Eamus, F. Chevallier, J. Joiner, B. Poulter, Y. Zhang, L. Guanter, and W. Meyer. 2016. Drought rapidly diminishes the large net CO 2 uptake in 2011 over semi-arid Australia. Scientific reports **6**:37747.

Mackay, D. S., D. E. Roberts, B. E. Ewers, J. S. Sperry, N. G. McDowell, and W. T. Pockman. 2015. Interdependence of chronic hydraulic dysfunction and canopy processes can improve integrated models of tree response to drought. Water Resources Research **51**:6156-6176.

Maherali, H., W. T. Pockman, and R. B. Jackson. 2004. Adaptive variation in the vulnerability of woody plants to xylem cavitation. Ecology **85**:2184-2199.

Martínez-Vilalta, J., and N. Garcia-Forner. 2017. Water potential regulation, stomatal behaviour and hydraulic transport under drought: deconstructing the iso/anisohydric concept. Plant, cell & environment **40**:962-976.

Martínez-Vilalta, J., R. Poyatos, D. Aguadé, J. Retana, and M. Mencuccini. 2014. A new look at water transport regulation in plants. New phytologist **204**:105-115.

Martínez-Vilalta, J., D. Vanderklein, and M. Mencuccini. 2007. Tree height and age-related decline in growth in Scots pine (Pinus sylvestris L.). Oecologia **150**:529-544.

McDowell, N., W. T. Pockman, C. D. Allen, D. D. Breshears, N. Cobb, T. Kolb, J. Plaut, J. Sperry, A. West, and D. G. Williams. 2008. Mechanisms of plant survival and mortality during drought: why do some plants survive while others succumb to drought? New phytologist **178**:719-739.

Meinzer, F. C., D. M. Johnson, B. Lachenbruch, K. A. McCulloh, and D. R. Woodruff. 2009. Xylem hydraulic safety margins in woody plants: coordination of stomatal control of xylem tension with hydraulic capacitance. Functional Ecology **23**:922-930.

Mielke, M. S., M. A. Oliva, N. F. de Barros, R. M. Penchel, C. A. Martinez, S. da Fonseca, and A. C. de Almeida. 2000. Leaf gas exchange in a clonal eucalypt plantation as related to soil moisture, leaf water potential and microclimate variables. Trees **14**:263-270.

Monteith, J. L. 1965. Evaporation and environment. Page 4 *in* Symp. Soc. Exp. Biol.

Morillas, L., R. Pangle, G. Maurer, W. Pockman, N. McDowell, C. W. Huang, D. Krofcheck, A. Fox, R. Sinsabaugh, and T. Rahn. 2017. Tree mortality decreases water availability and ecosystem resilience to drought in piñon‐juniper woodlands in the southwestern USA. Journal of Geophysical Research: Biogeosciences.

Mueller, R. C., C. M. Scudder, M. E. Porter, R. T. Trotter, C. A. Gehring, and T. G. Whitham. 2005. Differential tree mortality in response to severe drought: evidence for long-term vegetation shifts. Journal of Ecology **93**:1085-1093.

Naithani, K. J., B. E. Ewers, and E. Pendall. 2012. Sap flux-scaled transpiration and stomatal conductance response to soil and atmospheric drought in a semi-arid sagebrush ecosystem. Journal of Hydrology **464**:176-185.

Neufeld, H. S., D. A. Grantz, F. C. Meinzer, G. Goldstein, G. M. Crisosto, and C. Crisosto. 1992. Genotypic variability in vulnerability of leaf xylem to cavitation in water-stressed and well-irrigated sugarcane. Plant physiology **100**:1020-1028.

Novick, K. A., D. L. Ficklin, P. C. Stoy, C. A. Williams, G. Bohrer, A. C. Oishi, S. A. Papuga, P. D. Blanken, A. Noormets, and B. N. Sulman. 2016. The increasing

importance of atmospheric demand for ecosystem water and carbon fluxes. Nature Climate Change **6**:1023-1027.

Oren, R., B. E. Ewers, P. Todd, N. Phillips, and G. Katul. 1998. Water balance delineates the soil layer in which moisture affects canopy conductance. Ecological Applications **8**:990-1002.

Oren, R., J. Sperry, G. Katul, D. Pataki, B. Ewers, N. Phillips, and K. Schäfer. 1999. Survey and synthesis of intra‐and interspecific variation in stomatal sensitivity to vapour pressure deficit. Plant, cell & environment **22**:1515-1526.

Otkin, J. A., M. C. Anderson, C. Hain, and M. Svoboda. 2014. Examining the relationship between drought development and rapid changes in the evaporative stress index. Journal of Hydrometeorology **15**:938-956.

Overpeck, J., and B. Udall. 2010. Dry times ahead. science **328**:1642-1643.

Pangle, R. E., J. P. Hill, J. A. Plaut, E. A. Yepez, J. R. Elliot, N. Gehres, N. G. McDowell, and W. T. Pockman. 2012. Methodology and performance of a rainfall manipulation experiment in a piñon–juniper woodland. Ecosphere **3**:1-20.

Pangle, R. E., J. M. Limousin, J. A. Plaut, E. A. Yepez, P. J. Hudson, A. L. Boutz, N. Gehres, W. T. Pockman, and N. G. McDowell. 2015. Prolonged experimental drought reduces plant hydraulic conductance and transpiration and increases mortality in a piñon–juniper woodland. Ecology and evolution **5**:1618-1638.

Peng, C., Z. Ma, X. Lei, Q. Zhu, H. Chen, W. Wang, S. Liu, W. Li, X. Fang, and X. Zhou. 2011. A drought-induced pervasive increase in tree mortality across Canada's boreal forests. Nature Climate Change **1**:467-471.

Pinheiro, J., D. Bates, S. DebRoy, and D. Sarkar. 2014. R Core Team (2014) nlme: linear and nonlinear mixed effects models. R package version 3.1-117. Available at h ttp://CRAN. R-project. org/package= nlme.

Plaut, J. A., W. D. Wadsworth, R. Pangle, E. A. Yepez, N. G. McDowell, and W. T. Pockman. 2013. Reduced transpiration response to precipitation pulses precedes mortality in a pinon–juniper woodland subject to prolonged drought. New phytologist **200**:375-387.

Poulter, B., D. Frank, P. Ciais, R. B. Myneni, N. Andela, J. Bi, G. Broquet, J. G. Canadell, F. Chevallier, and Y. Y. Liu. 2014. Contribution of semi-arid ecosystems to interannual variability of the global carbon cycle. Nature **509**:600.

Pretzsch, H. 2005. Diversity and productivity in forests: evidence from long-term experimental plots. Forest diversity and function:41-64.

Raffa, K. F., B. H. Aukema, B. J. Bentz, A. L. Carroll, J. A. Hicke, M. G. Turner, and W. H. Romme. 2008. Cross-scale drivers of natural disturbances prone to anthropogenic amplification: the dynamics of bark beetle eruptions. AIBS Bulletin **58**:501-517.

Raz-Yaseef, N., E. Rotenberg, and D. Yakir. 2010. Effects of spatial variations in soil evaporation caused by tree shading on water flux partitioning in a semi-arid pine forest. Agricultural and Forest Meteorology **150**:454-462.

Reichstein, M., E. Falge, D. Baldocchi, D. Papale, M. Aubinet, P. Berbigier, C. Bernhofer, N. Buchmann, T. Gilmanov, and A. Granier. 2005. On the separation of net ecosystem exchange into assimilation and ecosystem respiration: review and improved algorithm. Global Change Biology **11**:1424-1439.

Reichstein, M., J. D. Tenhunen, O. Roupsard, J. m. Ourcival, S. Rambal, F. Miglietta, A. Peressotti, M. Pecchiari, G. Tirone, and R. Valentini. 2002. Severe drought effects on ecosystem CO2 and H2O fluxes at three Mediterranean evergreen sites: revision of current hypotheses? Global Change Biology **8**:999-1017.

Rich, P. M., D. D. Breshears, and A. B. White. 2008. Phenology of mixed woody-herbaceous ecosystems following extreme events: net and differential responses. Ecology **89**:342-352.

Rodrigues, A., G. Pita, J. Mateus, C. Kurz-Besson, M. Casquilho, S. Cerasoli, A. Gomes, and J. Pereira. 2011. Eight years of continuous carbon fluxes measurements in a Portuguese eucalypt stand under two main events: Drought and felling. Agricultural and Forest Meteorology **151**:493-507.

Royer, P. D., N. S. Cobb, M. J. Clifford, C. Y. Huang, D. D. Breshears, H. D. Adams, and J. C. Villegas. 2011. Extreme climatic event-triggered overstorey vegetation loss increases understorey solar input regionally: primary and secondary ecological implications. Journal of Ecology **99**:714-723.

Ruehr, N. K., J. G. Martin, and B. E. Law. 2012. Effects of water availability on carbon and water exchange in a young ponderosa pine forest: Above-and belowground responses. Agricultural and forest meteorology **164**:136-148.

Schuler, T. M. 2006. Crop tree release improves competitiveness of northern red oak growing in association with black cherry. Northern Journal of Applied Forestry **23**:77-82.

Schwalm, C. R., W. R. Anderegg, A. M. Michalak, J. B. Fisher, F. Biondi, G. Koch, M. Litvak, K. Ogle, J. D. Shaw, and A. Wolf. 2017. Global patterns of drought recovery. Nature **548**:202.

Schwalm, C. R., C. A. Williams, K. Schaefer, D. Baldocchi, T. A. Black, A. H. Goldstein, B. E. Law, W. C. Oechel, T. P. U. Kyaw, and R. L. Scott. 2012. Reduction in carbon uptake during turn of the century drought in western North America. Nature Geoscience **5**:551-556.

Shaw, J. D., B. E. Steed, and L. T. DeBlander. 2005. Forest inventory and analysis (FIA) annual inventory answers the question: what is happening to pinyon-juniper woodlands? Journal of Forestry **103**:280-285.

Simard, S. W., T. Blenner-Hassett, and I. R. Cameron. 2004. Pre-commercial thinning effects on growth, yield and mortality in even-aged paper birch stands in British Columbia. Forest ecology and management **190**:163-178.

Skelton, R. P., A. G. West, and T. E. Dawson. 2015. Predicting plant vulnerability to drought in biodiverse regions using functional traits. Proceedings of the National Academy of Sciences **112**:5744-5749.

Slik, J., G. Paoli, K. McGuire, I. Amaral, J. Barroso, M. Bastian, L. Blanc, F. Bongers, P. Boundja, and C. Clark. 2013. Large trees drive forest aboveground biomass variation in moist lowland forests across the tropics. Global ecology and biogeography **22**:1261-1271.

Sperry, J., U. Hacke, R. Oren, and J. Comstock. 2002. Water deficits and hydraulic limits to leaf water supply. Plant, Cell & Environment **25**:251-263.

Sperry, J. S. 2000. Hydraulic constraints on plant gas exchange. Agricultural and Forest Meteorology **104**:13-23.

Sperry, J. S., and D. M. Love. 2015. What plant hydraulics can tell us about responses to climate‐change droughts. New Phytologist **207**:14-27.

Sperry, J. S., and N. Z. Saliendra. 1994. Intra-Plant and Inter-Plant Variation in Xylem Cavitation in Betula-Occidentalis. Plant Cell and Environment **17**:1233-1241.

Sperry, J. S., Y. Wang, B. T. Wolfe, D. S. Mackay, W. R. Anderegg, N. G. McDowell, and W. T. Pockman. 2016. Pragmatic hydraulic theory predicts stomatal responses to climatic water deficits. New Phytologist **212**:577-589.

Stevens-Rumann, C. S., K. B. Kemp, P. E. Higuera, B. J. Harvey, M. T. Rother, D. C. Donato, P. Morgan, and T. T. Veblen. 2017. Evidence for declining forest resilience to wildfires under climate change. Ecology letters.

Tardieu, F., and T. Simonneau. 1998. Variability among species of stomatal control under fluctuating soil water status and evaporative demand: modelling isohydric and anisohydric behaviours.

von Buttlar, J., J. Zscheischler, A. Rammig, S. Sippel, M. Reichstein, A. Knohl, M. Jung, O. Menzer, M. A. Arain, and N. Buchmann. 2018. Impacts of droughts and extreme-temperature events on gross primary production and ecosystem respiration: a systematic assessment across ecosystems and climate zones. Biogeosciences **15**:1293.

Ward, J. S. W. J. 2008. Intensity of precommercial crop tree release increases diameter growth and survival of upland oaks. Canadian Journal of Forest Research **39**:118-130.

Warnock, D. D., M. E. Litvak, L. Morillas, and R. L. Sinsabaugh. 2016. Drought-induced piñon mortality alters the seasonal dynamics of microbial activity in piñon–juniper woodland. Soil Biology and Biochemistry **92**:91-101.

Weiss, J. L., D. S. Gutzler, J. E. A. Coonrod, and C. N. Dahm. 2004. Long-term vegetation monitoring with NDVI in a diverse semi-arid setting, central New Mexico, USA. Journal of Arid Environments **58**:249-272.

West, A., K. Hultine, K. Burtch, and J. Ehleringer. 2007. Seasonal variations in moisture use in a piñon–juniper woodland. Oecologia **153**:787-798.

West, N. E. 1999. Distribution, composition, and classification of current juniper–pinyon woodlands and savannas across western North America.*in* In: Monsen, SB, Stevens, R.,(Eds.), Proceedings: Ecology and Management of Pinyon–juniper Communities within the Interior West. USDA For. Serv. Proc. RMRS-P-9. Citeseer.

Williams, A. P., C. D. Allen, A. K. Macalady, D. Griffin, C. A. Woodhouse, D. M. Meko, T. W. Swetnam, S. A. Rauscher, R. Seager, and H. D. Grissino-Mayer. 2013. Temperature as a potent driver of regional forest drought stress and tree mortality. Nature Climate Change **3**:292-297.

Williams, A. P., C. D. Allen, C. I. Millar, T. W. Swetnam, J. Michaelsen, C. J. Still, and S. W. Leavitt. 2010. Forest responses to increasing aridity and warmth in the southwestern United States. Proceedings of the National Academy of Sciences **107**:21289-21294.

Williams, D. G., and J. R. Ehleringer. 2000. Intra- and interspecific variation for summer precipitation use in pinyon-juniper woodlands. Ecological Monographs **70**:517-537.

Wolf, S., T. F. Keenan, J. B. Fisher, D. D. Baldocchi, A. R. Desai, A. D. Richardson, R. L. Scott, B. E. Law, M. E. Litvak, and N. A. Brunsell. 2016. Warm spring reduced carbon cycle impact of the 2012 US summer drought. Proceedings of the National Academy of Sciences:201519620.

Xiao, J., Q. Zhuang, B. E. Law, D. D. Baldocchi, J. Chen, A. D. Richardson, J. M. Melillo, K. J. Davis, D. Y. Hollinger, and S. Wharton. 2011. Assessing net ecosystem carbon exchange of US terrestrial ecosystems by integrating eddy covariance flux measurements and satellite observations. Agricultural and Forest Meteorology **151**:60-69.

Xu, L., and D. D. Baldocchi. 2003. Seasonal trends in photosynthetic parameters and stomatal conductance of blue oak (Quercus douglasii) under prolonged summer drought and high temperature. Tree physiology **23**:865-877.

Zhang, Y., R. Oren, and S. Kang. 2011. Spatiotemporal variation of crown-scale stomatal conductance in an arid Vitis vinifera L. cv. Merlot vineyard: direct effects of hydraulic properties and indirect effects of canopy leaf area. Tree physiology **32**:262-279.

Zhao, M., and S. W. Running. 2010. Drought-induced reduction in global terrestrial net primary production from 2000 through 2009. science **329**:940-943.